Natural Resources Canada | Ressources naturelles Canada

GEOLOGICAL SURVEY OF CANADA
OPEN FILE 8765

Review of space weather events in solar cycle 23 (1998-2005)

L. Trichtchenko

2021

Canada

GEOLOGICAL SURVEY OF CANADA
OPEN FILE 8765

Review of space weather events in solar cycle 23 (1998-2005)

L. Trichtchenko

2021

Permanent link: https://doi.org/10.4095/327886

This publication is available for free download through GEOSCAN (https://geoscan.nrcan.gc.ca/).

Recommended citation
Trichtchenko, L., 2021. Review of space weather events in solar cycle 23 (1998-2005); Geological Survey of Canada, Open File 8765, 88 p. https://doi.org/10.4095/327886

Publications in this series have not been edited; they are released as submitted by the author.

INTRODUCTION

The presented review covers the space weather events that occurred in years 1998-2005 and includes descriptions of the solar, interplanetary and geomagnetic activity and other space weather parameters during each year together with the main characteristics of the most significant events. These are presented through annual plots and short descriptions, which are useful for space weather scientists and forecasters for comparisons with modern events and for detailed event studies. The information includes the overall space weather activity: from their solar sources through the solar wind propagation to effects on the ground and in the near-earth environment. Annual plots are presented for each year showing the variation in sunspots, F10.7 flux, energetic protons and electrons on GOES, interplanetary magnetic field and solar wind parameters extracted from ACE data, global geomagnetic indices, such as PC North, Kp and Dst, and local (Canadian) geomagnetic hourly range indices at polar, auroral and subauroral stations. Each annual review also contains detailed descriptions of the major space weather events of each year. These descriptions vary from year to year and include many interesting features, from description of space weather during Extra-Vehicular Activities on the International Space Station to satellite anomalies, and to geomagnetically induced currents in power grids over the globe. In addition to the data sources referred to in the report, the catalogue of space storms (APEV) at http://dbserv.sinp.msu.ru/apev/, with more details on solar sources, is recommended.

PART 1

Review of space weather in year 1998

Summary

This part presents a synopsis of solar activity, solar wind conditions, global geomagnetic activity, and geomagnetic activity in Canada for the entire year 1998, highlighting the causes and ground effects of the space weather event on May 4. To put this activity into context we also present relevant solar, solar wind, and global geomagnetic parameters. Five major interplanetary disturbances with high geo-effectiveness can be identified. The geomagnetic response to these events is seen at high latitudes in the PC index, at mid-latitudes in the ap and Kp indices and at low latitudes in the Dst index. During 1998 only one geomagnetic storm reached the Kp value of 9- (May 4), with corresponding Dst = -205 nT. During this event, geomagnetically induced currents (GIC) in the Nova Scotia power system reached a value of ~ 70 A. No operational impacts were reported.

Solar activity

Year 1998 was in the ascending part of the solar cycle, with the daily sunspot numbers and F10.7 flux variations as presented in Figure 1.1. The sunspot numbers were the highest in September, April and August, while the F10.7 values were the largest in August-September and December.

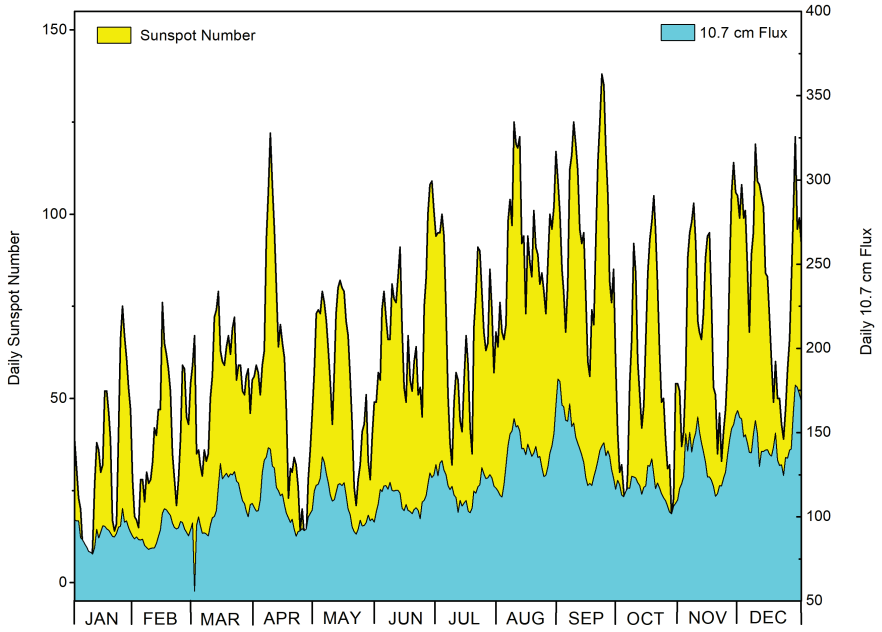

Figure 1.1. Daily sunspot number (yellow) (ftp://ftp.ngdc.noaa.gov/STP/space-weather/solar-data/solar-indices/sunspot-numbers/) and F10.7 adjusted solar flux density (blue) in flux units 10^{-22} Joules/s/m^2/Hz (https://spaceweather.gc.ca/solarflux/sx-en.php)

Solar Proton Events

The most significant solar proton events were evaluated based on daily fluences of high energy protons (>10 MeV and >100MeV) measured by the GOES satellite (Figure 1.2).

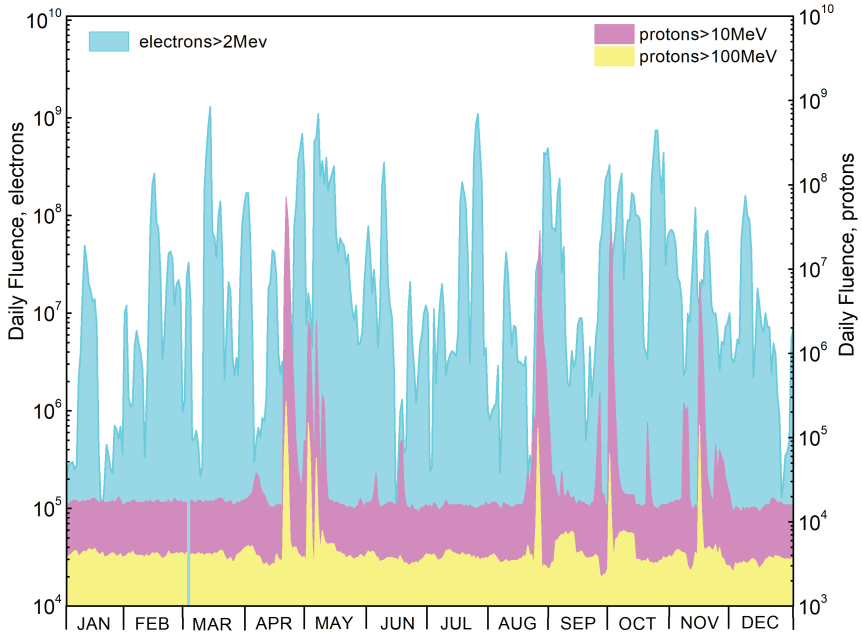

Figure 1.2. Daily fluences of electrons with energies>2MeV (blue), protons > 10 MeV (pink) and >100 MeV (yellow) extracted from GOES satellite data ftp://ftp.ngdc.noaa.gov/STP/SOLAR_DATA/SATELLITE_ENVIRONMENT/.

Table 1.1.
The most significant solar energetic proton events during 1998 (https://umbra.nascom.nasa.gov/SEP)

Start	max	PFU>10 MeV	CME	Flare max	Flare Xray/optical	AR location	AR number
Apr 20/1400	Apr 21/1205	1,700	W/20 1007	Apr 20/1021	M1/EPL	S43W90	8194
May 02/1420	May 02/1650	150	Halo/02 1406	May 02/1342	X1/3B	S15W15	8210
May 06/0845	May 06/0945	210	W/06 0829	May 06/0809	X2/1N	S11W65	8210
Aug 24/2355	Aug 26/1055	670	NA	Aug 24/2212	X1/3B	N30E07	8307
Sep 25/0010	Sep 25/0130	44	NA	Sep 23/0713	M7/3B	N18E09	8340
Sep 30/1520	Oct 01/0025	1,200	NA	Sep 30/1350	M2/2N	N23W81	8340
Nov 08/0245	Nov 08/0300	11	?		none		
Nov 14/0810	Nov 14/1240	310	NA	Nov 14/0518	C1/BSL	N28W90	8375?

Among the events listed in Table 1.1, the most significant in its interplanetary response, according to ftp://ftp.ngdc.noaa.gov/STP/swpc_products/weekly_reports/PRFs_of_SGD/, were the May events, initiated by the Active Region (AR) 8210 (S17, on 02 May) which started producing major flares even at the end of April:
-X1/2B at 27 April /0920UT, Type IV radio burst and a halo-CME
-M6/3B at 29 April /1637UT, Type IV radio burst and a halo-CME.
- X1/3B at 02 May /1342UT with an associated 1300 SFU Tenflare, Type IV, and partial-halo CME (Table1.1, line 2).

The May 2 event produced several Solar Energetic Proton (SEP) events, such as:
Protons with energies >10 MeV reached a peak of 150 PFU at 02/1650UT;
Protons with energies > 100 MeV reached a peak of 7.6 PFU at 02/1450UT (ended on 03 May).
A polar cap absorption (PCA) event occurred in response to the SEP (est. maximum absorption 3.7 dB).

The same active region produced the SEP event on May 6, following the X2/2N flare. Protons with energies > 10 MeV flux reached a peak of 210 PFU at 06/1650UT and protons with energies> 100 MeV reached a peak of 2.9 PFU at 06/0840UT.

September solar events:
Activity has been associated with AR 8340 (N20, on 21 September) which produced M6/3B flare at 23/0713UT with Types II and IV radio bursts. Solar energetic protons with energies> 10 MeV reached 44 PFU at 25/0130UT. A Forbush decrease of -15% was detected by the Thule neutron monitor.

November solar events:
Activity has been associated mostly with AR 8375 (N18, on 05 November) with the following largest flares:

- M8/2B at 05/1955UT with Type II, and a full-halo CME.
- Protons with energies >10 MeV (the last in Table1.1, 14/0810UT) reached a peak of 310 PFU at 14/1240UT. Protons with energies> 100 MeV reached a peak of 6.1 PFU at 14/0950UT.

Interplanetary conditions

The interplanetary magnetic field (IMF) components in the geocentric solar-magnetospheric coordinate system (GSM) obtained from ACE satellite data are presented in Figure 1.3. The largest negative values of the Bz component of IMF (<-20 nT) were recorded in May, November and September 1998.

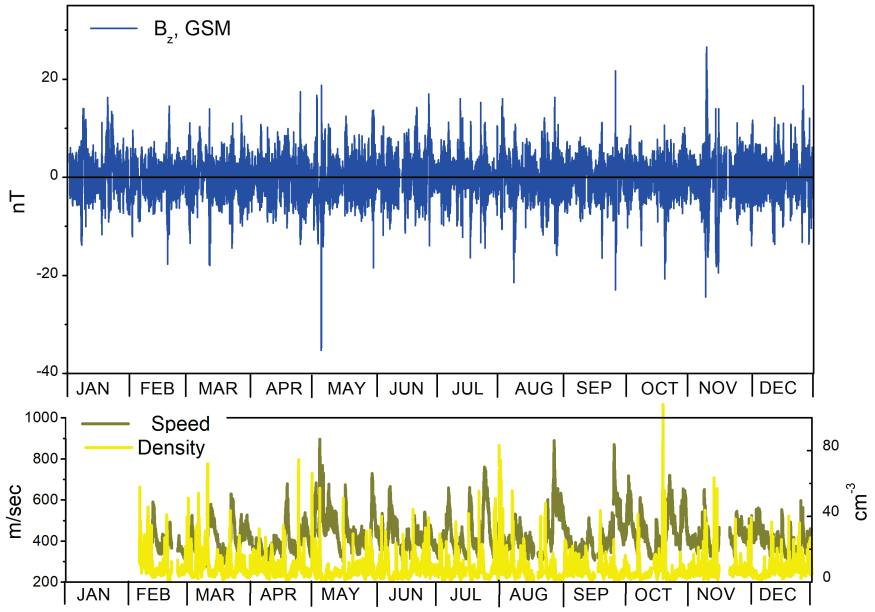

Figure 1.3. Top panel: 4-min. average of IMF Bz; bottom panel: hourly solar wind speed (dark yellow) and density (yellow) at ACE satellite http://www.srl.caltech.edu/ACE/ASC/.

During May 4, 1998 SW event, the IMF Bz was minimum - 40 nT, solar wind velocity increased to 840 km/sec and particle densities increased to 18 p/cc on 04 May following an interplanetary shock passage at 04/0229UT.

During September 24-25, 1998 SW event, the IMF Bz was minimum -27 nT, solar wind velocity increased to 880 km/sec, and particle densities increased to 14 p/cc early on 25 September.

During 07 - 08 November, the IMF Bz was -25 nT, velocity increased to 660 km/sec, particle densities increased to 27 p/cc.

Global Geomagnetic Activity

Variations of the global geomagnetic indices Kp (ap), Dst and the polar cap index for Thule (PC-North) are presented in Figure 1.4.

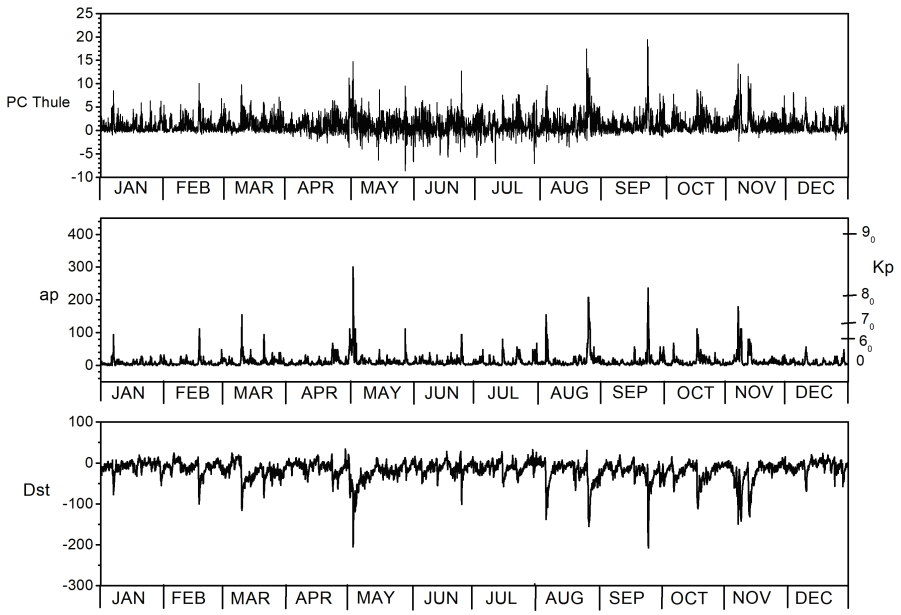

Figure 1.4. Geomagnetic indices for the year 1998 (http://isgi.unistra.fr/data_download.php)
Top: 15-min PC index at Thule
Middle: 3-hour ap and Kp indices
Bottom: 1-hour Dst (nT)

During the year 1998 there were global disturbances with Kp=9- (May 4) and Kp=8+ (September 25), one with Kp=8o (August 27) and one with Kp=8- (November 8).
For the Dst index the September 25 storm was the largest (Dst=-207 nT), closely followed by May 4 (-205 nt), and significantly smaller Dst index values during August 27 (-155 nT) and November 8 (-149 nT).
The highest value of the Thule PC index occurred in September, followed by the August and May geomagnetic storms.

Geomagnetic Activity in Canada

The hourly ranges at three Canadian magnetic observatories (https://spaceweather.gc.ca/data-donnee/indices/si-en.php), Resolute (RES, GML =83.1°), Poste-de-la-Baleine (PBQ, 66.8°) and Ottawa (OTT, 57.0°) which represent geomagnetic activity in polar cap, auroral and subauroral regions in Canada, are presented in Figures 1.5-1.7.

Hourly ranges at the magnetic observatories in Canada show the major differences between three zones. Thus, the largest disturbance in RES occurred on May 29, i.e. when solar wind and global geomagnetic indices show very moderate activity. The largest disturbance in the auroral zone (PBQ) was the September event and the largest in the subauroral zone was the May 4 event (i.e. the overall largest in Kp). Except for RES, the major disturbances coincided with the major events seen in the ACE data.

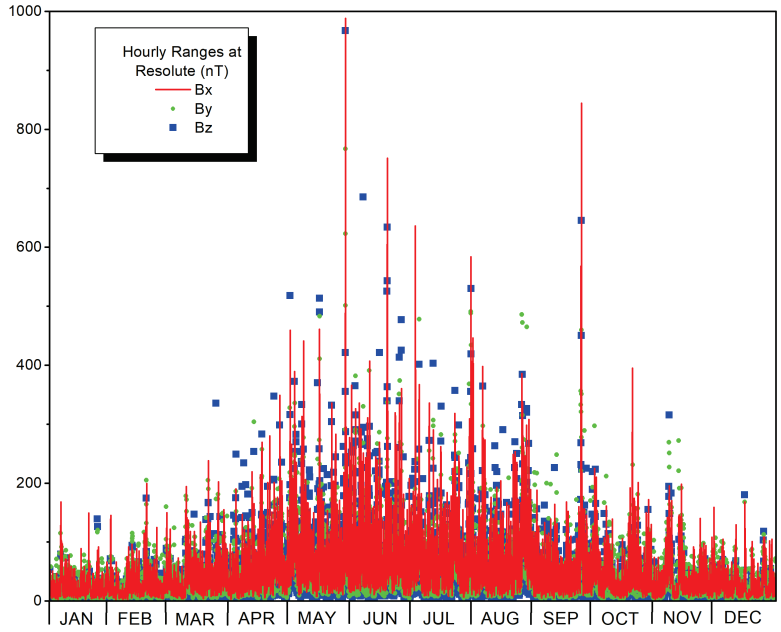

Figure 1.5. Hourly ranges of the magnetic field components at Resolute.

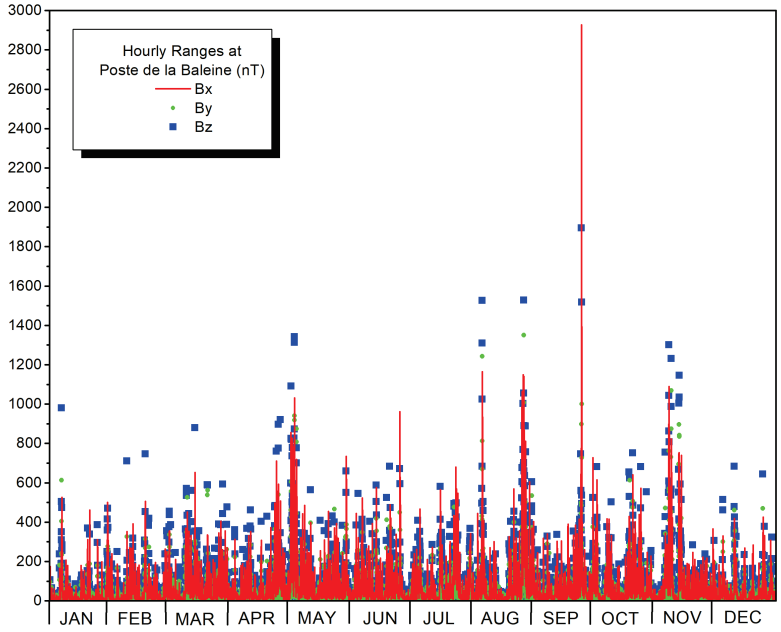

Figure 1.6. Hourly ranges of the magnetic field components at Poste-de-la-Baleine.

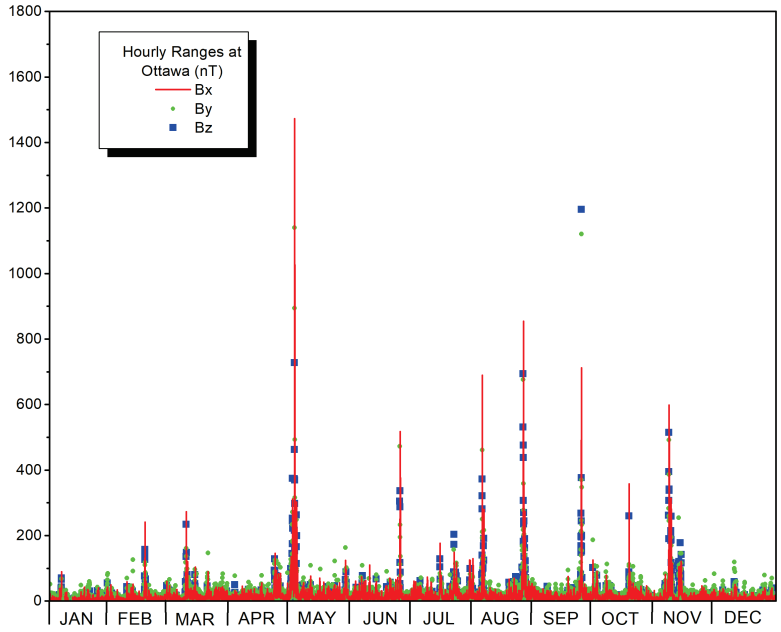

Figure 1.7. Hourly ranges of the magnetic field components at Ottawa.

Details of the largest space weather event and GIC

The largest identified space weather event on May 4 produced significant variations in the interplanetary magnetic field (IMF) and also had an impact on ground electric power utilities, as presented in Figures 1.8-1.10.

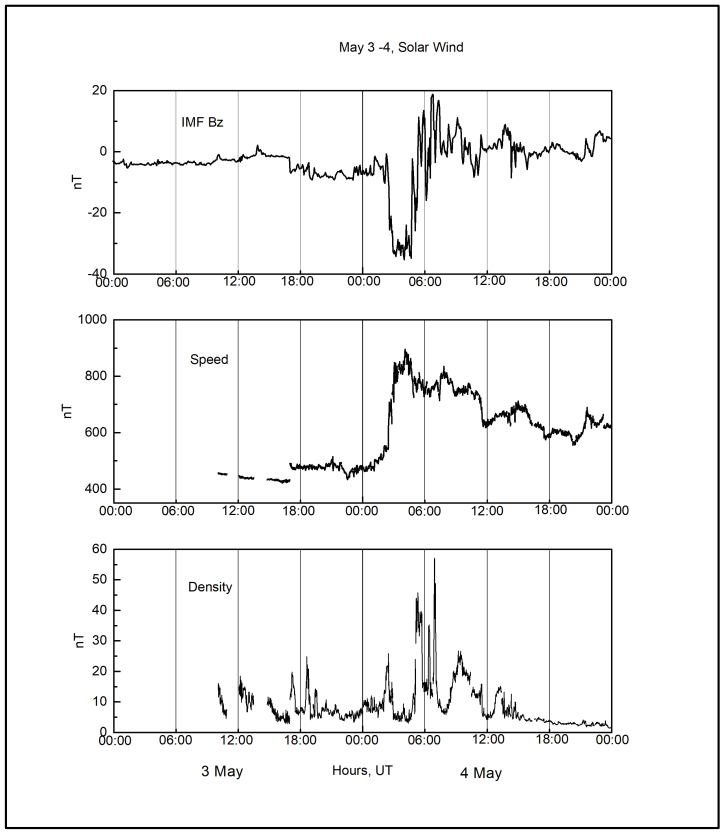

Figure 1.8. Variations of the interplanetary parameters during October 21-22 1998; top panel is IMF Bz middle panel is solar wind speed and the bottom panel is solar wind density, obtained at ACE.

At the time of the event, the ACE satellite had just started its operations thus there were some data gaps, especially in data from the solar wind instruments, and less in the magnetic measurements.

Geomagnetically Induced Currents

The examples of the ground geomagnetic field, the modelled geoelectric field at two geomagnetic observatories in Canada (Ottawa and St John's) and the geomagnetically induced currents in the Nova Scotia power grid recorded during the May 3-4 event are presented in Figures 1.9 and 1.10.

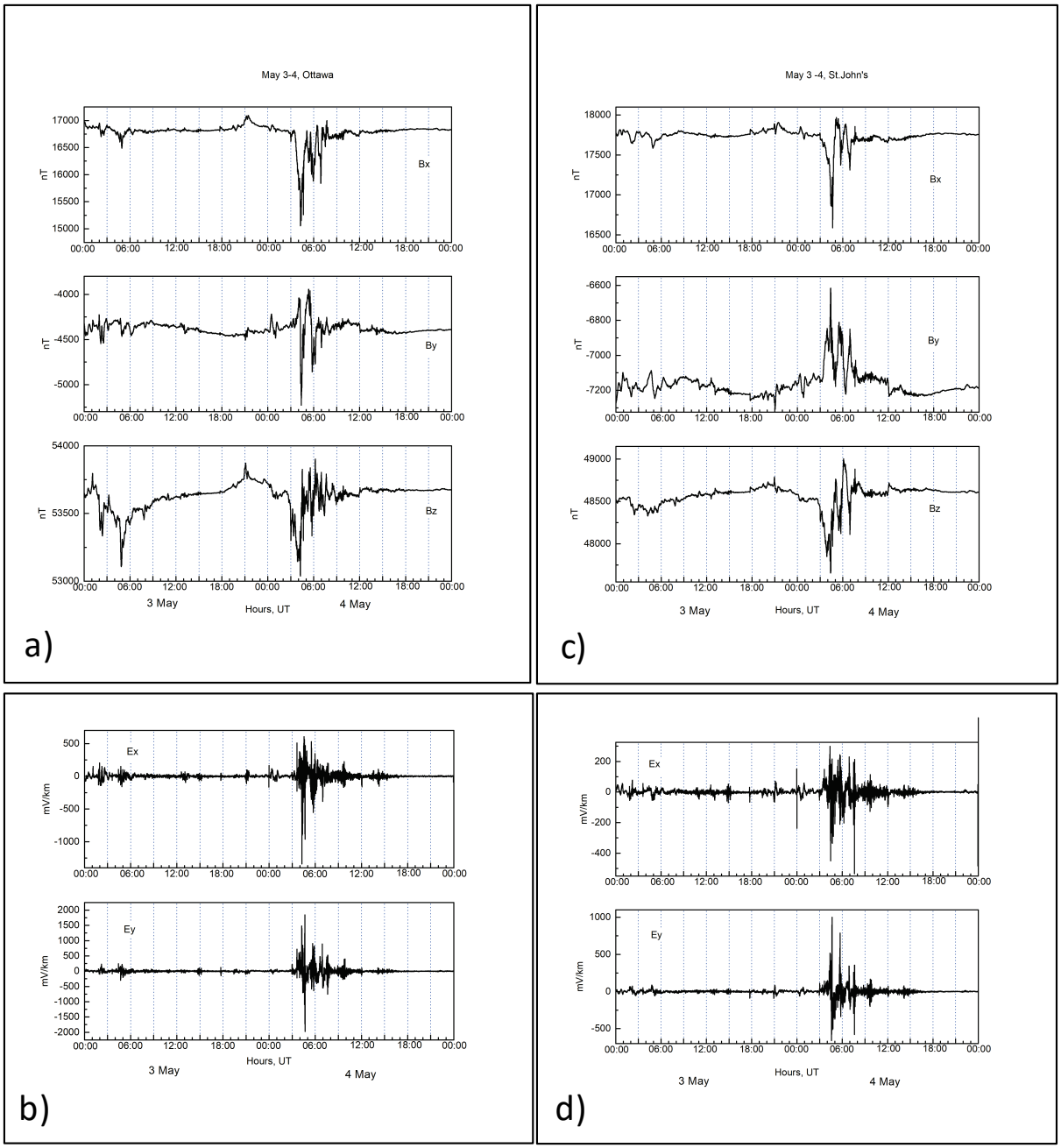

Figure 1.9. Ground effects of space weather on 3rd and 4th May 1998; a) geomagnetic variations (three components) at OTT Observatory and b) corresponding modelled geoelectric field components; and c) geomagnetic variations (three components) at STJ Observatory and d) corresponding modelled geoelectric field components.

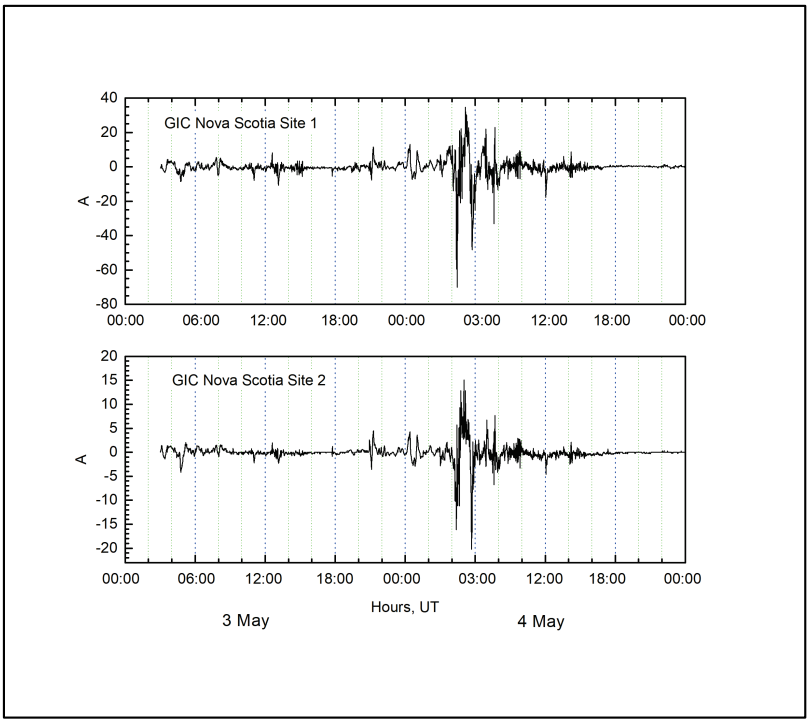

Figure 1.10. Ground effects of magnetic disturbances. GIC variations at two different sites of Nova Scotia Power grid. Significant difference in the GIC values between the two sites is clearly seen

PART 2

Review of space weather in year 1999

Summary

An overview of the space weather activity for year 1999 is presented, with an emphasis on the ground geomagnetic and technological effects across Canada. To put this activity into context, the relevant solar, solar wind, and global geomagnetic parameters are presented for the whole year and for the only significant event in the year. The largest event of the year occurred on October 22, with Kp max=8o, and is presented in more detail, including the observations of the geomagnetic filed, recordings of the geoelectric field and measurements on the power grids.

Solar activity

Year 1999 was in the ascending part of the solar cycle, with the daily sunspot numbers and F10.7 flux variations as presented in Figure 2.1. It follows, that the sunspot numbers were the highest in June, July and November, while the F10.7 values were the largest in August and November.

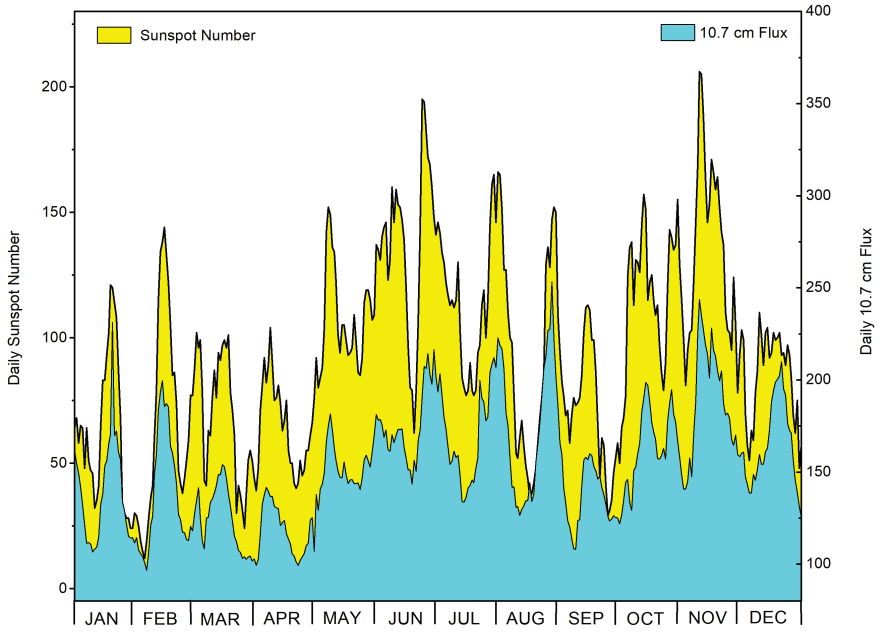

Figure 2.1. Daily sunspot number (yellow) (ftp://ftp.ngdc.noaa.gov/STP/space-weather/solar-data/solar-indices/sunspot-numbers/) and F10.7 adjusted solar flux density (blue) (https://spaceweather.gc.ca/solarflux/sx-en.php) in flux units 10^{-22} Joules/s/m^2/Hz.

Solar Proton Events

The most significant solar proton events are evaluated based on daily fluences of high energy protons (>10 MeV and >100MeV) at GOES satellite (Figure 2.2 and Table 2.1)).

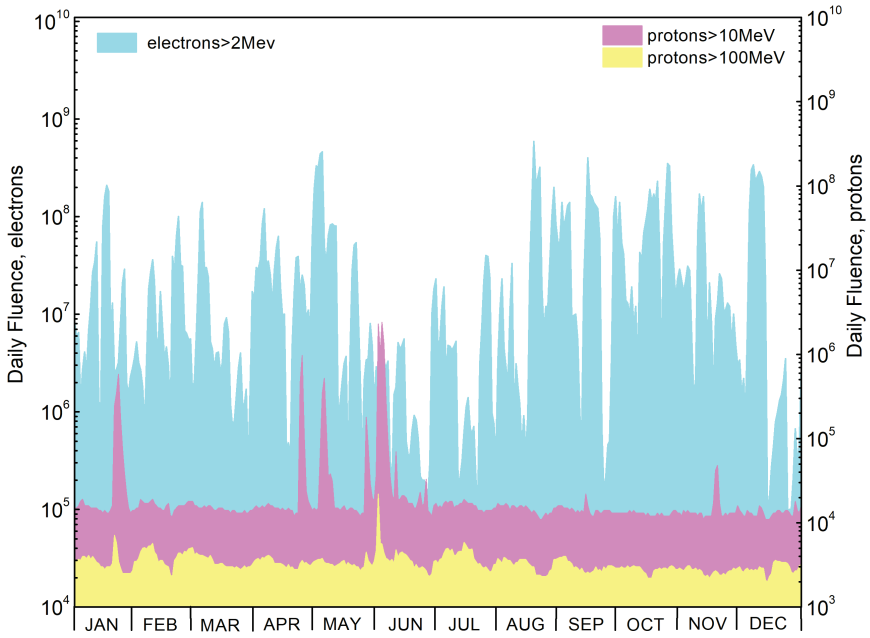

Figure 2.2. Daily fluences of electrons with energies>2MeV (blue), protons > 10 MeV (pink) and >100 MeV (yellow) extracted from GOES satellite data ftp://ftp.ngdc.noaa.gov/STP/SOLAR_DATA/SATELLITE_ENVIRONMENT/ .

Table 2.1.
The most significant solar proton events in 1999 are (https://umbra.nascom.nasa.gov/SEP)

start	max	PFU>10 MeV	CME	Flare max	Flare Xray/optical	AR location	AR number
Jan 23/1105	Jan 23/1135	14	NA	Jan 20/2005	M5	N27E90	?
Apr 24/1804	Apr 25/0055	32	Halo/24 1331		none		
May 05/1820	May 05/1955	14	Halo/03 0606	May 3/0602	M4/N2	N15E32	8525
Jun 02/0245	Jun 02/1010	48	Halo/01 ~1937	Jun 01/~1930	CME	W limb	
Jun 04/0925	Jun 04/1055	64	NW/04 0726	Jun 04/0703	M3/2B	N17W69	8552

Interplanetary conditions

The interplanetary magnetic field (IMF) components in geocentric solar-magnetospheric coordinate system (GSM) obtained from the ACE satellite data are presented in Figure 2.3.

The several large negative values of the Bz component of IMF (<-20 nT) were recorded in February, September, and October (the largest). The description below is based on ftp://ftp.ngdc.noaa.gov/STP/swpc_products/weekly_reports/PRFs_of_SGD/

-The February IMF event has been associated with the CME from AR 8462 (N20 W09), which passed the ACE spacecraft about 18/0200UT accompanied by a velocity increase to 700 km/sec, and IMF Bz =-28 nT.

- The solar wind disturbance occurred during 22 - 23 September with a velocity increase to 630 km/sec, IMF Bz =- 20 nT, and brief increases in density. The origin could be a high speed streams from coronal holes, or slow partial-halo Coronal Mass Ejection (CME) following a disappearing solar filament (DSF) on 16/1508-1615UT.

- The largest event of the year occurred on October 22, with Kp max=8o. In the solar wind the IMF Bz was below 30 nT, with a solar wind speed of ~ 700 km/sec. The most possible solar source of this disturbance is high speed streams, although the solar activity was high from October16 to October 22, producing multiple C-and M-class flares, Type II radio bursts and filament eruption on 1999/10/17 (23:12 UT). The latter resulted in s Sudden Impulse (SI), but did not produce IMF Bz negative, thus was not geo-effective.

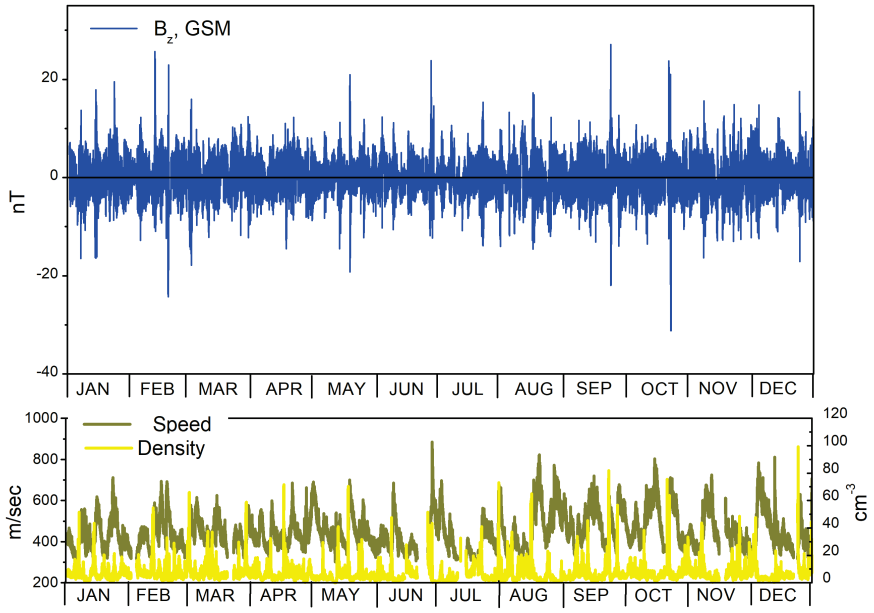

Figure 2.3. Interplanetary magnetic field components and solar wind parameters at ACE satellite http://www.srl.caltech.edu/ACE/ASC/ .

Note, that January and June proton events were not accompanied by significant negative Bz, nor by appreciable geomagnetic activity.

Global Geomagnetic Activity

Variations of the global indices Kp (ap), Dst and the polar cap index for Thule (PC-North) are presented in Figure 2.4.

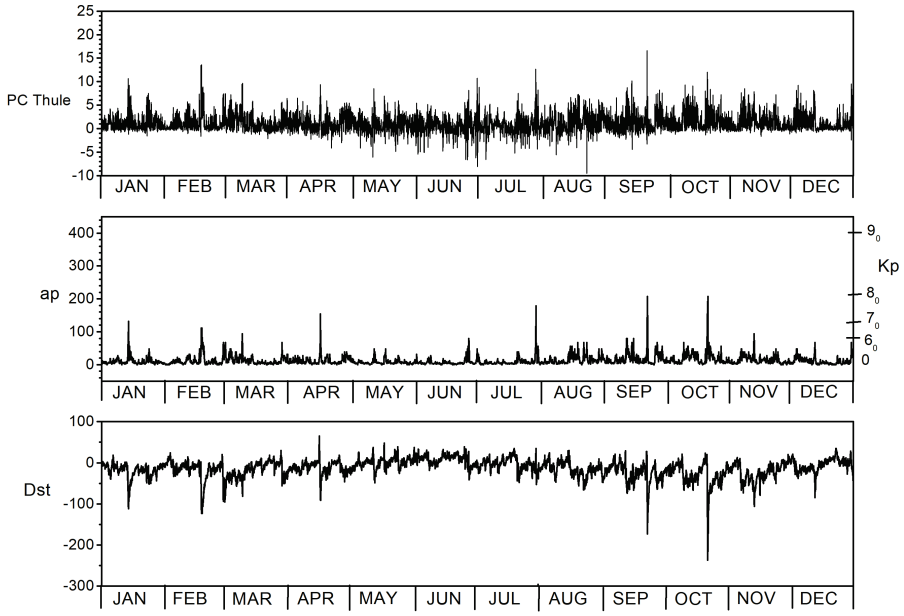

Figure 2.4. Geomagnetic indices for the year 1999 http://isgi.unistra.fr/data_download.php .
Top:15-min PC index at Thule
Middle:3-hour ap and Kp indices
Bottom:1-hour Dst index nT

The year1999 was very moderate in terms of geomagnetic activity, with the largest Kp=8 occurring on October 22. Minor geomagnetic storms occurred on September 22 (Kp=7o) and 18 – 19 February (Kp=7-). The largest disturbance in terms of Dst index (-237 nT) has also occurred on October 22. High values of the Thule PC index occurred in February and September.

Geomagnetic Activity in Canada

The hourly ranges at three Canadian magnetic observatories, Resolute (RES, GML =83.1°), Poste-de-la-Baleine (PBQ, 66.8°) and Ottawa (OTT, 57.0°) which represent geomagnetic activity in polar cap, auroral and subauroral regions in Canada (https://spaceweather.gc.ca/data-donnee/indices/si-en.php), are shown in Figures 2.5-2.7.

Hourly ranges at the magnetic observatories in Canada show that the largest disturbance in all zones was in July, but the relative size of disturbances during other events depends on the local conditions. Disturbances in RES mostly occurred in summer time, with the largest in June and next in size in May, July and September, due to the seasonal variations in ionospheric conductivity. At auroral latitudes, (PBQ), the disturbances were more evenly distributed throughout the year and have the largest amplitude in February. At subauroral latitudes (OTT) there were fewer disturbances which stand out more clearly against the background activity level. The major disturbance was in October, with smaller ones in April and September.

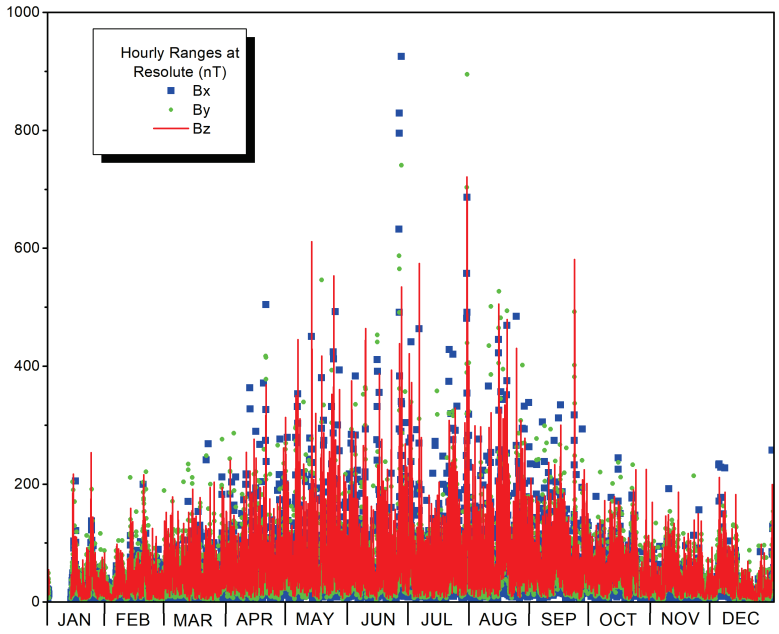

Figure 2.5. Hourly ranges of the magnetic field components at Resolute.

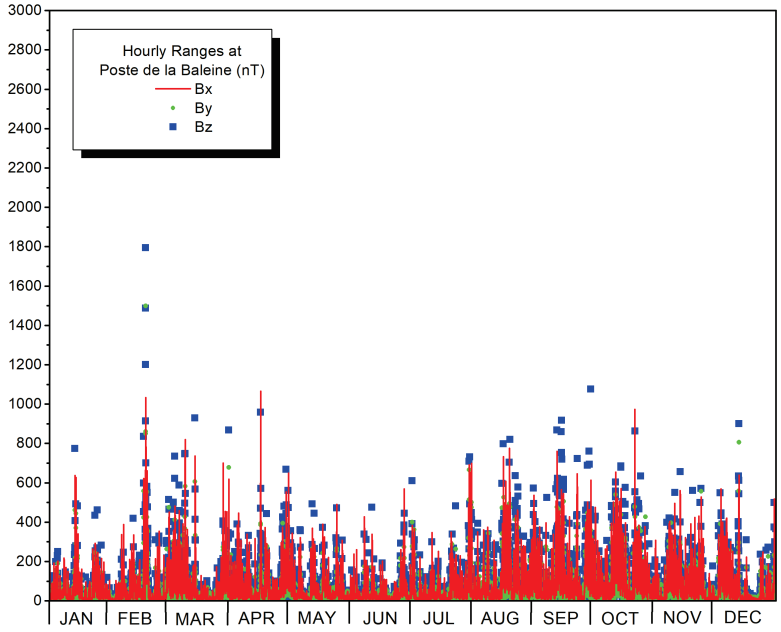

Figure 2.6. Hourly ranges of the magnetic field components at Poste-de-la-Baleine.

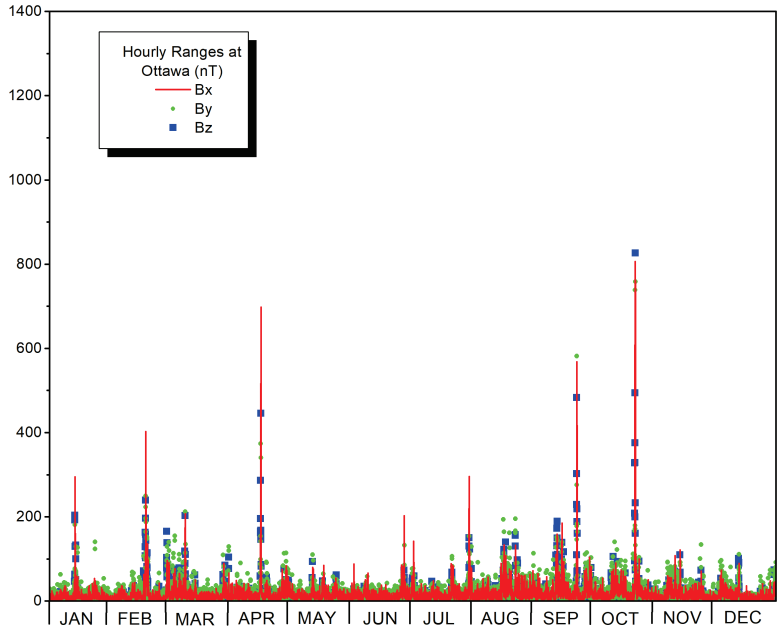

Figure 2.7. Hourly ranges of the magnetic field components at Ottawa.

Details of the largest space weather event and GIC

The largest identified space weather event on 21-22 October produced significant variations in the IMF and had an impact on ground electric power utilities, as presented in Figures 2.8-2.9.

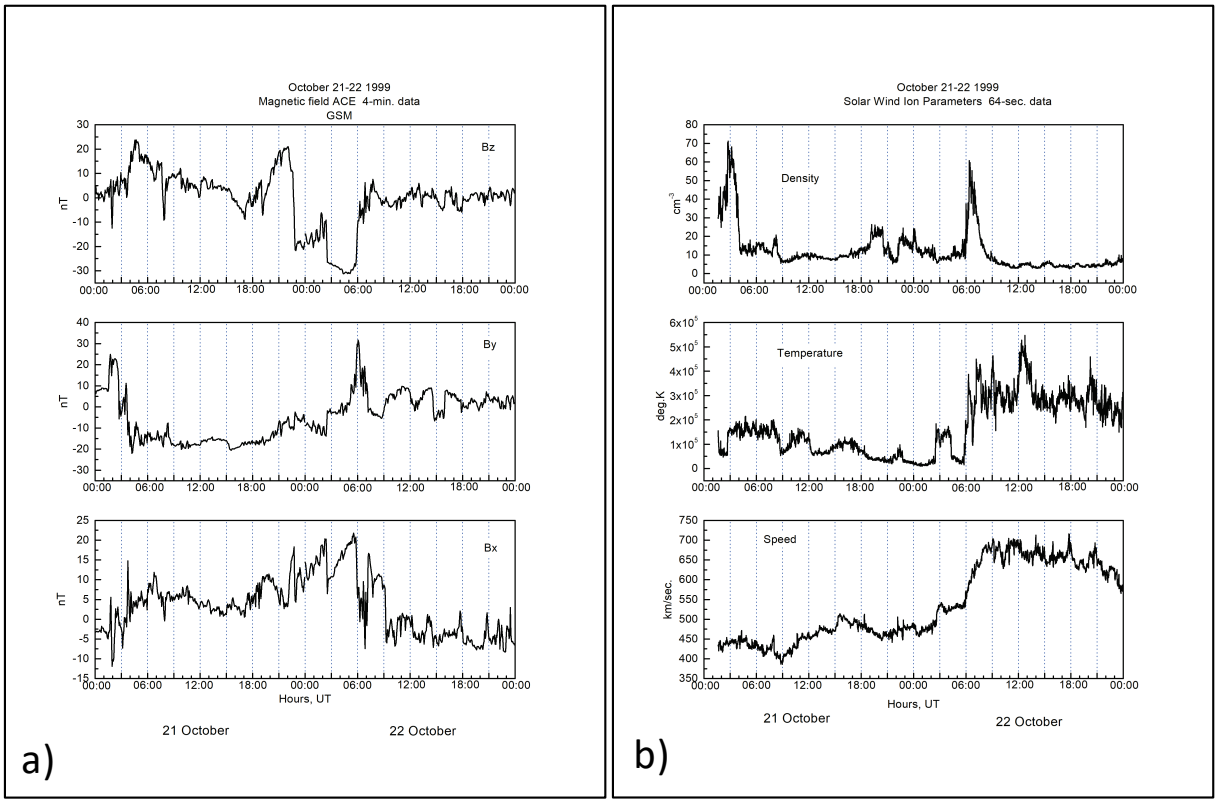

Figure 2.8. Variations of the interplanetary parameters during October 21-22 1999: a) three components of the IMF, top to bottom-Bz, By and Bx; b) solar wind density (top), temperature (middle) and speed (bottom), obtained at ACE.

Geomagnetically Induced Currents

The examples of recordings of the ground geomagnetic field (Ottawa, Ontario), geoelectric field (Lindsay, Ontario) and geomagnetically induced currents in the Nova Scotia power and harmonics and asymmetry in Hydro Quebec systems during the October 21-22 are presented in Figure 2.9.

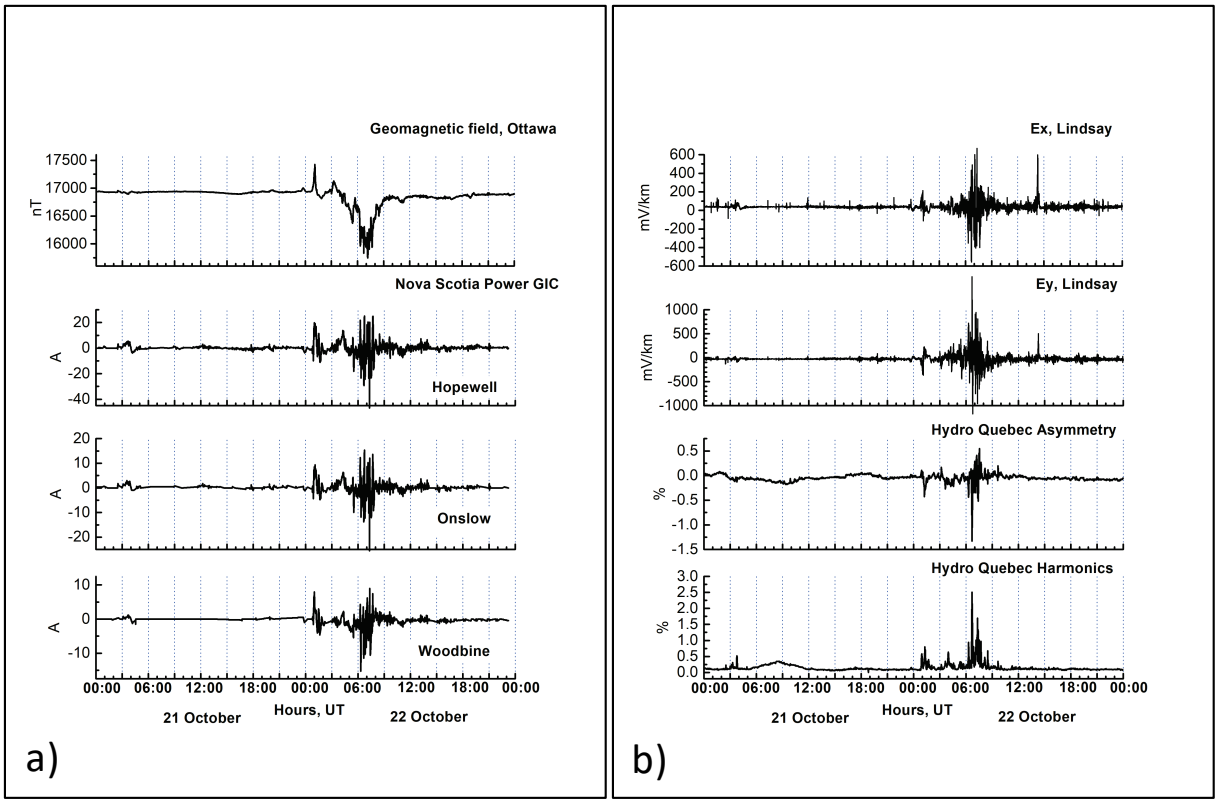

Figure 2.9. Ground effects of magnetic disturbances; a) top panel-geomagnetic field variations at Ottawa Observatory, other panels-GIC variations at different sites of Nova Scotia Power grid; b) top two panels geoelectric field variations measured at Lindsay, Ontario, and the bottom two panels are Hydro Quebec asymmetry and harmonics variations during the event.

The event of October 22, 1999 was not particular large, with the GIC below 50 A, geoelectric field less than 1000mV/km, and harmonic levels below 2.5%.

PART 3

Review of space weather in year 2000

Summary

An overview of geomagnetic activity for year 2000 is presented, with an emphasis on ground geomagnetic and technological effects across Canada. Five major interplanetary disturbances with high geo-effectiveness are identified. The global geomagnetic response to these events is seen at high latitudes in the PC index, at mid-latitudes in the ap and Kp indices and at low latitudes in the Dst index. The largest event occurred on 15 July, with IMF Bz = - 43 nT, producing geomagnetic disturbances with Kp = 9 and Dst = -295 nT. Geomagnetic activity in Canada was high during the year, with the largest disturbance in all zones (polar, auroral, subauroral) in July. The relative sizes of the disturbances in the different zones varied from event to event depending on the movements of the auroral electrojets. For example, the September 17-18 event shows the most significant fluctuations in Ottawa, but can barely be seen in magnetic hourly ranges at auroral latitudes (PBQ), yet is clearly seen in the polar cap (RES). Some power systems experienced geomagnetically induced currents; e.g., about 10 A (Ontario, April) and up to 100 A (Nova Scotia, July). An evaluation of the short-term NRCan geomagnetic forecasts during the first part of the year 2000 is included.

Solar activity

Year 2000 was close to the solar cycle maximum, with the daily sunspot numbers and F10.7 flux variations as presented in Figure 3.1. It follows that the sunspot numbers were the highest in July, May and August, while the F10.7 values were the largest in July, May and September.

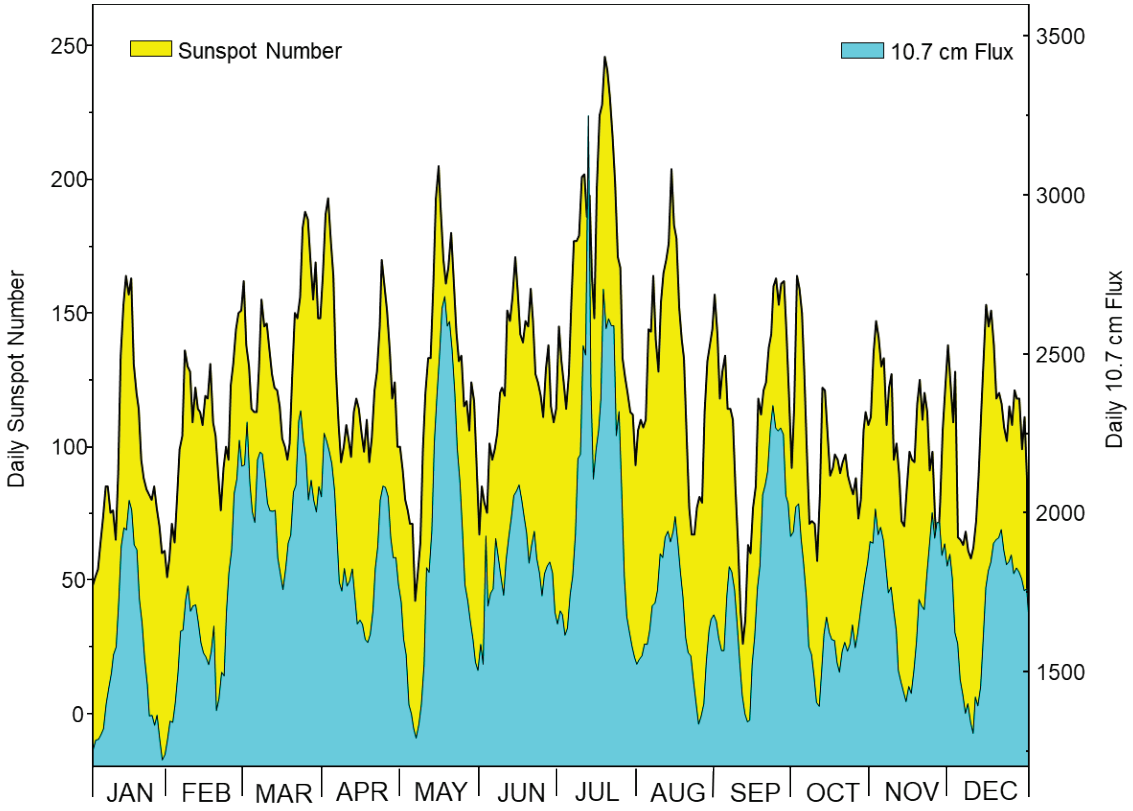

Figure 3.1. Daily sunspot number (yellow) ftp://ftp.ngdc.noaa.gov/STP/space-weather/solar-data/solar-indices/sunspot-numbers/ and F10.7 adjusted solar flux density (blue) https://spaceweather.gc.ca/solarflux/sx-en.php in flux units 10^{-22} Joules/s/m^2/Hz.

Solar Proton Events

The most significant solar proton events are evaluated based on daily fluences of high energy protons (>10 MeV and >100MeV) at GOES satellite (Figure 3.2). These are 5 events, marked after the first letters of the corresponding months, as A, M, Jn, Jl, Au, S, N1 and N2.

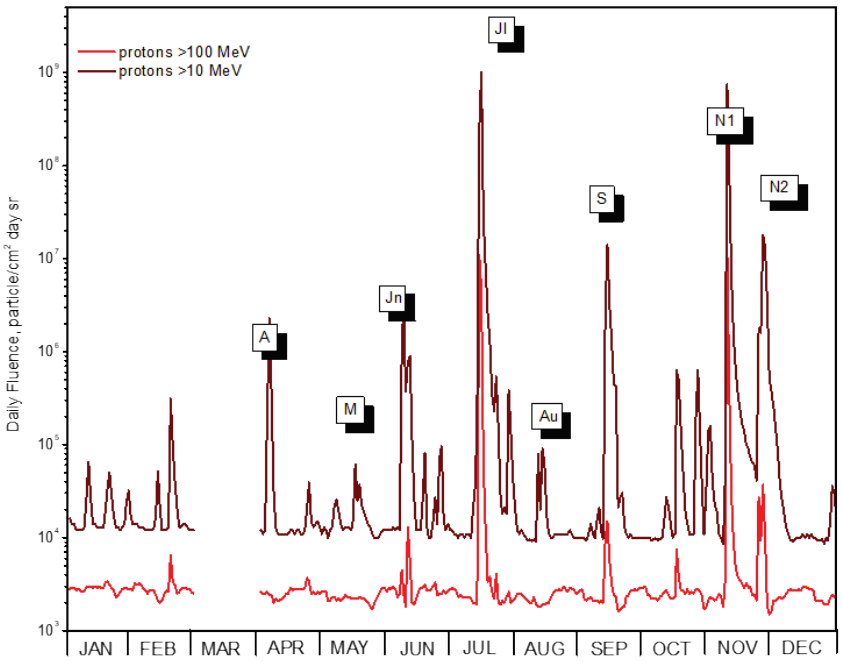

Figure 3.2. Daily fluences of protons with energies > 10 MeV and >100 MeV (GOES data) ftp://ftp.ngdc.noaa.gov/STP/SOLAR_DATA/SATELLITE_ENVIRONMENT/ .

The most significant solar proton events during 2000 are:
(ftp://ftp.ngdc.noaa.gov/STP/swpc_products/weekly_reports/PRFs_of_SGD/)

- A (April): A halo CME with speed of 600 km/s following C9/2F flare which occurred on 4/1632, causing proton event peaking at 5/0930.
- M (May): A CME associated with LDE C7/1N of 20/0535, accompanied by Type 4 and Type 2 radiobursts, with speed of 500 km/s.
- Jn (June): A X2/3B flare followed by a full halo CME of 06/1554 with speed of 908 km/s was responsible for the >10 MeV Proton Event at 07/1335.
- Jl (Bastille Day event): A full halo CME of 14/1054 associated with X5.7/3B flare, with the speed 1775 km/s.
- Au (August): A full halo CME of 9/1630 with speed of 575 km/s as a result of sub-flare activity.
- S (September): There were multiple occurrences of CMEs prior to the geomagnetic event: the first one at 15/1150 with speed of 377 km/s was probably associated with C9.5 flare, the 2nd one at 15/1506 with speed of 467 km/s was probably associated with M2 flare and the 3rd

one at 15/2150 with speed of 370 km/s may be associated with C7 flare. There was also a full halo CME at 16/0526 with speed of 692 km/s.

- N1 (November): The LDE M7/3F, beginning at 08/2306, was responsible for the proton event which began on Nov 8 and peaked on Nov 9. This solar radiation storm was the fourth largest since 1976.
- N2 (November): The X2/3B flare beginning on 24/0455 was responsible for the proton event of November 24.

Interplanetary conditions

The interplanetary magnetic field (IMF) components in geocentric solar-magnetospheric coordinate system (GSM) obtained from the ACE satellite data are presented in Figure 3.3.
The largest negative values of the Bz component of IMF (<-20 nT) were recorded in April, May, July, August and September. Two other IMF components also peak at that time showing that there are the increases in total IMF amplitude during these events. These disturbances in IMF are numbered 1-5, as many of them do not coincide with the solar proton events.

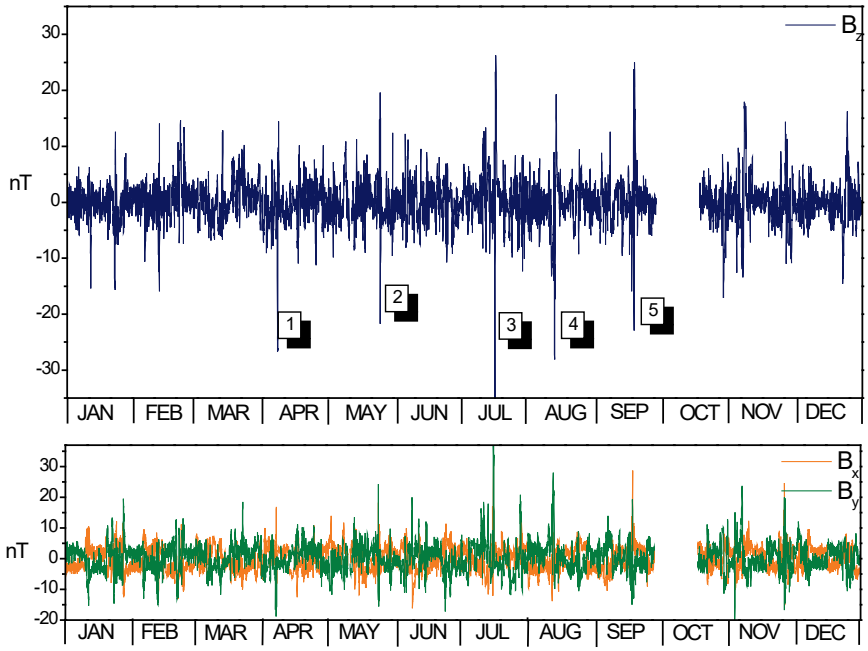

Figure 3.3. Hourly average of the interplanetary magnetic field components in GSM coordinate system at ACE satellite. http://www.srl.caltech.edu/ACE/ASC/

Note, that the June maximum in protons was not accompanied by significant negative IMF Bz nor by appreciable ground geomagnetic activity. Two large proton events in November also are not associated with any of 5 largest IMF events, although the associated spikes can be seen in IMF, and these produce only medium increase in global geomagnetic indices.

Satellite environment and satellite anomalies

The energetic electron daily fluences, together with high energy protons (as possible source of satellite anomalies and also electron detector contamination) are plotted in Figure 3.4 together with time of satellite anomalies (failures). These anomalies occurred at different satellites on different orbits, and are presented here for the possible identification of the anomaly source.

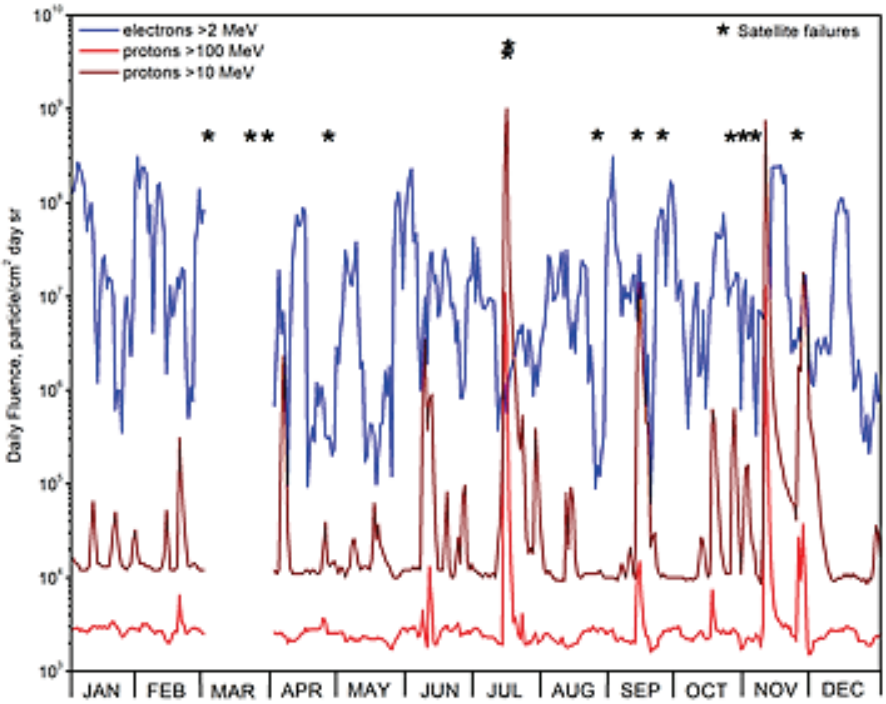

Figure 3.4. Daily fluences of electrons with energies >2 MeV, and protons with energies > 10 MeV and >100 MeV (GOES satellite data). Stars indicate satellite anomalies, extracted in 2001from http://www.sat-nd.com/failures/

As can be seen from Figure 3.4, most of these anomalies do not coincide with the increase in electron fluence, while several of them are associated with the peaks in solar proton fluences.

Global Geomagnetic Activity

Variations of the global indices Kp (ap), Dst and the polar cap index for Thule (PC-North) are presented in Figure 3.5.

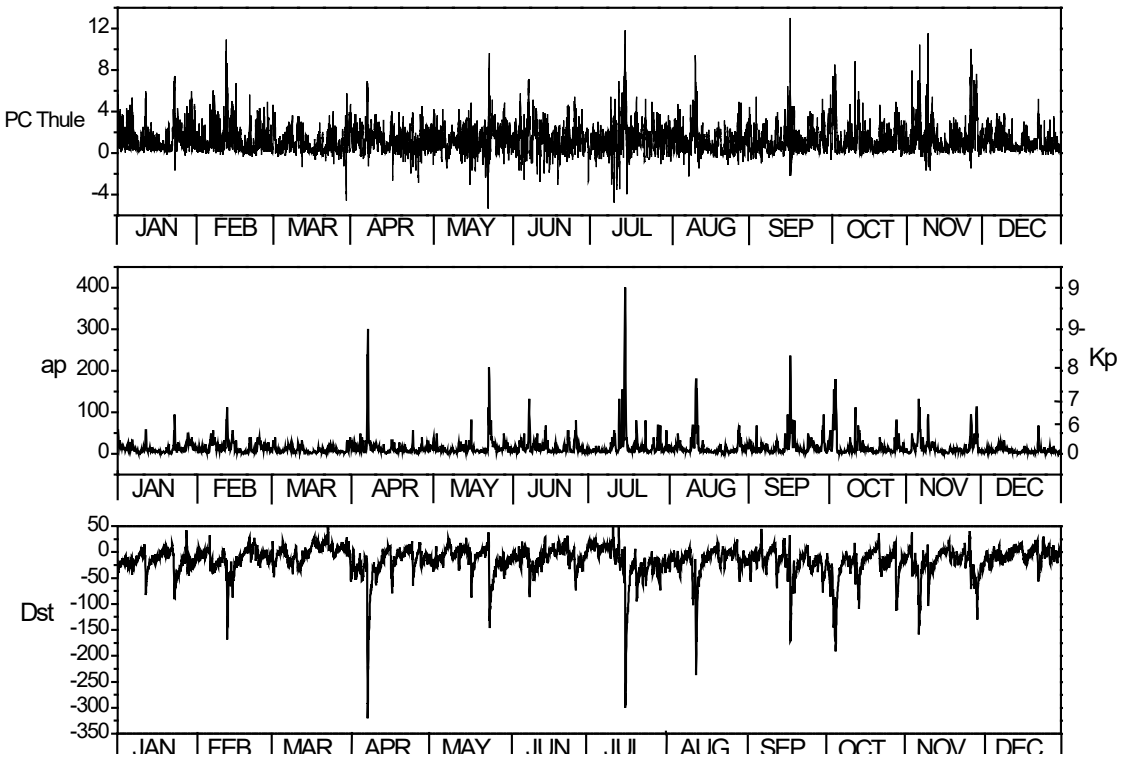

Figure 3.5. Geomagnetic indices for the year 2000 http://isgi.unistra.fr/data_download.php .
Top: 15-min PC index at Thule;
Middle: 3-hour ap and Kp indices;
Bottom: 1-hourly Dst (nT).

During the year 2000 there were two global disturbances with Kp=9- (April) and Kp=9 (July) and a few more with Kp > 7 (May, August, September and October). For the Dst index the April storm was the largest (Dst=-321 nT), July follows with Dst=-295 nT. Next on the Dst amplitude scale are August (-237 nT), February, September and October. High values of the Thule PC index occurred in July, September, May, February and November.

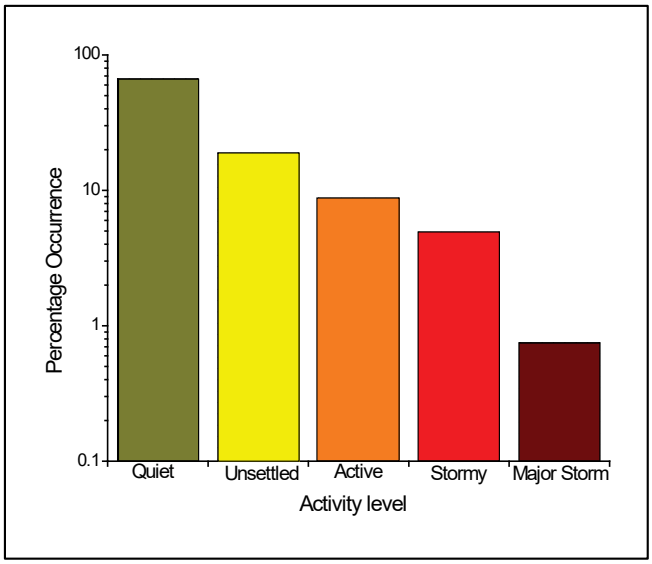

Figure 3.6. Statistics of the global geomagnetic activity, based on ap index.

ap < 15

15<ap<27

27<ap<48

48<ap<140

140<ap

Statistics of different activity levels for the year 2000, as is presented in Figure 3.6, shows the levels defined as: quiet (ap<15), unsettled (15<ap < 27, active (27<ap< 48), stormy (48<ap<140) and major storm (ap>140). As can be seen, only 0.8 % of ap index values were at the level of major storm.

Geomagnetic Activity in Canada

The hourly ranges at three Canadian magnetic observatories https://spaceweather.gc.ca/data-donnee/indices/si-en.php , Resolute (RES, GML =83.1°), Poste-de-la-Baleine (PBQ, 66.8°) and Ottawa (OTT, 57.0°) which represent geomagnetic activity in the polar cap, auroral and subauroral regions in Canada, are presented in Figures 3.7-3.9.

Hourly ranges at the magnetic observatories in Canada show that the largest disturbance in all zones was in July, but the relative size of disturbances during other events depends on the local conditions. Disturbances in RES mostly occurred in summer time, with the largest in July and next in size in May and September, due to the seasonal variations in ionospheric conductivity. At auroral latitudes, (PBQ), the disturbances were more evenly distributed throughout the year and have large amplitude (the largest in July, next in February and November). At subauroral latitudes (OTT) there were fewer disturbances which stand out more clearly against the background activity level. The major disturbances coincided with the major events seen in the ACE data.

Small diagrams on the top of each plot show the percentage occurrence of hourly ranges at different geomagnetic activity levels.

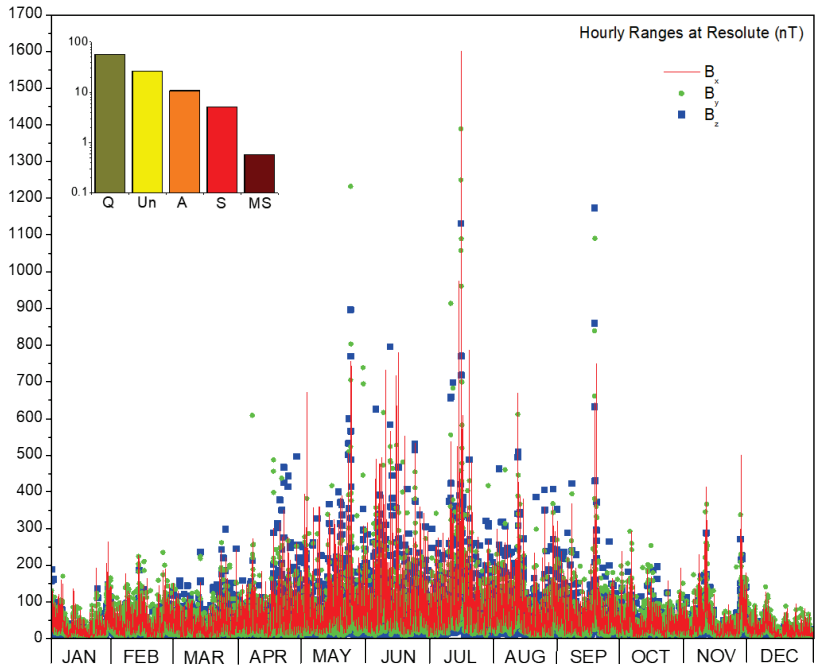

Figure 3.7. Hourly ranges of the magnetic field components at Resolute.
Q <50 nT, 50<**Un** <100 nT, 100<**A**<175 nT, 175>**S**>450 nT, **MS**>450 nT

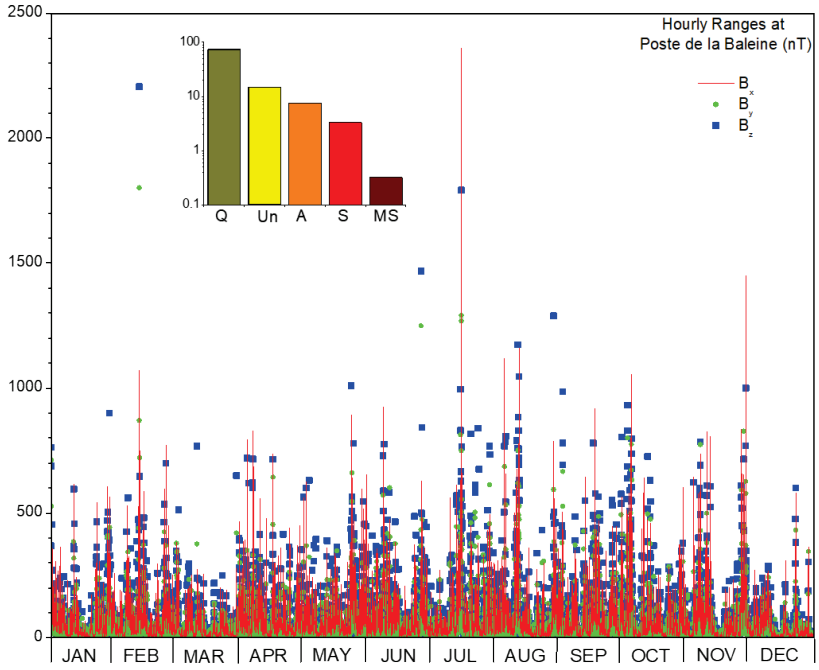

Figure 3.8. Hourly ranges of the magnetic field components at Poste-de-la-Baleine.
Q <90 nT, 90<**Un** <180 nT, 180<**A**<315 nT, 315>**S**>700 nT, **MS**>450 nT

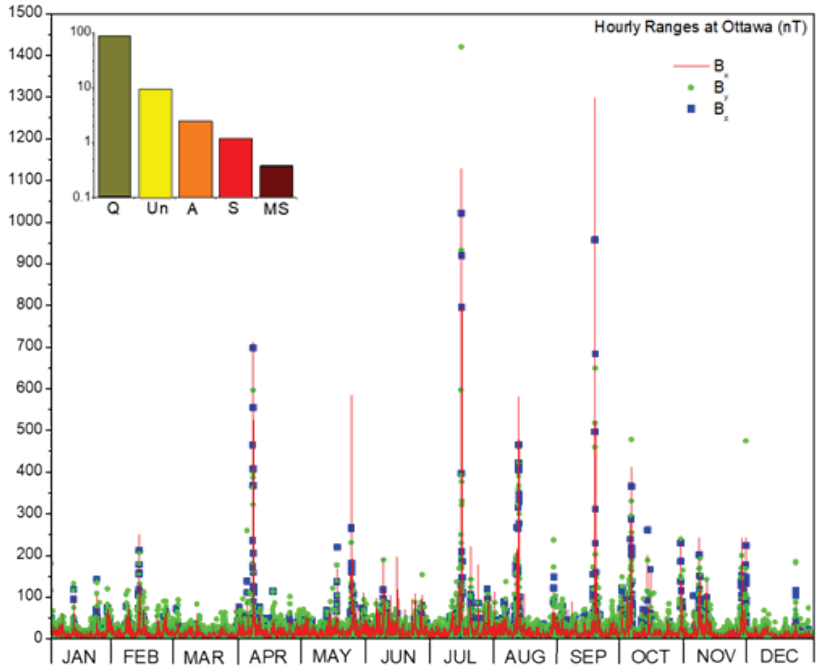

Figure 3.9. Hourly ranges of the magnetic field components at Ottawa. **Q** <30 nT, 30<**Un** <60 nT, 60<**A**<105 nT, 105>**S**>300 nT, **MS**>300 nT

Details of the largest space weather events

All five identified space weather events produce significant variations in the solar wind (IMF) and at the geostationary orbit, as presented in Figures 3.10-3.14.

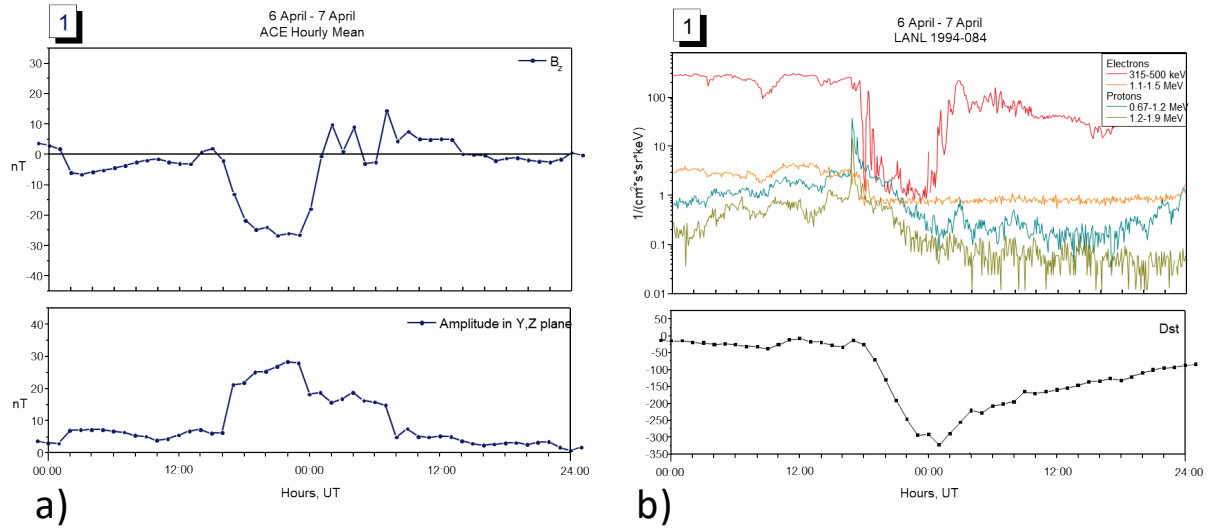

Figure 3.10. Event 6-7 April: a) top panel-hourly IMF Bz, bottom panel-hourly IMF amplitude in YZ plane; b) top panel- electrons and protons at geostationary orbit (LANL satellite), bottom panel – hourly Dst index.

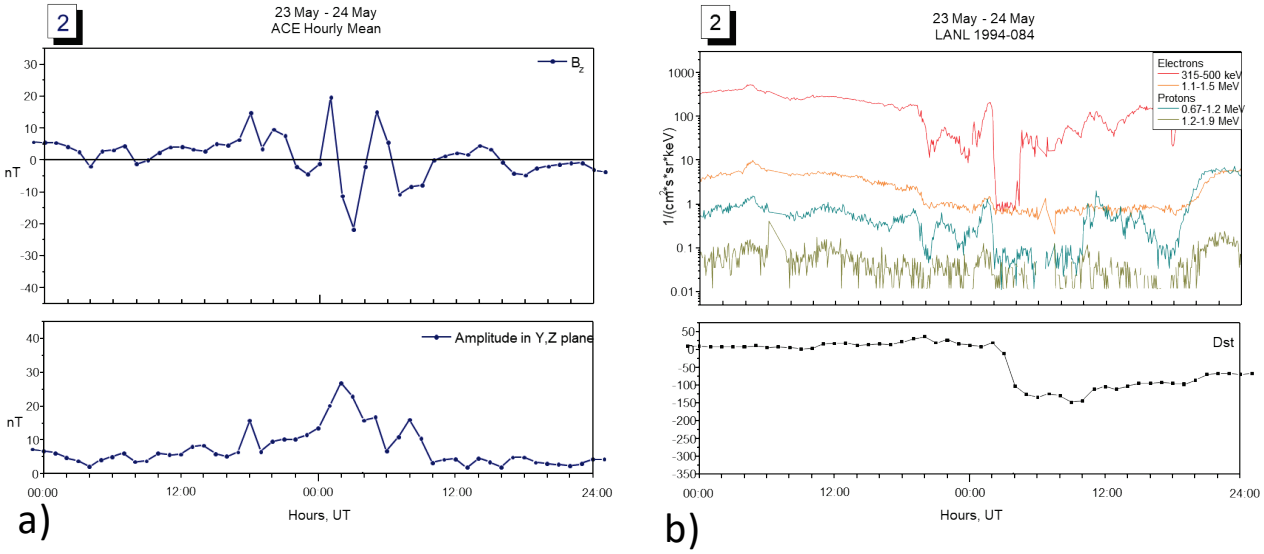

Figure 3.11. Event 23-24 May: a) top panel-hourly IMF Bz, bottom panel-hourly IMF amplitude in YZ plane; b) top panel- electrons and protons at geostationary orbit (LANL satellite), bottom panel – hourly Dst index.

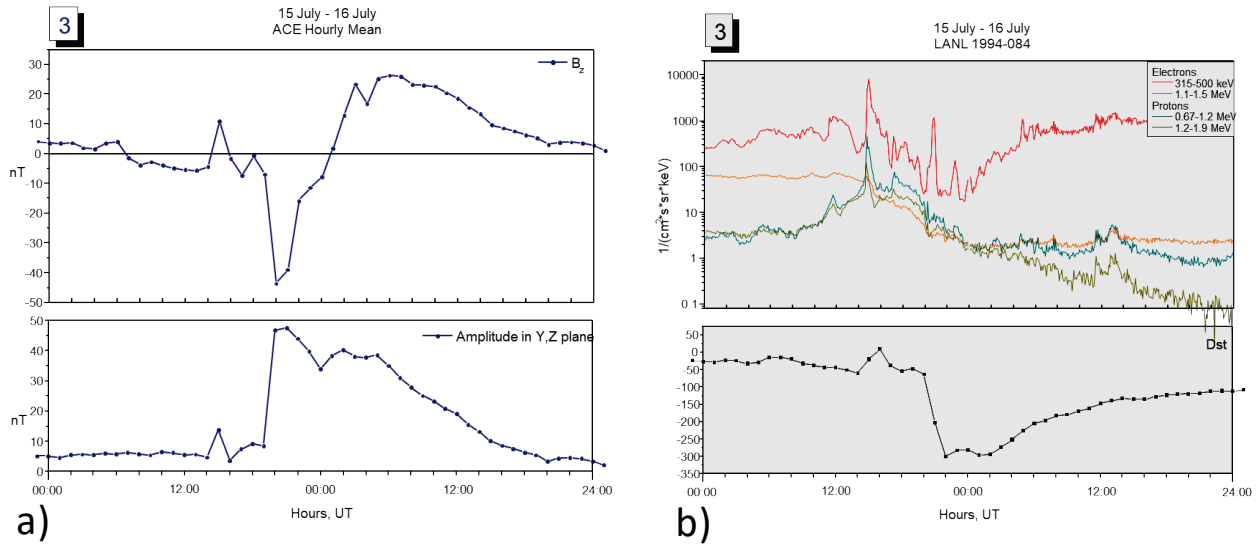

Figure 3.12. Event 15-16 July: a) top panel-hourly IMF Bz, bottom panel-hourly IMF amplitude in YZ plane; b) top panel- electrons and protons at geostationary orbit (LANL satellite), bottom panel – hourly Dst index.

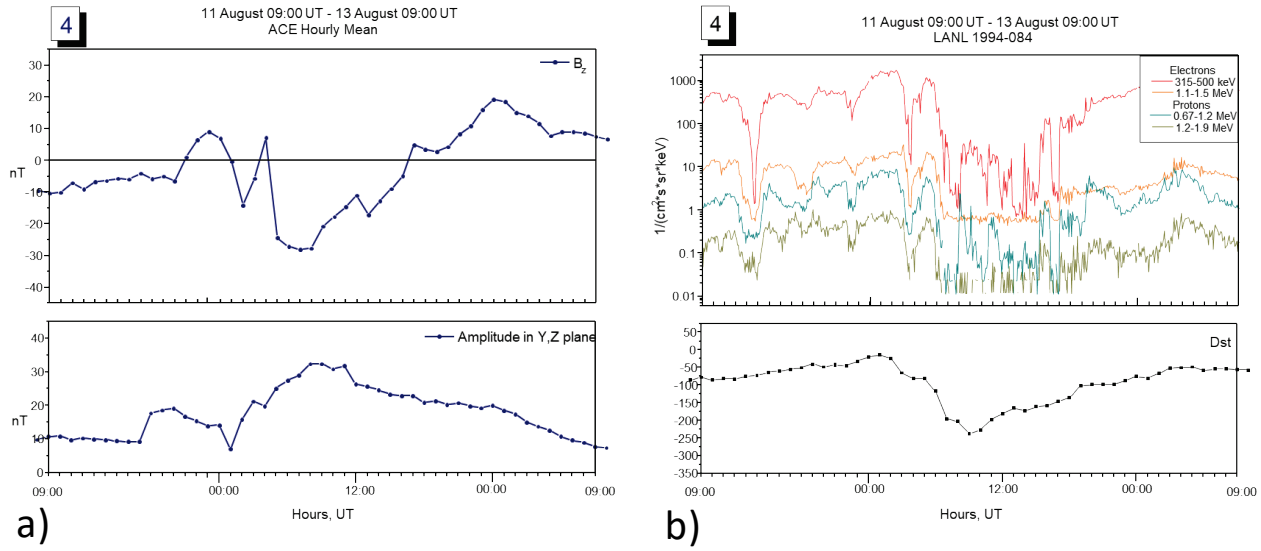

Figure 3.13. Event 11-13 August: a) top panel-hourly IMF Bz, bottom panel-hourly IMF amplitude in YZ plane; b) top panel- electrons and protons at geostationary orbit (LANL satellite), bottom panel – hourly Dst index.

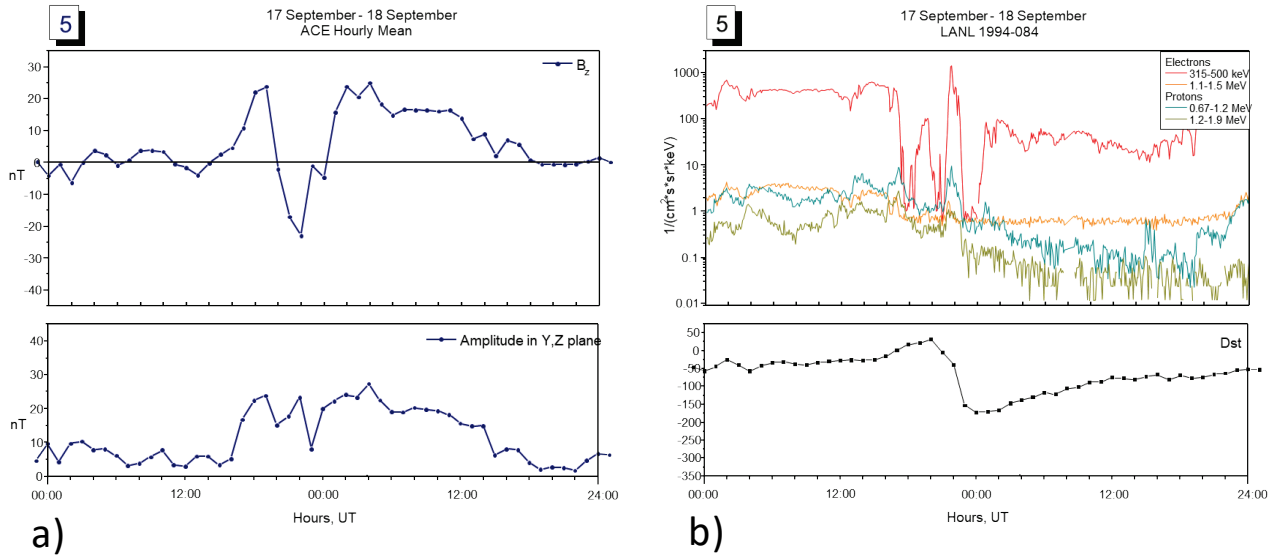

Figure 3.14. Event 17-18 September: a) top panel-hourly IMF Bz, bottom panel-hourly IMF amplitude in YZ plane; b) top panel- electrons and protons at geostationary orbit (LANL satellite), bottom panel – hourly Dst index.

As can be inferred from the comparisons of different plots presented in Fig.3.10-3.14, variations of electrons with energies 315-500 keV better correspond to the variations of IMF Bz, while variations of protons with energies 0.67-1.2MeV better correspond to the variations of Dst index.

Geomagnetically Induced Currents

All five space weather events examined here produced significant geomagnetically induced currents in ground technological systems in Canada. The examples of geomagnetically induced currents in the Ontario and Nova Scotia power systems and potential variations on the Maritimes pipelines recorded during the April 6-7 (Event 1), July 15 (Event 3) and September 17 - 18 (Event 5) are presented in Figures 3.15-3.16. During the April 6-7 event a magnetic disturbance of approximately 800 nT was accompanied by electric fields up to 800 mV/km. These produced pipe-to-soil potential variations of 500 mV and GIC at Lakehead in Ontario of 10A. On July 15, the disturbance reached 1500 nT producing GIC up to 100 A at substations in Nova Scotia. On September 17-18 the magnetic disturbance again reached nearly 1500 nT and produced GIC of 60 A in Nova Scotia.

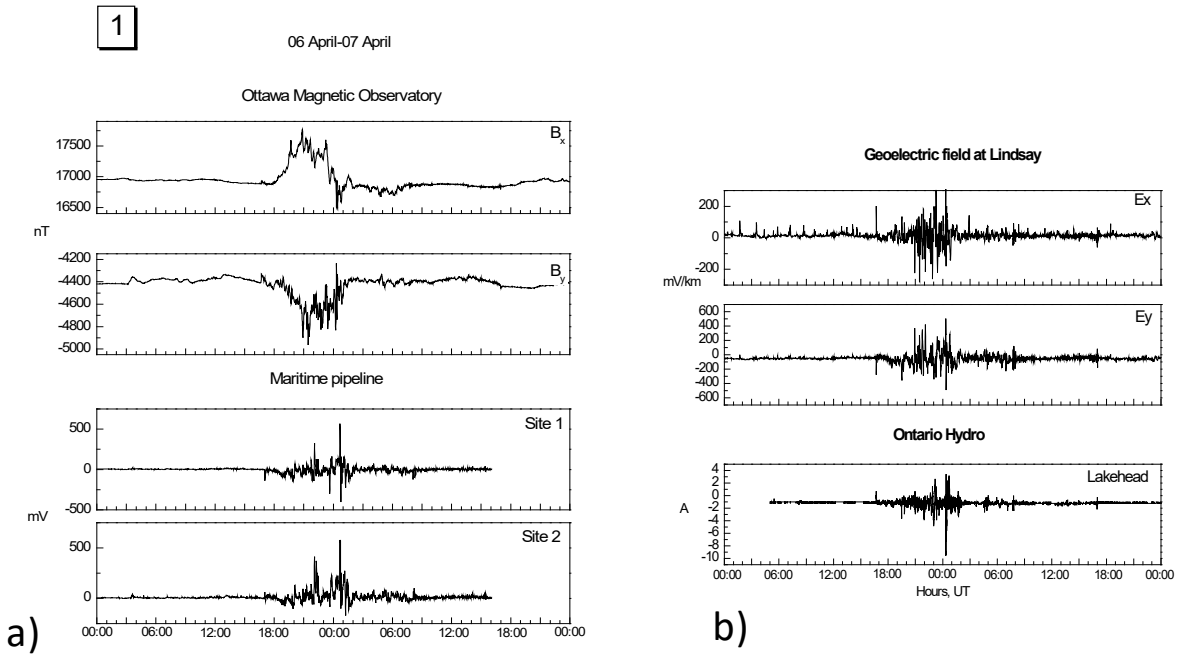

Figure 3.15. Ground effects of magnetic disturbances on 6-7 April.

a) Magnetic field variations (OTT) and pipe- to-soil voltage on the Maritimes Pipeline.

b) Geoelectric field variations measured at Lindsay and GIC in the Ontario power system.

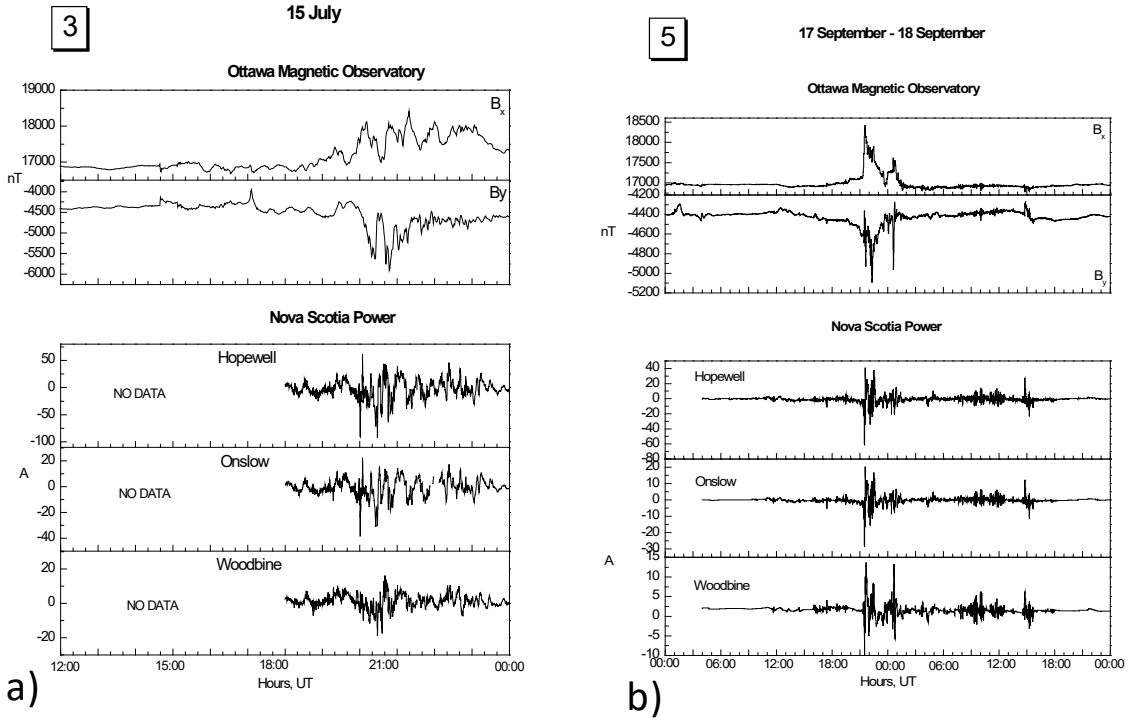

Figure 3.16. Ground effects of magnetic disturbances (magnetic variations and GIC)

a) July 15.

b) September 17-18.

Forecast

The NRCan/RWC Canada short term forecasts for the next six-hours are produced by an automated expert system, using a number of solar, solar wind, and geomagnetic data inputs. The forecasts are also evaluated automatically on a weekly basis using several techniques. The public forecasts, available via the Web, are presented in the form of words; however, the forecast process actually generates quantitative forecasts, in the form of hourly ranges in nT. The diagrams (Figure 3.17) show examples of one simple (historical) form of evaluation.

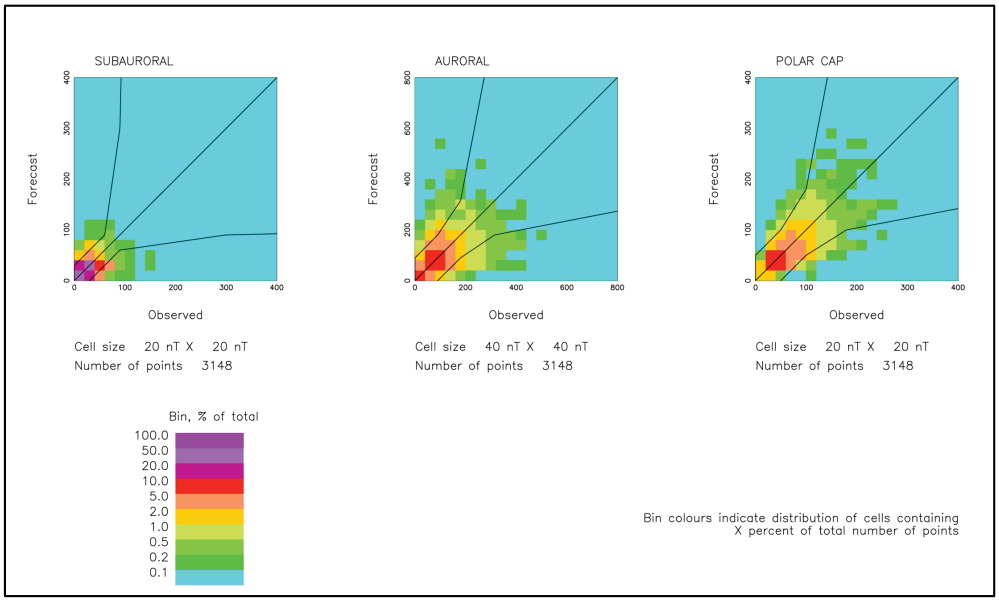

Figure 3.17. "Next 6 - hour" forecast evaluation for days 1- 200 of the year 2000. Bin colours indicate distribution of cells containing X percent of total number of points.

In this presentation, the quantitative forecast values are compared with the corresponding observed values. All forecast/observed pairs that fall within a particular bin are counted and the total is expressed as a percentage of the total number of pairs. The goal of a forecaster (machine or human) is to have only the bins along the diagonal of the diagram coloured as non-zero. The examples shown are for the first half of year 2000.

References

L. Trichtchenko, R. Coles, D. H. Boteler, H.-L. Lam, Geomagnetic Activity 2000: The Northern Perspective, poster presented at the Space Weather Week in Boulder, April, 2001.

PART 4

Review of space weather in year 2001

Summary

An overview of solar events, solar wind disturbances and geomagnetic activity for year 2001 is presented with an emphasis on ground geomagnetic and technological effects across Canada. Four major interplanetary disturbances with high geo-effectiveness were identified, such as on March 31, April 11, November 6 and November 24, all most probably due to halo CME events. The global geomagnetic response to these events is seen at high latitudes in the PC index, at mid latitudes in the ap and Kp indices and at low latitudes in the Dst index. Geomagnetic activity in Canada was high during these events, as shown by the hourly ranges of the magnetic field variations in three zones (polar, auroral, subauroral). The relative sizes of the disturbances in the different zones vary from event to event depending on the position of the auroral electrojets. Geomagnetically induced currents, experienced by power systems in subauroral (Canada, USA) and low latitude (Vietnam) zones, correlated well with the local geomagnetic activity.

Solar activity

Daily sunspot number and 10.7 flux density variations show the general solar activity during the year (Figure 4.1). Significant increase in both characteristics at the second half of March-April produced the increase of the geomagnetic activity at that period. Increases in SSN and 10.7 flux in June and September had only moderate effect on the ground.

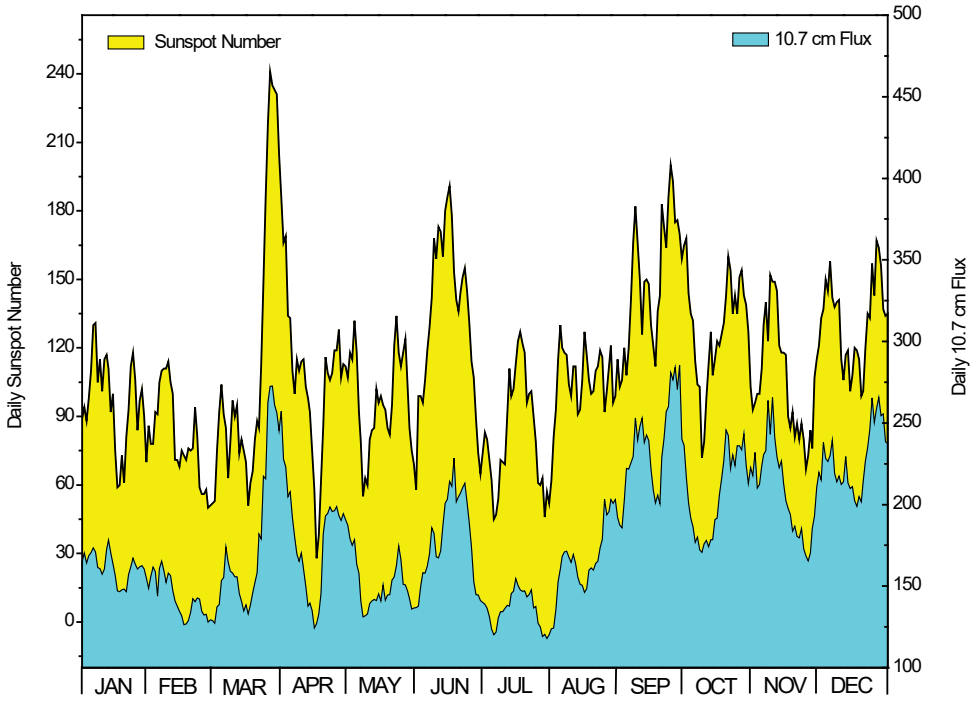

Figure 4.1. Daily sunspot number ftp://ftp.ngdc.noaa.gov/STP/space-weather/solar-data/solar-indices/sunspot-numbers/ and 10.7 adjusted solar flux density https://spaceweather.gc.ca/solarflux/sx-en.php in units 10^{-22} Joules/s/m^2/Hz

Solar Proton Events

Variations in daily fluences of high energy protons (>10 MeV and >100MeV) at GOES satellite are presented together with the daily electron fluxes in Figure 4.2.

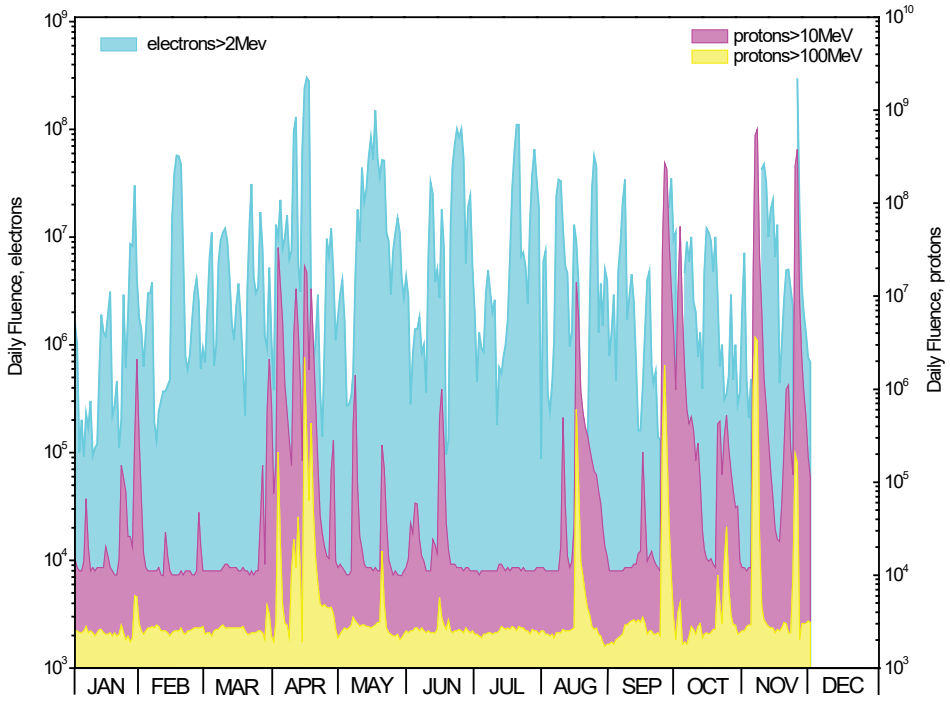

Figure 4.2. Daily fluences of electrons >2MeV (blue), protons > 10 MeV (pink) and >100 MeV (yellow) (ftp://ftp.ngdc.noaa.gov/STP/SOLAR_DATA/SATELLITE_ENVIRONMENT/).

The most significant solar proton events, as per ftp://ftp.ngdc.noaa.gov/STP/swpc_products/weekly_reports/PRFs_of_SGD/ :

1. The end of March until the end of April period, which produced multiple peaks in proton fluences with the highest being on
   - April 3: (CME (W) and flare of X20 with Type II radiobursts),
   - April 11 (a full halo CME of 10/0850 POS speed 1678, associated with X2/3B flare and Type II, Type IV radiobursts),
   - April 15 (CME on 15/1350 associated with X14/2B flare, Type II and Type IV radiobursts).
2. September 24-25:A full halo CME of 24/1030 with plane of sky (POS) speed of 2200 km/s associated with X2.6/2B flare, caused proton event peaking at 25/2235.
3. November 4-6: A full halo CME on 04/1620 with POS speed of 1620 km/s associated with X1/3B flare, accompanied by Type II and Type IV radiobursts caused this proton event with maximum at 06/0215.
4. November 22-24: Two flares (M3.8/2B and M9.9/2N) accompanied by two Type II radiobursts followed by two halo CMEs, of 22/2055 with POS speed 1246 km/s and of 22/2330 with POS speed of 1500 km/s were responsible for two IP shocks and the proton event at 24/0555.

Interplanetary conditions

Figure 4.3 shows the interplanetary magnetic field (IMF) components in geocentric solar-magnetospheric coordinate system (GSM) obtained from the ACE satellite data.
The largest negative Bz component (<-20 nT) occurred in March 31, April 11, November 6 and November 24. The variance of the magnetic field also peaks at that time showing that there are increases in total IMF amplitude during these events. The maximum negative Bz was on 6 November and equals –69.6 nT, the second largest was on 31 March (-41 nT). Note, that September maximum in protons was not accompanied by significant negative IMF Bz.

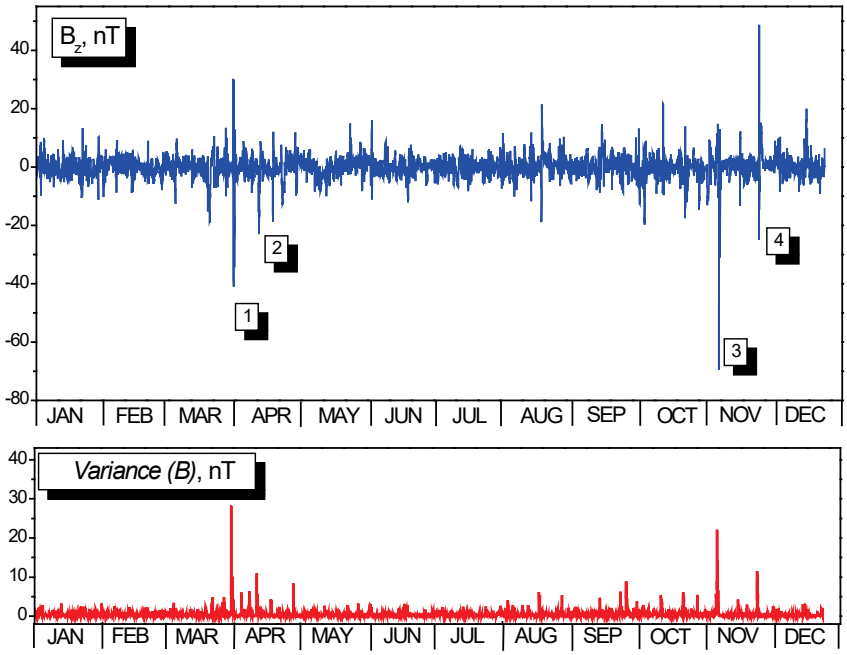

Figure 4.3. Hourly average of Bz magnetic field component and variance of total IMF at ACE satellite http://www.srl.caltech.edu/ACE/ASC/ . The largest Bz are numbered 1-4 and are further investigated.

Global Geomagnetic Activity

Variations of the global indices Kp (ap), Dst and the polar cap index for Thule (PC-North) are presented in Figure 4.4.

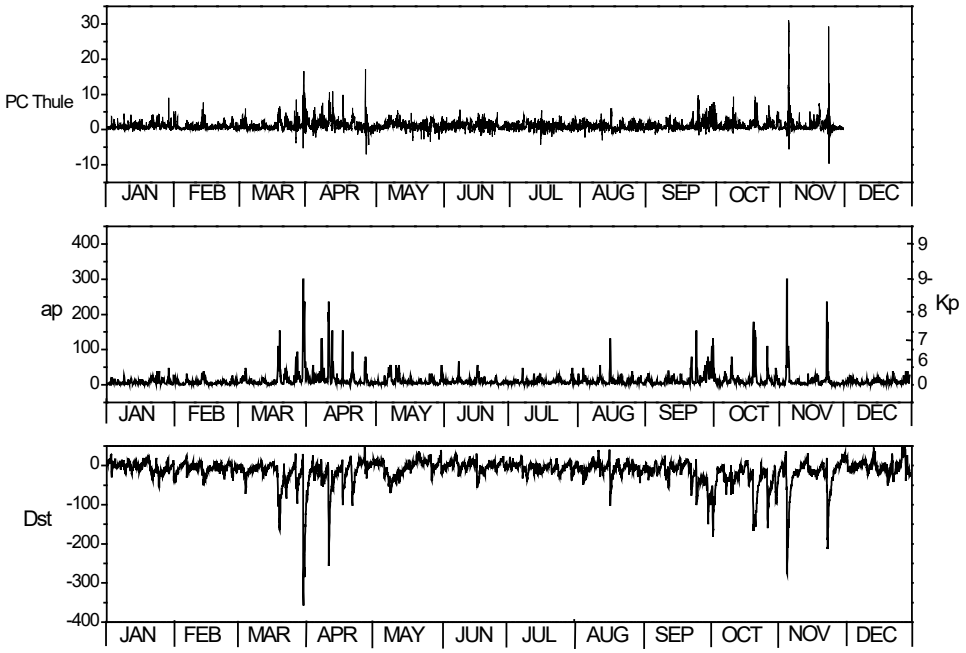

Figure 4.4. Geomagnetic indices for the year 2001. Top to bottom:Top-15-min PC index at Thule, Middle-3-hour ap (left scale) and Kp (right scale) indices and Bottom-Dst index. http://isgi.unistra.fr/data_download.php

During the year 2001 there were

- two global disturbances with Kp=9- , on 31 March and 6 November,
- one with Kp=8+ (24 November),
- one with Kp=8 (11 April),
- one with Kp=8- (21 October),
- and a few more with Kp ~ 7 (March, April, September).

For the Dst index

- March 31 storm was the largest (Dst=-358 nT),
- November 6 follows with Dst=-277 nT.
- Next on the Dst amplitude scale are April 11 storm (-256 nT) and November 24 (Dst=-213 nT).

High values of the Thule PC index occurred on 6 November, 24 November, 28 April and 31 March. Based on global geomagnetic and solar wind events, 4 periods with high activity (31 March, 11-12 April, 5-6 November, 23-24 November) were chosen for more close investigations of their ground effects.

Geomagnetic Activity in Canada

Figures 4.5-4.7show the hourly ranges of the magnetic field components at three Canadian magnetic observatories, Resolute (RES, GML =83.1°), Poste-de-la-Baleine (PBQ, 66.8°) and Ottawa (OTT, 57.0°) which represent geomagnetic activity in the polar cap, auroral and subauroral regions in Canada. https://spaceweather.gc.ca/data-donnee/indices/si-en.php

Hourly ranges at these magnetic observatories in Canada show that the largest disturbance in polar cap and subauroral zones was on 24 November, but the relative size of disturbances during other events depends on the local conditions. The largest disturbance in the auroral zone (PBQ, Y-component) was the September event, which can also be clearly seen in RES (polar zone) Y-component, where it is third largest.

November 6 event was significant in all three zones. In the polar and auroral regions the April 11-12 storm was larger than the one on March 31. In the sub-auroral region the larger event was on March 31.

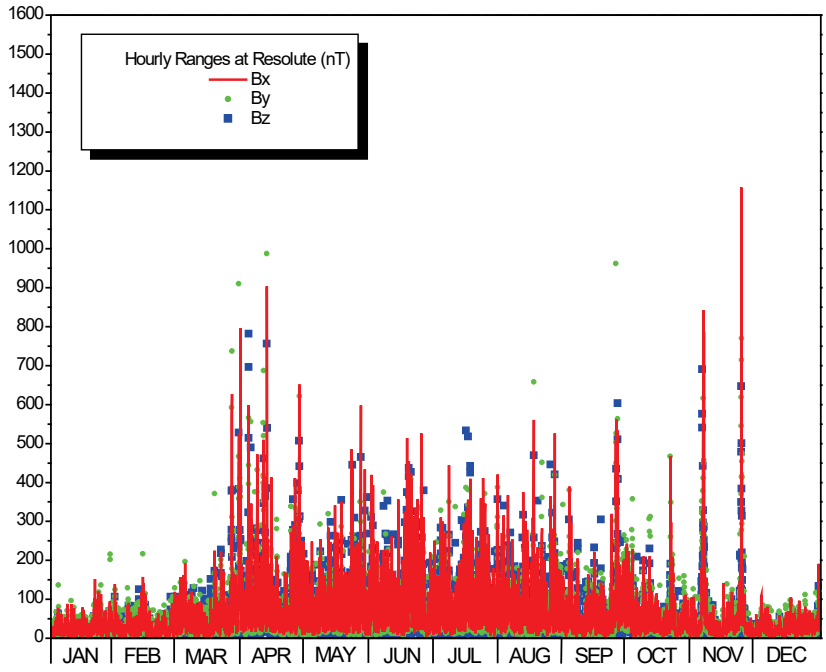

Figure 4.5. Hourly ranges of the magnetic field components at Resolute.

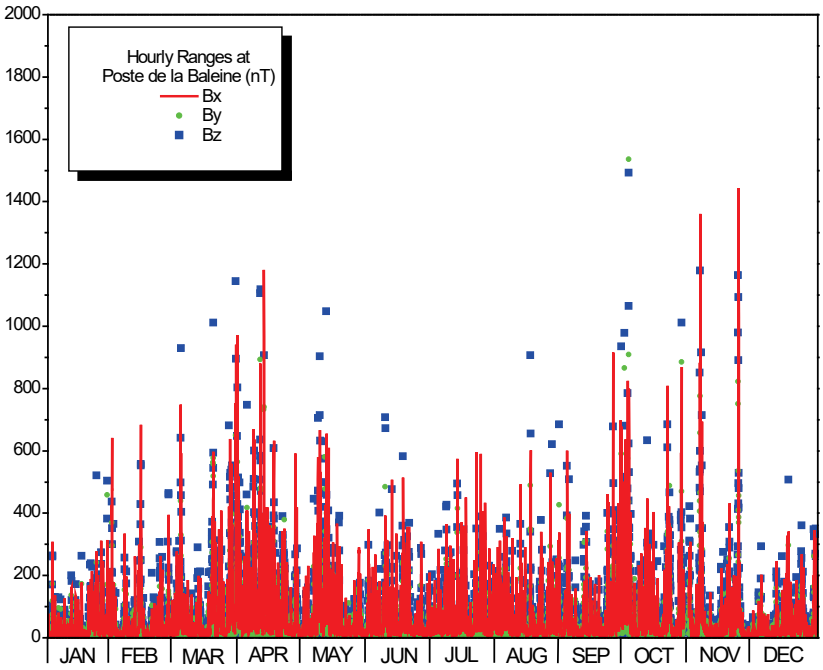

Figure 4.6. Hourly ranges of the magnetic field components at Poste-de-la-Baleine.

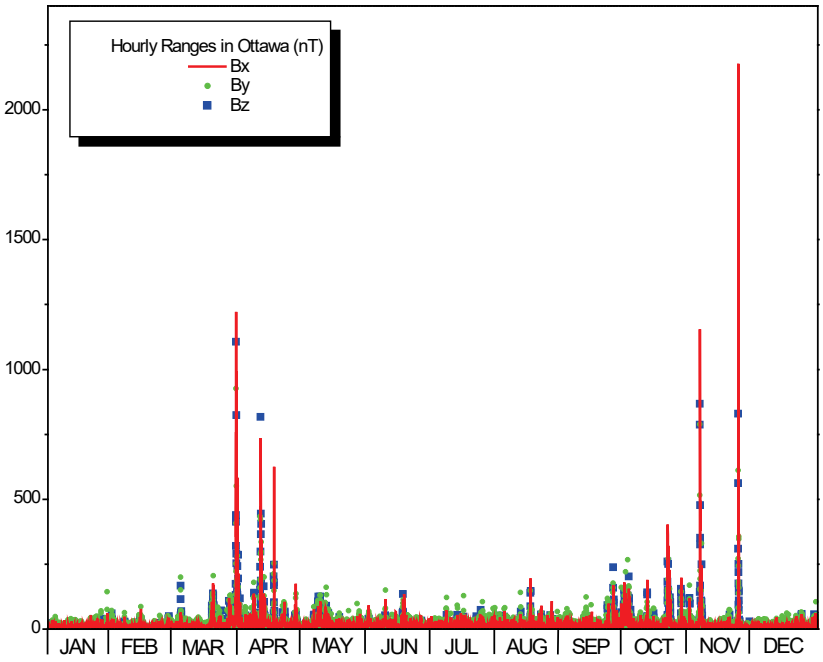

Figure 4.7. Hourly ranges of the magnetic field components at Ottawa.

Details of the largest space weather events and GIC

All four space weather events identified above produced significant geomagnetically induced currents in ground technological systems over the globe, presented in Figures 4.8 and 4.9.

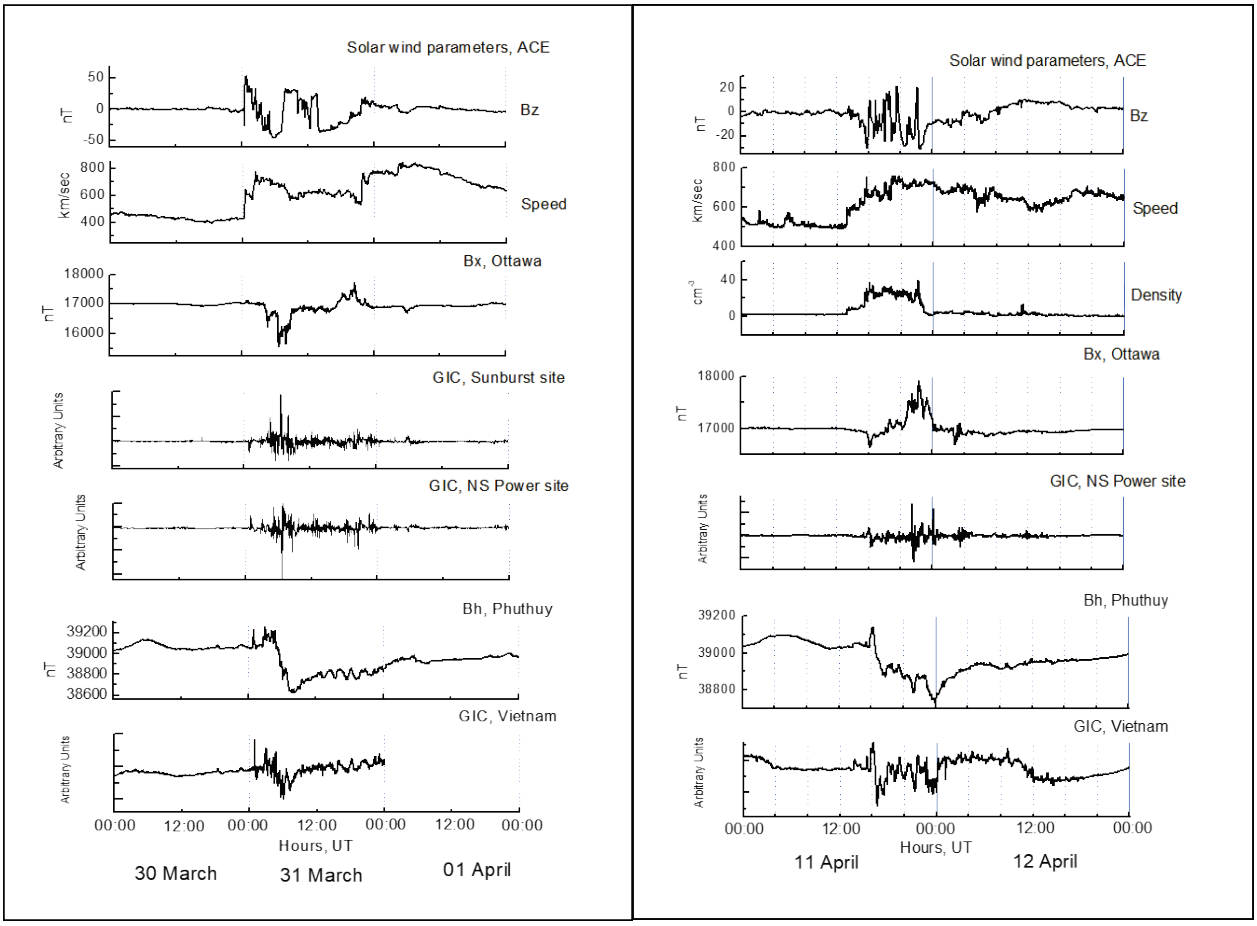

Figure 4.8. Ground effects of space weather events. Presented for each event are solar wind parameters, geomagnetic variations and geomagnetically induced currents in different locations over the globe.

a) March 30-April 1

b) April 11-12

All four space weather events examined here produced significant geomagnetically induced currents in ground technological systems in the subauroral zone (North America) and at low latitudes (Vietnam). Solar wind plasma discontinuities, seen on ACE and WIND as sharp changes in solar wind speed and plasma density, interact with the magnetosphere producing sudden impulses (SI) in geomagnetic field and bursts of GIC. The relative size of these features, seen clearly during events 1 and 3 (less in the other two) is different at different latitudes (larger in low latitudes). The southward turning of IMF coincided with the further development of substorms and GIC activity in all 4 events

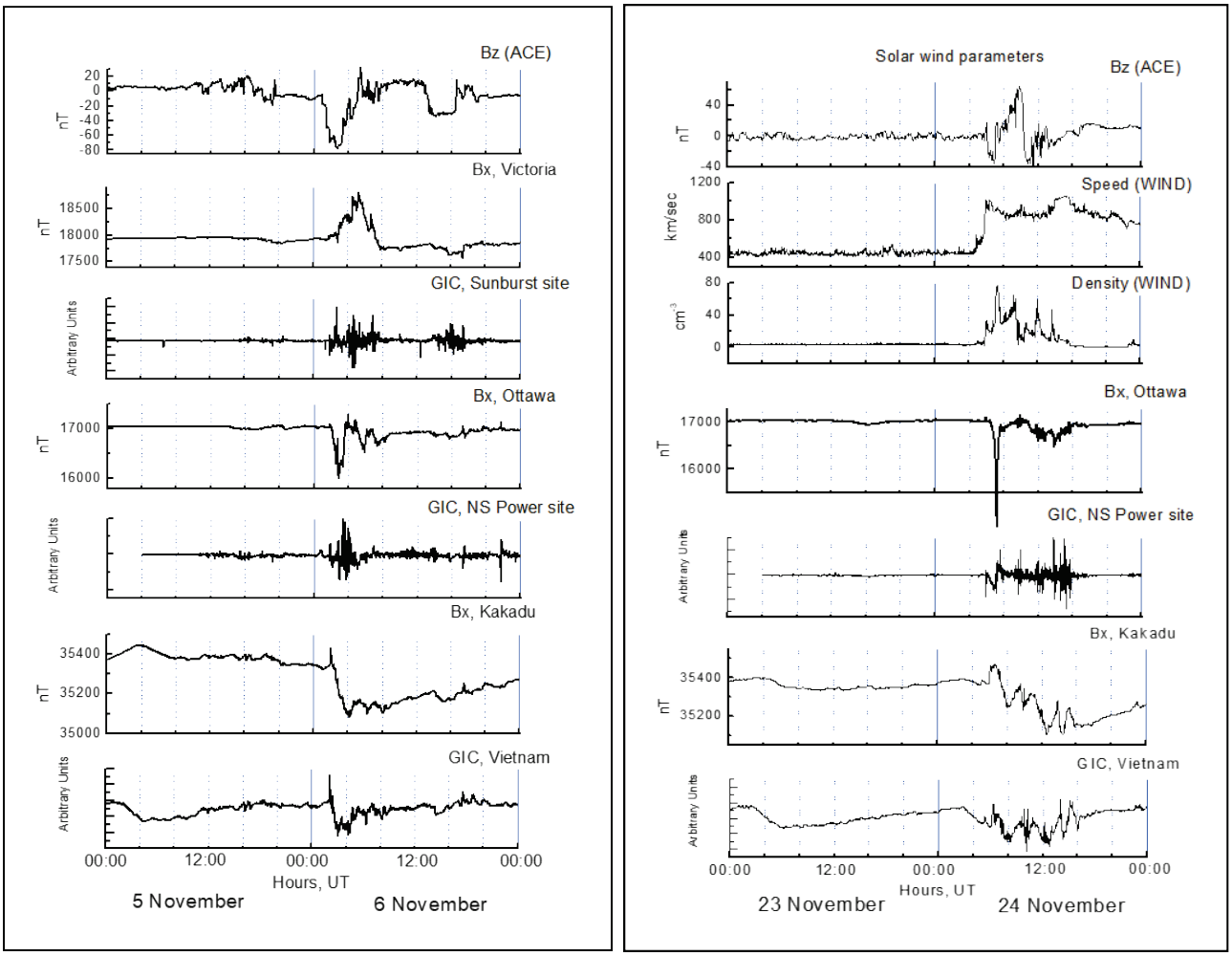

Figure 4.9. Ground effects of space weather events. Presented for each event are solar wind parameters, geomagnetic variations and geomagnetically induced currents in different locations over the globe.

a) November 5-6

b) November 24-25

References

L. Trichtchenko, Geomagnetic Activity and GIC in Year 2001, poster presented at the Space Weather Week in Boulder, April 2002.

PART 5

Review of space weather in year 2002

Summary

Part 5 presents an overview of solar events, solar wind disturbances and geomagnetic activity for year 2002 with an emphasis on ground geomagnetic and technological effects across Canada. This year started the declining phase of the solar cycle 23. The most pronounced solar event with high geo-effectiveness was identified on May 22-23 (Kp=8+), initiated by a full halo CME. Some of other periods of strong geomagnetic activity (Kp=7+) were associated with halo CMEs and flare activity (April 17-20, September 7-8) or becoming of more mixed origin (October 1-4) or related to coronal holes (November 21, Kp=7-). The relative sizes of the geomagnetic disturbances in three Canadian zones (polar, auroral, subauroral) vary from event to event as shown by hourly ranges of geomagnetic field at different observatories across Canada. Geomagnetically induced currents, experienced by power systems in the subauroral zone are shown to correlate better with the local geomagnetic activity.

Solar activity

Daily sunspot number and 10.7 flux density variations, presented in Figure 5.1, show the general solar activity during the year.

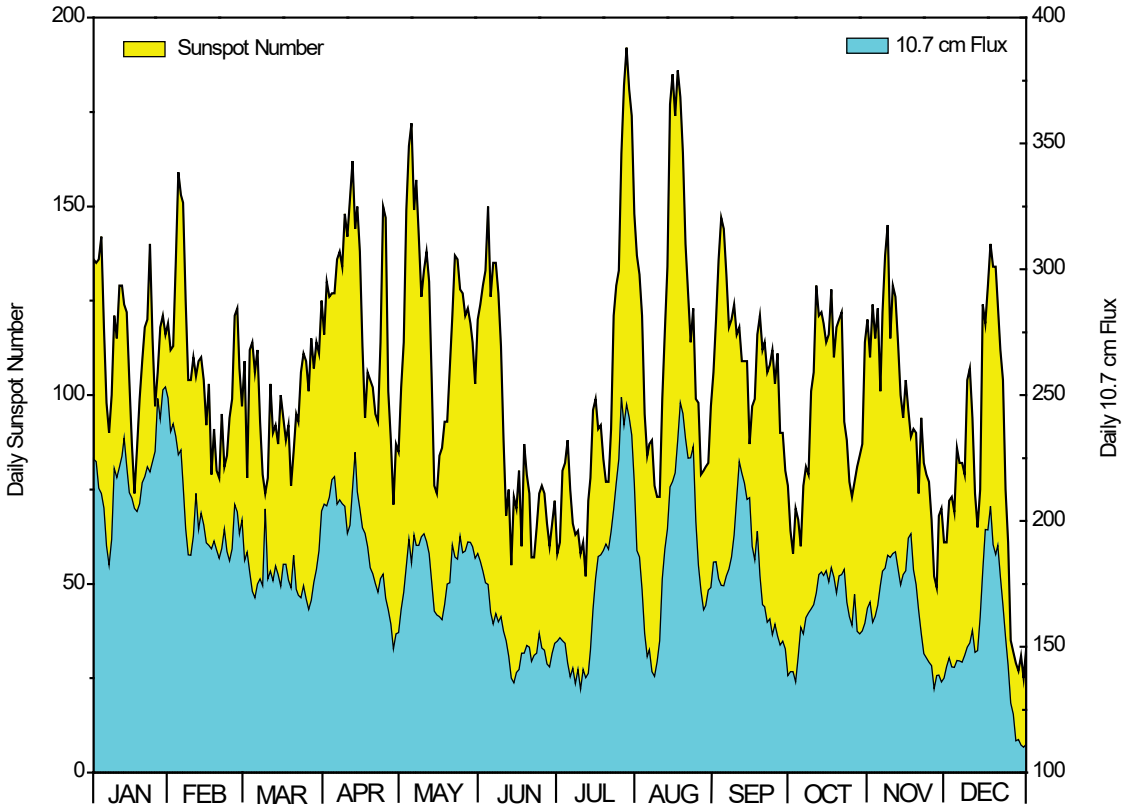

Figure 5.1. Daily sunspot number ftp://ftp.ngdc.noaa.gov/STP/space-weather/solar-data/solar-indices/sunspot-numbers/ and 10.7 adjusted solar flux density https://spaceweather.gc.ca/solarflux/sx-en.php in units 10^{-22} Joules/s/m^2/Hz.

Two distinctive peaks (in July and August) did not produce the important effects on the ground, but coincided with the elevated level of high energy particles at geostationary orbit (Figure 5.2). On the contrary, an increase in both characteristics at the second half of April and May produced the increase of the global geomagnetic activity at that period.

Solar Proton Events

The most significant solar proton events are evaluated based on daily fluences of high energy protons (>10 MeV and >100MeV), presented in Figure 5.2 together with the electron daily fluences at GOES satellite

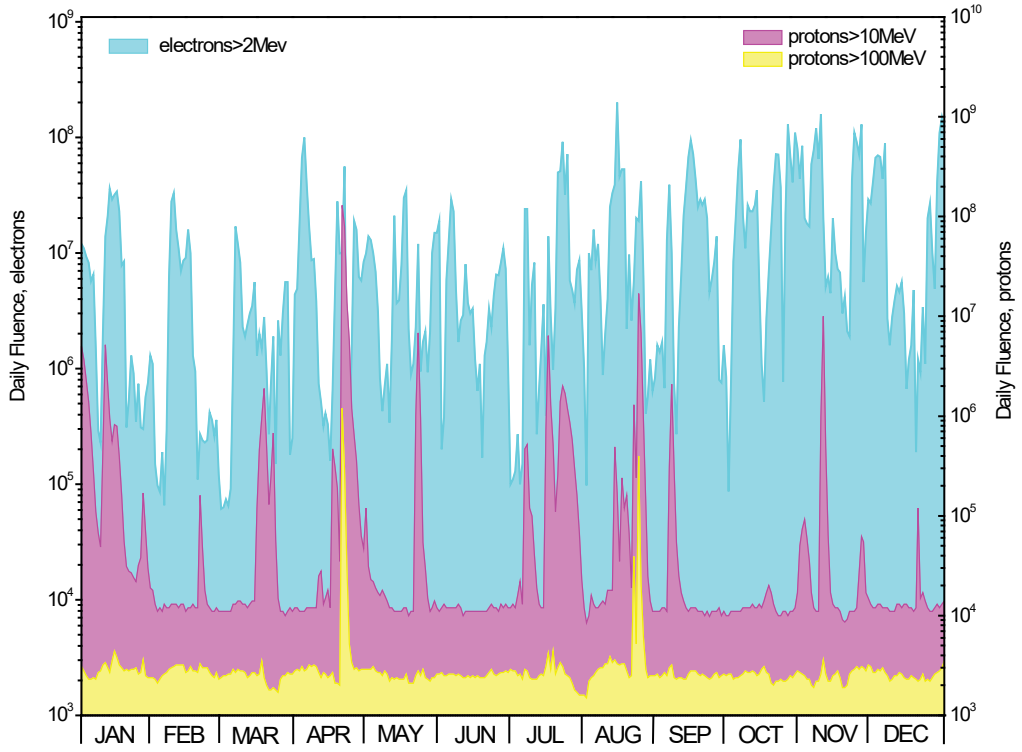

Figure 5.2. Daily fluences of electrons with energies>2MeV (blue), protons > 10 MeV (pink) and >100 MeV (yellow) from GOES satellite data ftp://ftp.ngdc.noaa.gov/STP/SOLAR_DATA/SATELLITE_ENVIRONMENT/ .

The most significant solar proton events during 2002 are https://umbra.nascom.nasa.gov/SEP:

- April: The full halo CME on 17/ 0826, associated with M2/2N flare and accompanied by Type II and Type IV radiobursts, caused proton event peaking at 17/1540. On April 21/ 0151 the full halo CME associated with X1/1F flare produces the largest proton event (21/2320), which affects satellites Nozomi (heliocentric) and Genesis (around L1).
- May: Full halo CME at 22/0326 with POS speed 1496 km/s associated with C5 flare, caused a proton event peaking at 23/1055.
- July: The largest in July was the proton event at 17/1600 produced by full halo CME and X3/3B flare at 15/2008 with Type IV radioburst.
- August : CME on 24/0112, associated with X3/1F flare and Type II, Type IV radiobursts caused proton event at 24/0835.

- September: Long duration C5 flare (max at 05/1706) with full halo CME on 05/1706 produced a proton event peaking at 07/1650.
- November: CME on 09/1331, associated with M4/2B flare and Type II, Type IV radiobursts caused proton event at 10/0540.

Energetic electrons at geostationary orbit

According to Figure 5.2, the >2 MeV relativistic electrons fluence values were high during the following time periods:

- 22 April;
- 22-25 July;
- August 15-18 (possible coronal hole effect);
- 14-16 September;
- November 5-9 (possible coronal hole effect);

Solar Wind conditions

Figure 5.3 shows the interplanetary magnetic field (IMF) southward component (Bz) (top panel); solar wind density and speed (bottom panel) in geocentric solar-magnetospheric coordinate system (GSM) available from ACE data. Significant southward Bz component (<-20 nT, GSM) occurred on (ftp://ftp.ngdc.noaa.gov/STP/swpc_products/weekly_reports/PRFs_of_SGD/)

- April: 17th (Bz min=-28 nT, halo CME effects) and 23rd (-20 nT, partial halo CME effect)
- May: 11th (Bz min=-20nT, coronal hole effects), and the largest negative Bz was on 23 May (-43 nT, speed ~1000km/s, CME effect).
- September: 7th (Bz min=-22nT, halo CME effect) and 30th (Bz min =-24 nT, probably the mixture of effects produced by M1.8 flare activity on 27/1312, partial halo CME on 29/0830 and coronal holes).
- November: 21st (Bz min=-27 nT, speed ~800 km/s, coronal hole effect) and 26th (Bz min=-27 nT, due to partial halo CME on 24th).

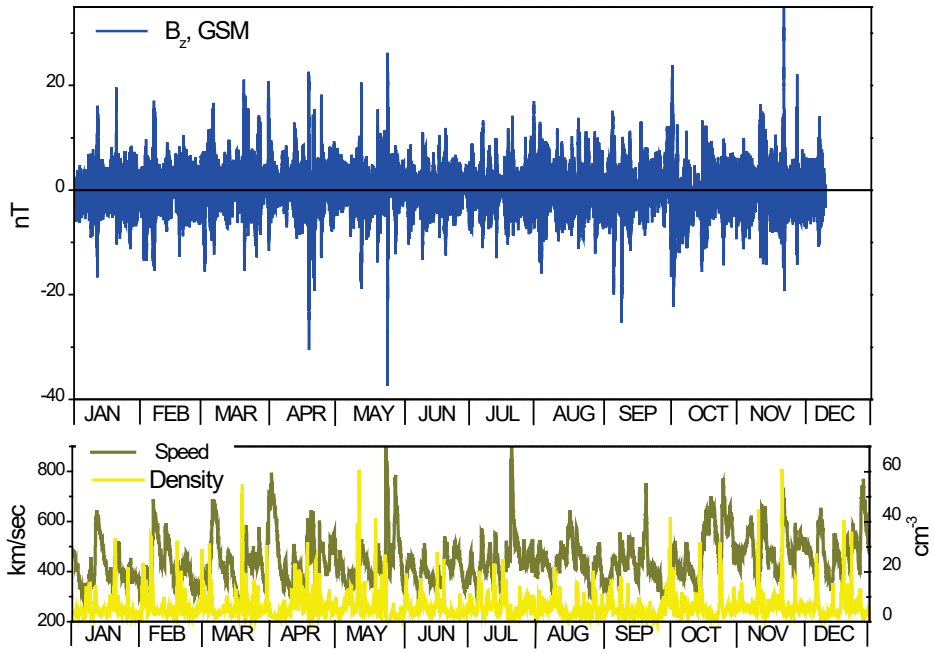

Figure 5.3. Top panel: 4-min. average of IMF Bz and, bottom panel: hourly solar wind speed (dark yellow) and density (yellow) at ACE satellite.

Global Geomagnetic Activity

Variations of the global indices Kp (ap), Dst and the polar cap index for Thule (PC-North) are presented in Figure 5.4.

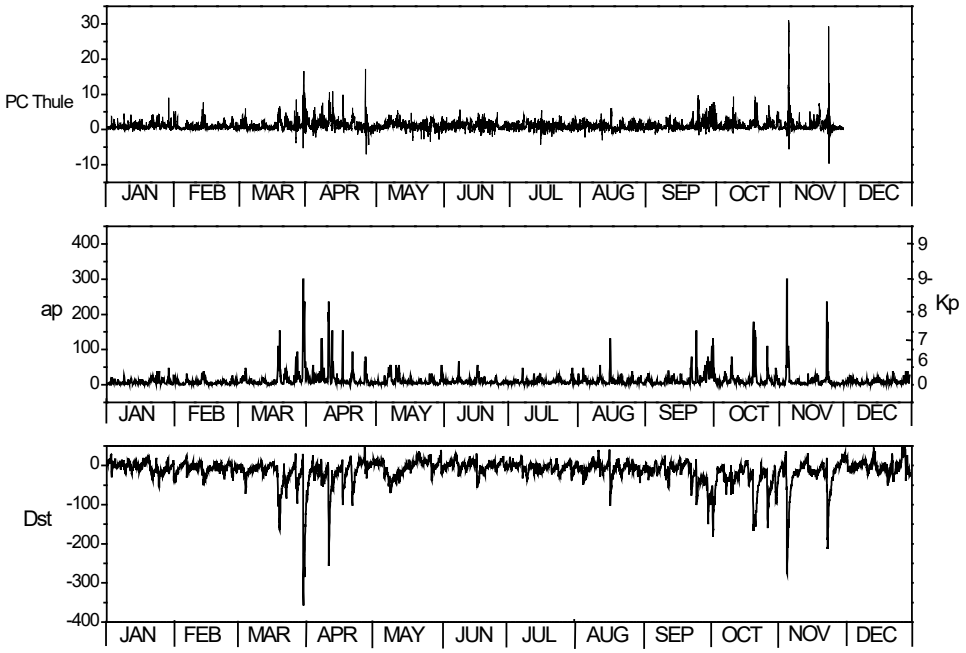

Figure 5.4. Geomagnetic indices http://isgi.unistra.fr/data_download.php for the year 2002. Top to bottom: Top-15-min PC index at Thule, Middle-3-hour ap (left scale) and Kp (right scale) indices and Bottom-Dst index.

There was one event with Kp=8+ (Dst min=-108nT) on 23 May, the result of solar activity which was followed from the Sun (fast halo CME on 22 May, proton event on 23rd) through the solar wind (IMF Bz=-43 nT) to the ground.

Kp index was 7+ on:

- October 1-4, result of the enhanced solar activity on 27-30 September of mixed origin, with Dst min=-179 nT on 1 October;
- April 17-20, due to flare activity and halo CMEs on 15 and 17 April. Dst min =-151nT
- September 7-8, clearly following from halo CME on September 5, proton event and <-20nT IMF Bz on September 7th. Dst min=-170 nT.

On May 11 and November 21 Kp index was 7- .

High values of the Thule PC index occurred on 23 May, 10-11 January, 19-23 April.

Geomagnetic Activity in Canada

Figures 5.5-5.7 show hourly ranges indices of the magnetic field components (https://spaceweather.gc.ca/data-donnee/indices/si-en.php) at three Canadian magnetic observatories, Resolute (RES, GML =83.1°), Poste-de-la-Baleine (PBQ, 66.8°) and Ottawa (OTT, 57.0°) which represent geomagnetic activity in the polar cap, auroral and subauroral regions in Canada.

The largest disturbance in RES was on 23 May, other significant disturbances on May 27, July 19, 29. The regular seasonal variation in polar cap can also be seen on Fig. 5.5.

The largest magnetic disturbance in auroral region (PBQ) was on September 7 followed by April 17-20, October 1-4 and May 11 (Fig. 5.6).

In subauroral region (OTT) (Fig.5.7), however, the April 17-20 disturbance was the largest, following by October 1-4, August 2 (from solar activity on 29 July) and September 7-8.

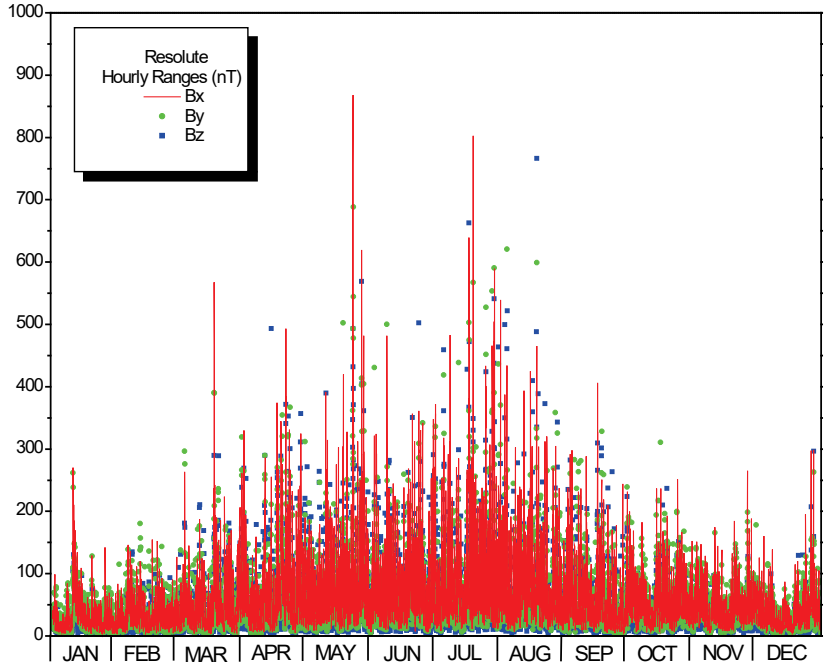

Figure 5.5. Hourly ranges of the magnetic field components at Resolute.

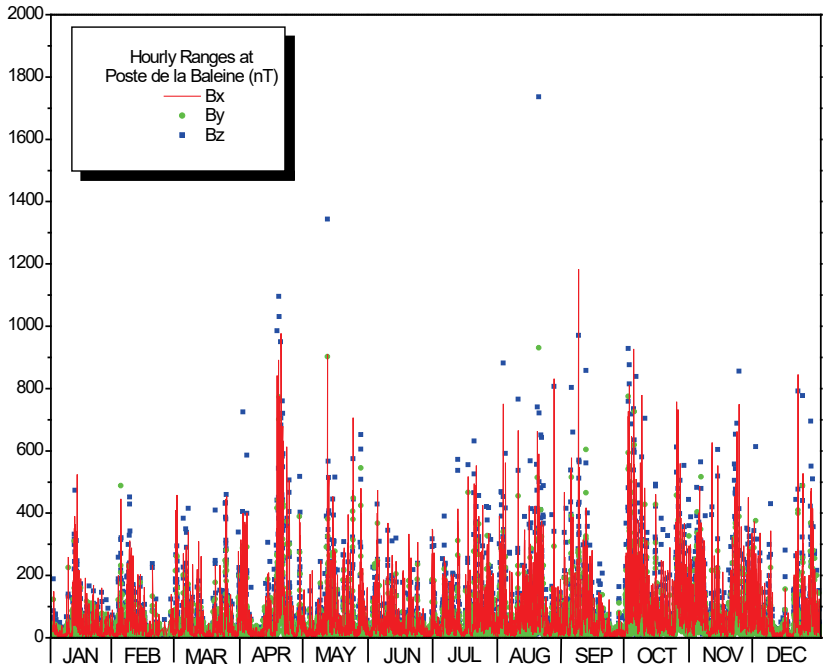

Figure 5.6. Hourly ranges of the magnetic field components at Poste-de-la-Baleine.

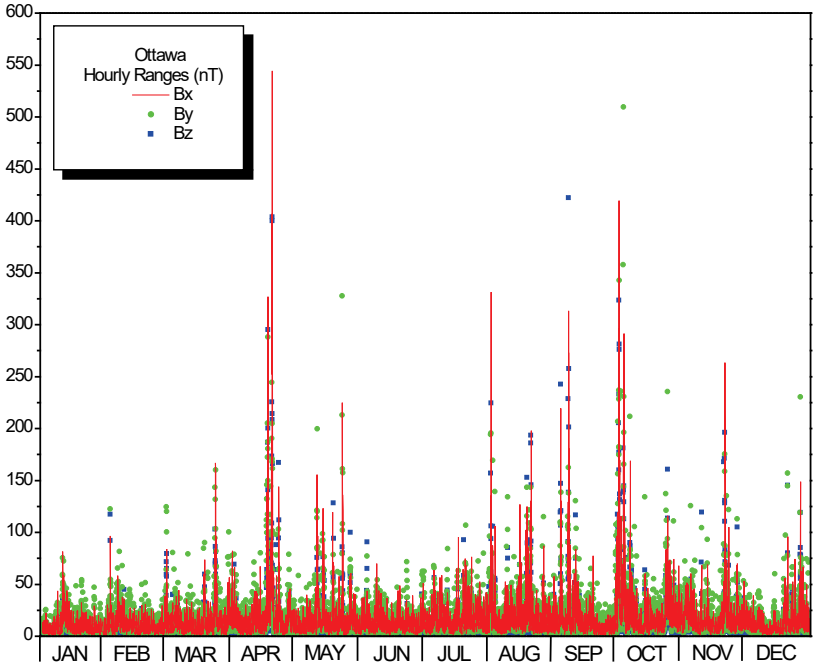

Figure 5.7. Hourly ranges of the magnetic field components at Ottawa.

Space Weather during EVAs on ISS

The space environment conditions were analysed for periods of time when Extra Vehicular Activities (EVAs) on International Space Station (ISS) were performed. It was made by using GOES electron flux data, Kp and Dst indices (Figure. 5.8).

For most of the EVAs there were no significant increase in the electron flux. The increase in radiation level at the ISS altitude might be expected on November 26 (GOES average electron flux ~ 6000 pfu) following the geomagnetic disturbance on November 21 with Kp=6 and Dst=-97. The lower response of the electron flux in October (average ~ 4000 pfu) was produced by more significant geomagnetic activity on 1-4 October with max Kp=7+ and max Dst= -179. Data on the actual conditions at ISS altitude were not available.

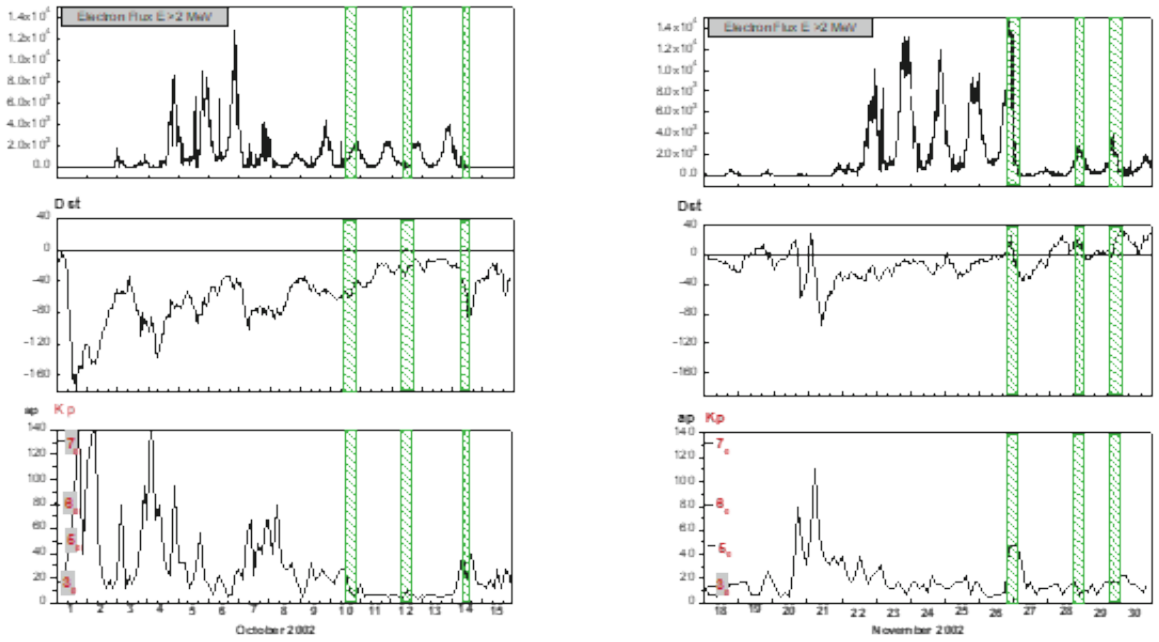

Figure 5.8. Space environment conditions during EVAs on ISS. Green areas show times of EVAs.Left Panel: October 2002; Right panel: November 2002.

Details of the largest space weather events and GIC

The most geoeffective event with Kp=8+ on 23 May produced moderate geomagnetically induced currents in ground technological systems in North America. On the other hand, the long enhanced level of geomagnetic activity (Kp=7+) on October 1-4 was more geoeffective in this area. In both events, changes in Bz are associated with the beginning of the ground geomagnetic effects (Figure 5.9). Solar wind plasma disturbances seen on ACE interact with the magnetosphere producing corresponding changes in geomagnetic field and bursts of GIC. The association of these features is seen clearly during the event on 23 May but less in the event 1-4 October (Kp=7+). However, the geomagnetically induced currents were twice as much during the second event.

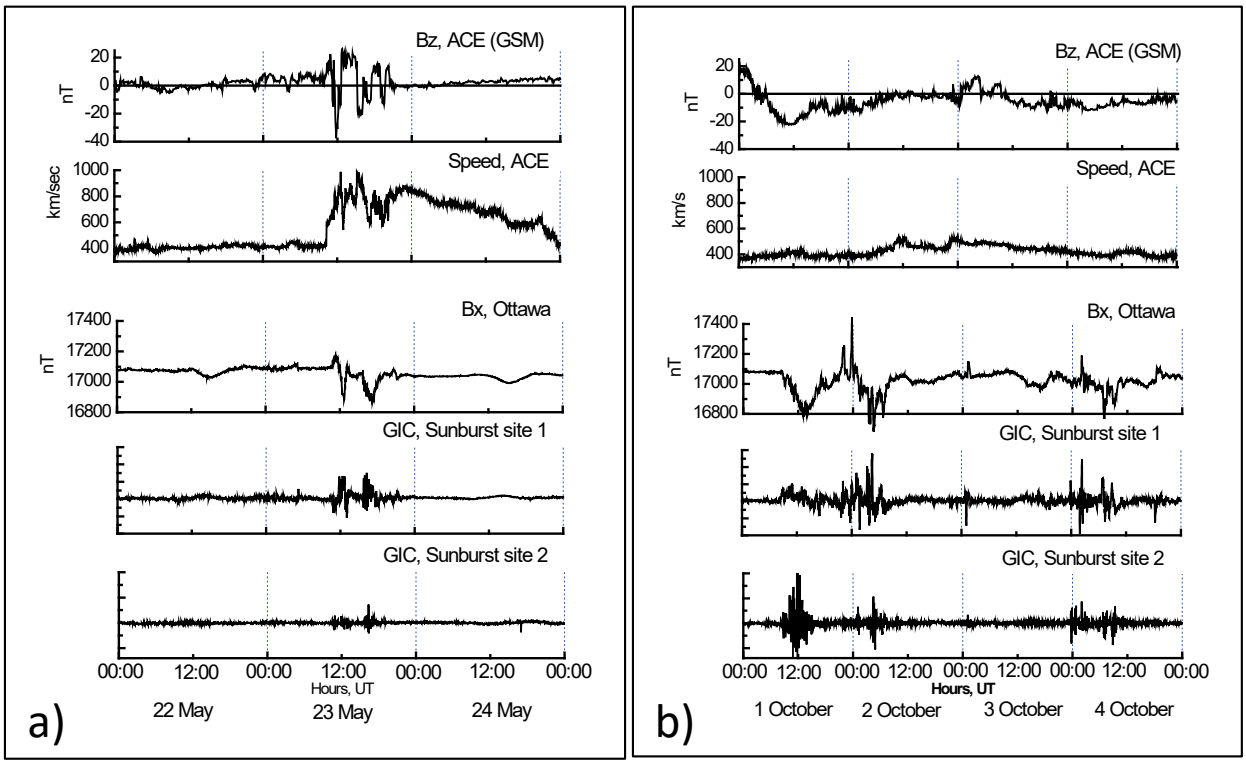

Figure 5.9. Ground effects of space weather events:a) May 22-24; b) October 1-4. Presented for each event are solar wind parameters (top two plots), geomagnetic variations (middle plot) and geomagnetically induced currents in different locations over the globe (two bottom plots).

References

L. Trichtchenko, Space Weather 2002 and Geomagnetic Activity in North America, poster presented at the Space Weather Week in Boulder, April 2003.

PART 6

Review of space weather in year 2003

Summary

Part 6 presents a synopsis of solar activity, solar wind conditions, global geomagnetic activity, and geomagnetic activity in Canada for the entire year 2003. There were three space weather events with high geo-effectiveness during the year. The most pronounced one occurred on October 29-31 with maximum geomagnetic indices of Kp=9 and Dst=-401. This famous event was initiated on October 28 by solar Active Region 486, which produced a X17/4B flare associated with a full halo CME with speed of about 2000 km/sec. Strong geomagnetic activity on May 29 with Kp=8+, Dst =-130, was due to two halo CMEs associated with X1 and X3 -flares accompanied by IMF Bz =–30 nT and solar wind speed of 800 km/sec. The geomagnetic storm on November 20 with Kp=9- and Dst=-453 was produced by a halo CME on November 18. The size of the geomagnetic disturbances during October 29-31 event in all three zones (polar, auroral, subauroral) was exceptionally large, while others varied from event to event as shown by the hourly ranges of geomagnetic field at different observatories. Power systems in North America experienced very strong geomagnetically induced currents during the October 29-31 event, although no power outages were reported in North America, while there was one short duration outage in Sweden.

Solar activity

Year 2003 is manifesting the second peak the solar cycle Daily sunspot number and 10.7 flux density variations show the general solar activity during the year (Figure 6.1).

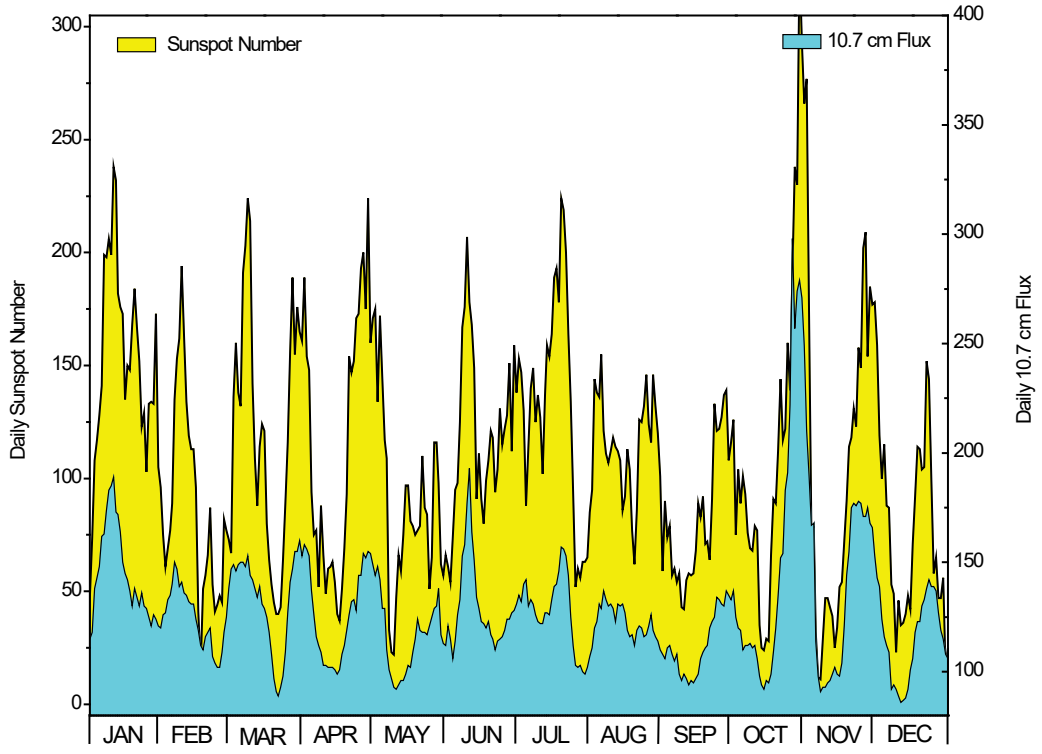

Figure 6.1. Daily sunspot number (yellow) ftp://ftp.ngdc.noaa.gov/STP/space-weather/solar-data/solar-indices/sunspot-numbers/ and F10.7 adjusted solar flux density (blue) https://spaceweather.gc.ca/solarflux/sx-en.php in units 10^{-22} Joules/s/m^2/Hz

The largest sunspot activity at the end of October coincided with the largest 10.7 flux value and produced important effects on the ground and the largest level of high energy particles at the geostationary orbit (Fig.6.2).

Solar Proton Events

The satellite environment is presented below as the daily fluences of electrons and protons at GOES satellite. The most significant solar proton events are evaluated based on daily fluences of high energy protons (>10 MeV and >100MeV), presented in Figure 6.2, together with the energetic electron fluences at GOES satellite.

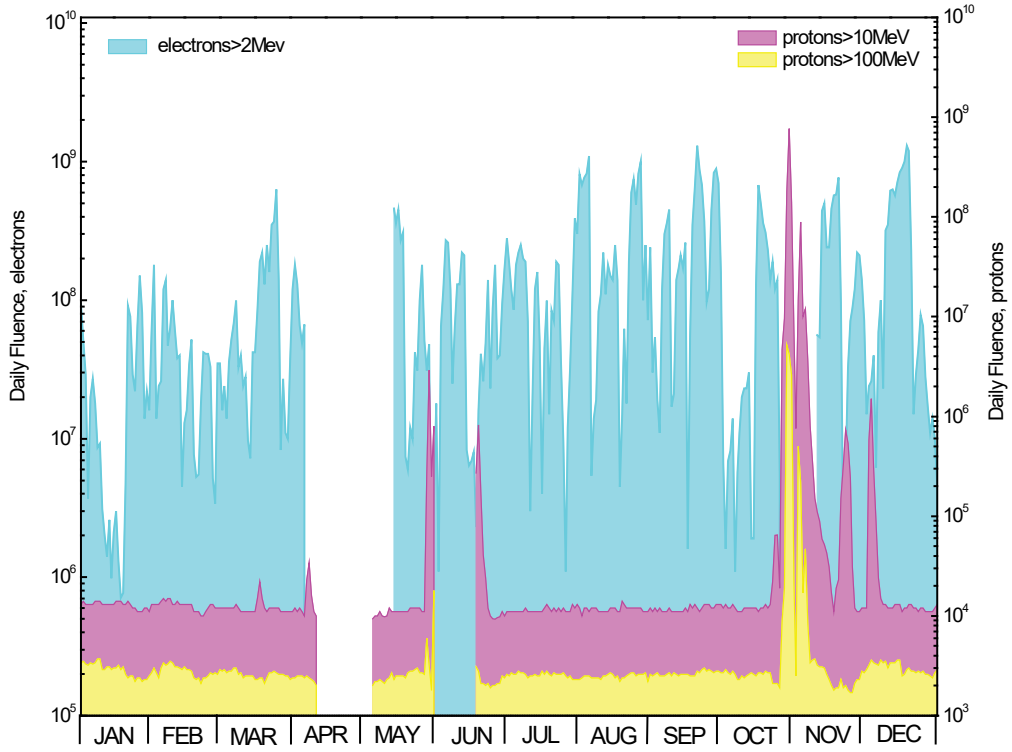

Figure 6.2. Daily fluences of electrons with energies>2MeV (blue), protons > 10 MeV (pink) and >100 MeV (yellow) from GOES satellite data ftp://ftp.ngdc.noaa.gov/STP/SOLAR_DATA/SATELLITE_ENVIRONMENT/ .

The most significant solar proton events during 2003 are (https://umbra.nascom.nasa.gov/SEP):

- May:
  - X1.4/2B of 27/2307 was accompanied by Type II (600 km/s), Type IV, and 10.7 cm (910 sfu) bursts.
  - X3.9/2B of 28/0016, accompanied by Type II (392 km/s), Type IV, and 10.7 cm (1600sfu), produced a proton event peaking at 29/1530.
  - X1.2/2B of 29/0105, accompanied Type II (955 km/s), Type IV, and 10.7 cm (810 sfu) bursts, caused a proton event peaking at 29/1530.

- October: The Sun was very active producing a few large flares with Type II, Type IV, and 10.7 bursts towards the end of October.
    - X5.4/1B (23/0835),
    - X1.2/2N (26/1819),
    - **X17.2**/4B (28/1110) (third largest x-ray flare since 1976), and
    - **X10**/2B (29/2049).

  Associated with the X17.2 and X10 flares were proton events:
    - 10 MeV> 1,000 pfu 28/1215-29/0615-29/1340 max: 29,500 pfu
    - 10 MeV> 1,000 pfu 29/1920-30/0300-30/2135 max : 2,790 pfu
    - 10 MeV>10,000 pfu 29/0030-29/0615-29/1050 max: 29,500 pfu
    - 100 MeV> 1 pfu 28/1150-29/0015-31/0145 max: 186 pfu

- November: The early part of the month was dominated by the remnants of intense flare activities from October.
    - X8.3/2B (2/1734),
    - X3/2B (3/0129), X3.9/2F (3/0935),
    - X28/3B (4/1953) (the most powerful x-ray flare since 1976 that saturated the GOES sensor for 11 minutes)

  The large proton events were:
    - 10 MeV> 1,000 pfu 02/2220-03/0815-03/1930 max: 1,570 pfu
    - 100 MeV>1 pfu 02/1740-02/1905-03/1720 max: 49 pfu

According to Figure 6.2, the >2 MeV relativistic electrons fluences were high throughout the year due to high-speed solar wind streams emanating from low latitude coronal holes on the Sun .

Solar Wind conditions

Figure 6.3 shows the vertical (Z) component of the interplanetary magnetic field (IMF) (top panel); solar wind density and speed (bottom panel) in geocentric solar-magnetospheric coordinate system available from ACE data and preliminary analysis on ftp://ftp.ngdc.noaa.gov/STP/swpc_products/weekly_reports/PRFs_of_SGD/ .

Significant southward Bz component (<-30 nT, GSM) occurred on

- May 29th : Bz min=-33 nT, speed ~ 800km/s, effect of the two CMEs;
- July 26th : Bz min=-32 nT, speed ~800 km/s, coronal hole effects;
- October 29th (- 48 nT) and 30th (-35 nT), due to the two extremely fast CMEs. The large proton events contaminated SWEPAM data on board ACE satellite, therefore plots of speed and density might be unreliable.
- The largest negative Bz was on November 20th (-53 nT, increase in speed of 350 km/s, from 450 to ~ 850 km/s due to halo CME).

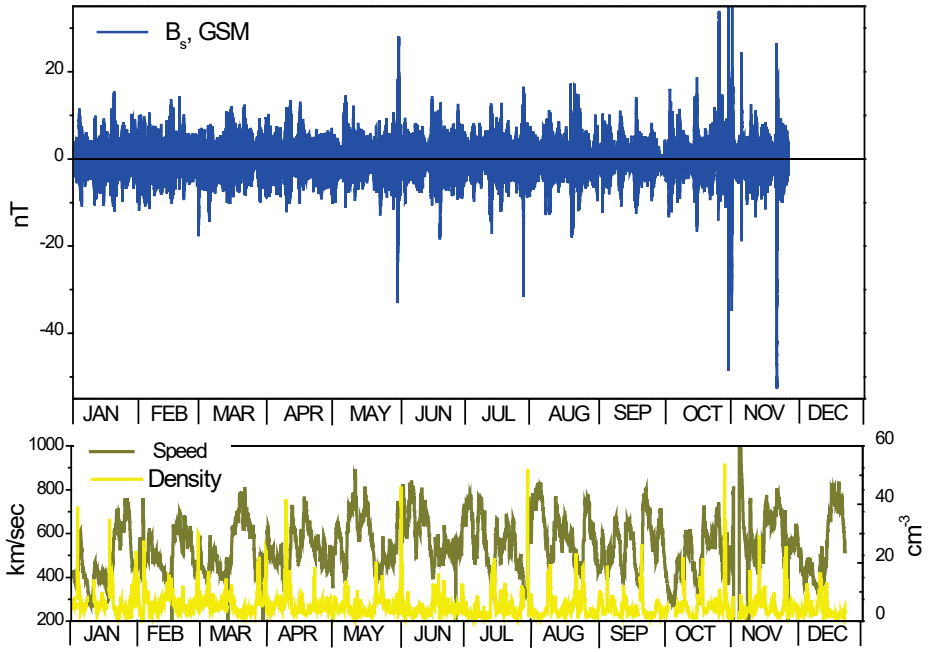

Figure 6.3. 4-min. Top panel: average of IMF Bz; Bottom panel: hourly solar wind speed and density at ACE satellite. http://www.srl.caltech.edu/ACE/ASC/

Global Geomagnetic Activity

Variations of the global indices Kp (ap), Dst and the polar cap index for Thule (PC-North) are presented in Figure 6.4.

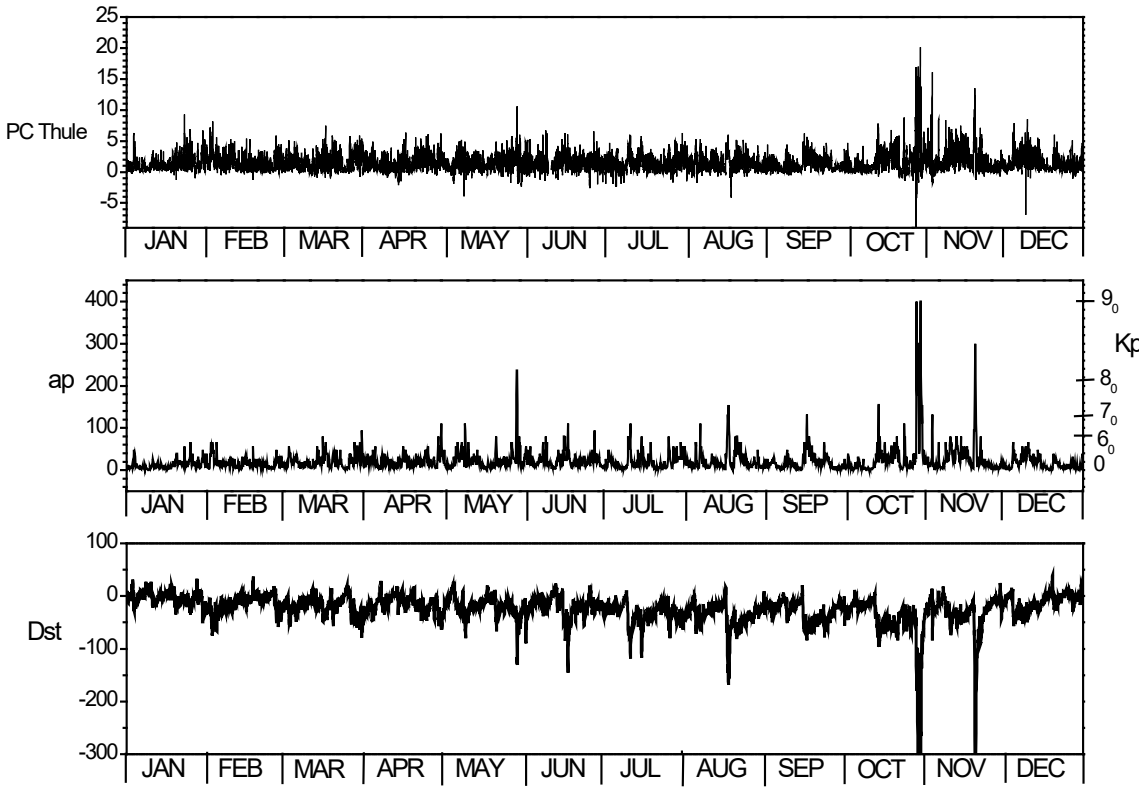

Figure 6.4. Geomagnetic indices http://isgi.unistra.fr/data_download.php for the year 2000. Top to bottom: Top-15-min PC index at Thule, Middle-3-hour ap (left scale) and Kp (right scale) indices and Bottom-Dst index.

The October 29-31 geomagnetic event is the consequence of solar activity which was related to Region 486 (two fast halo CMEs associated with X17 and X10 flares, numerous proton events and IMF Bz min=-48 nT), resulting in the largest value of the Kp index = 9. It was also the largest for the PC index, but only second for the Dst index = -401. The most significant event in terms of Dst index was on November 20-21 with Dst =-465 and Kp=9- (second largest in the year) due to a pair of M3 flares and associated halo CME on November 18. The third largest event in terms of Kp index=8+ (Dst= -131) occurred on May 29-30, due to two CMEs associated with X1 and X3 flares on 27-28 of May The third

largest event in terms of Dst, however, was on August 18-19 (Dst=-168, Kp=7+), possibly produced by long duration C7 flare of August 15th .

Geomagnetic Activity in Canada

Figures 6.5-6.7show the hourly ranges (https://spaceweather.gc.ca/data-donnee/indices/si-en.php) of the magnetic field components at three Canadian magnetic observatories, Resolute (RES, GML =83.1°), Poste-de-la-Baleine (PBQ, 66.8°) and Ottawa (OTT, 57.0°) which represent geomagnetic activity in the polar cap, auroral and subauroral regions in Canada.

The largest disturbance in all three zones was on 29-31 October with hourly ranges (HRX) of more than 2800 nT in RES, 2510 nT in PBQ and 1500 nT in OTT.

Other significant disturbance in polar cap was on May 29 with HRX =1020 nT. The regular seasonal variation in polar cap can also be seen on Fig. 6.5.

In auroral region (PBQ) the second largest disturbance was on August 18 with HRX=1850 nT followed by November 20-21 with HRX= 1690 nT.

In subauroral region (OTT), however, the May 29-30 was the second largest disturbance (915 nT), followed by November (450nT).

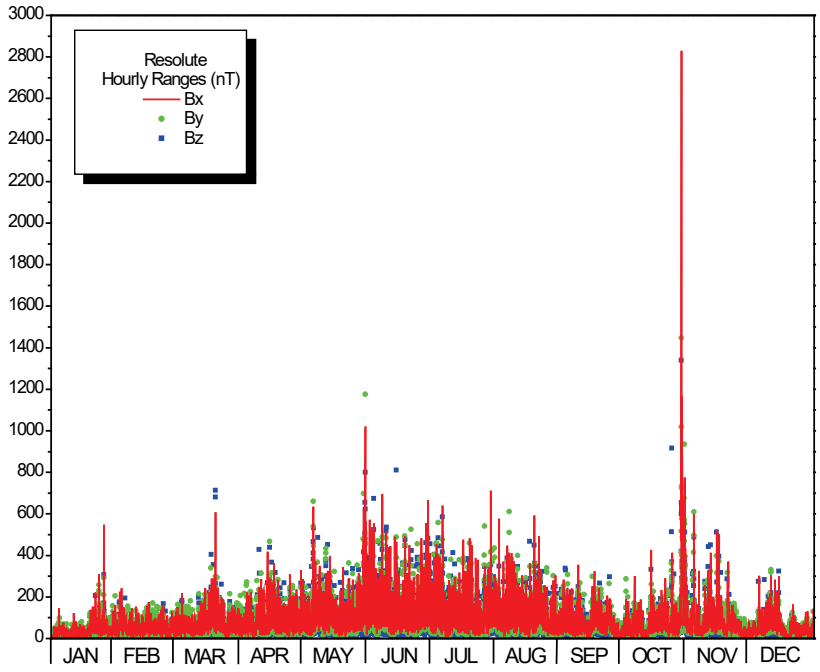

Figure 6.5. Hourly ranges of the magnetic field components at Resolute.

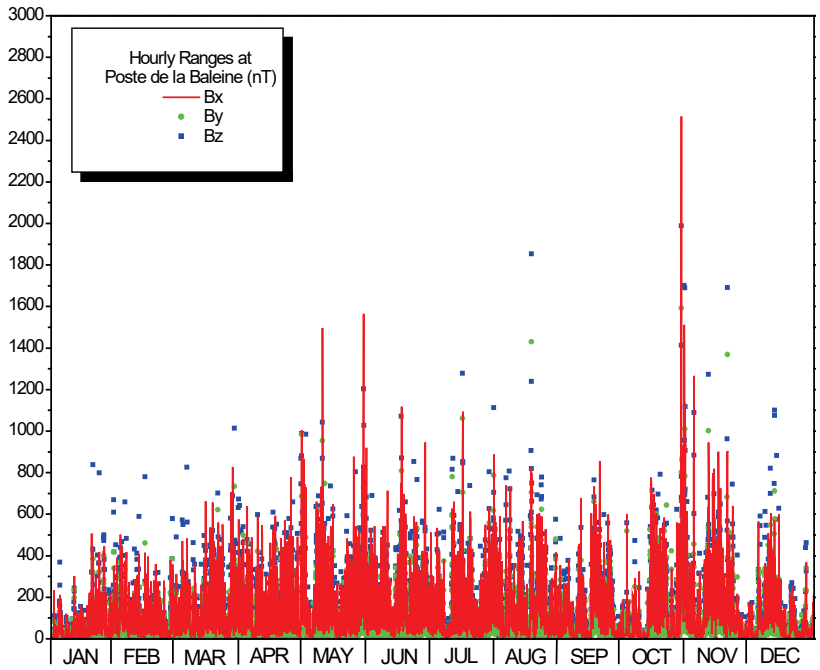

Figure 6.6. Hourly ranges of the magnetic field components at Poste-de-la-Baleine.

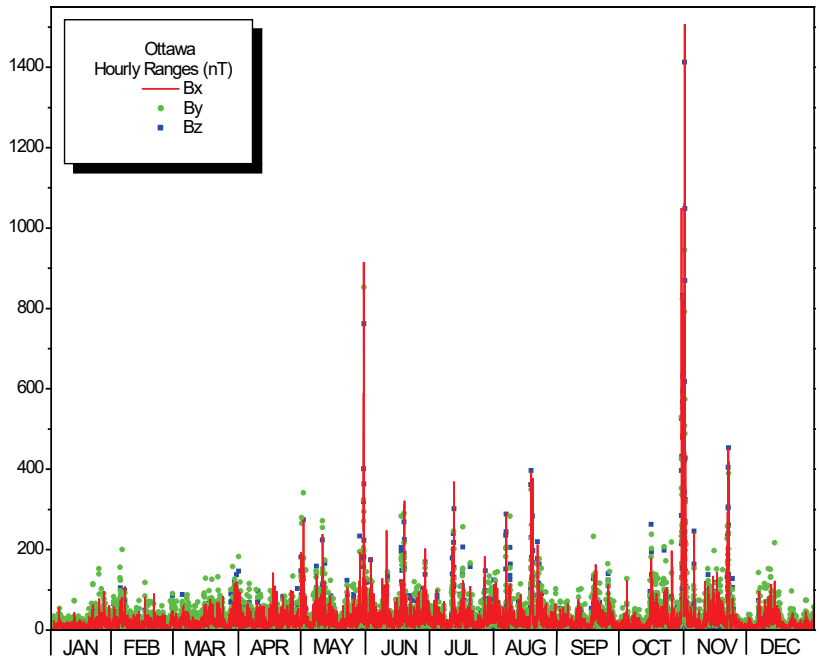

Figure 6.7. Hourly ranges of the magnetic field components at Ottawa.

Details of the largest space weather events and GIC

The IMF Bz, geomagnetic field at two observatories (Glenlea,GLN and Ottawa, OTT) and GIC variations at two sites of two power systems during the most disturbed periods of 2003 are presented on Figures 6.8-6.10.with their associated sonograms* (computed by sliding a 24 min. window through the data).

As presented in Figure 6.8, on May 29 rapid changes in the IMF Bz starting after ~1200 UT caused several spikes in the magnetometers at OTT and GLN until the IMF Bz became positive after ~0130UT on May 30. The sonogram for the three day period of IMF Bz indicates very little wave activity above 2 mHz except during the periods of rapid change.

The ground magnetic sonograms indicate Pc5 pulsations at ~ 3.5 mHz on May 30 during 0000 - 0230 UT especially at higher latitudes of GLN. GLN also recorded pulsations later the same day after ~1300 UT whereas OTT was quiet.

The GIC monitoring sites 1 (close to OTT) and 2 (close to GLN) show a wealth of wave activity in the Pc5 band, in contrast with that observed by the magnetometers. Of particular note is the activity at ~1300 UT on the last day where the frequency of waves is ~ 5 mHz.

As presented in Figure 6.9, on Oct 29 at 6 UT, IMF Bz turned southward for ~ 3 hrs before turning strongly northward until 18 UT, after which the IMF became strongly southward. There was some wave activity in the IMF at this onset time of IMF changes, which almost disappear for all period of disturbance (29-31 October). The ground magnetograms showed significant Pc5 activity during 9-18 UT at ~ 6 mHz, more significant at GLN than at OTT for most of the 3-day period. The wave frequency, as seen at GIC records, tends to be higher when IMF Bz is positive. The relative intensity for higher frequencies of wave activity is more evident with the GIC records than magnetograms.

As presented in Figure 6.10 for event on November 19-21, on Nov 20 the IMF is predominantly southward, and the Pc5 wave activity occurs at low frequencies. Once again the higher frequency wave activity is greater for the GIC monitoring stations, than for magnetic.

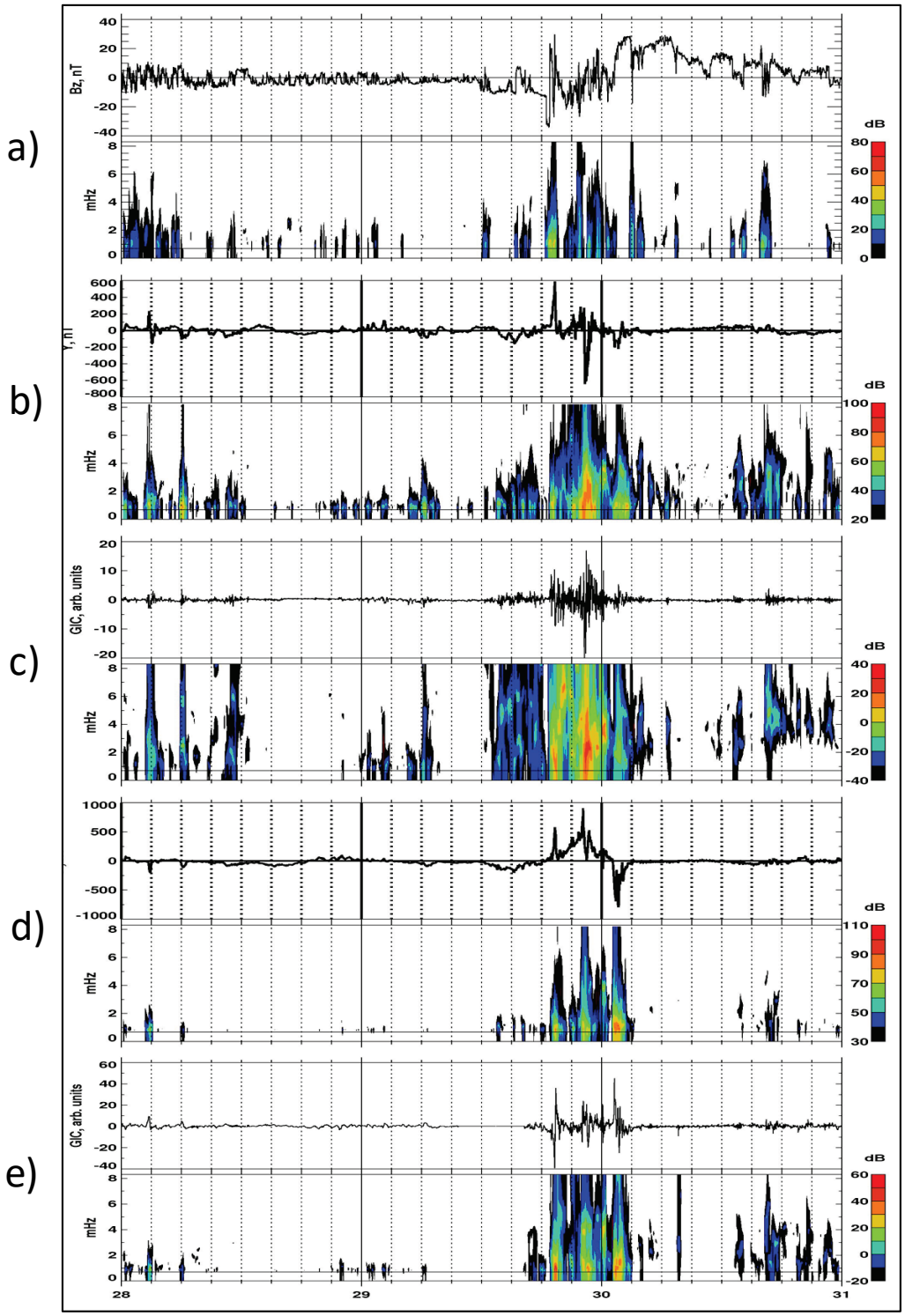

Figure 6.8. Space Weather Events on May 28-30:
a) IMF Bz and corresponding spectra (sonogram); b) magnetic field in OTT and corresponding sonogram; c) GIC in power system close to OTT and corresponding sonogram; d) magnetic field in GLN and corresponding sonogram; e) GIC in power system close to GLN and corresponding sonogram.

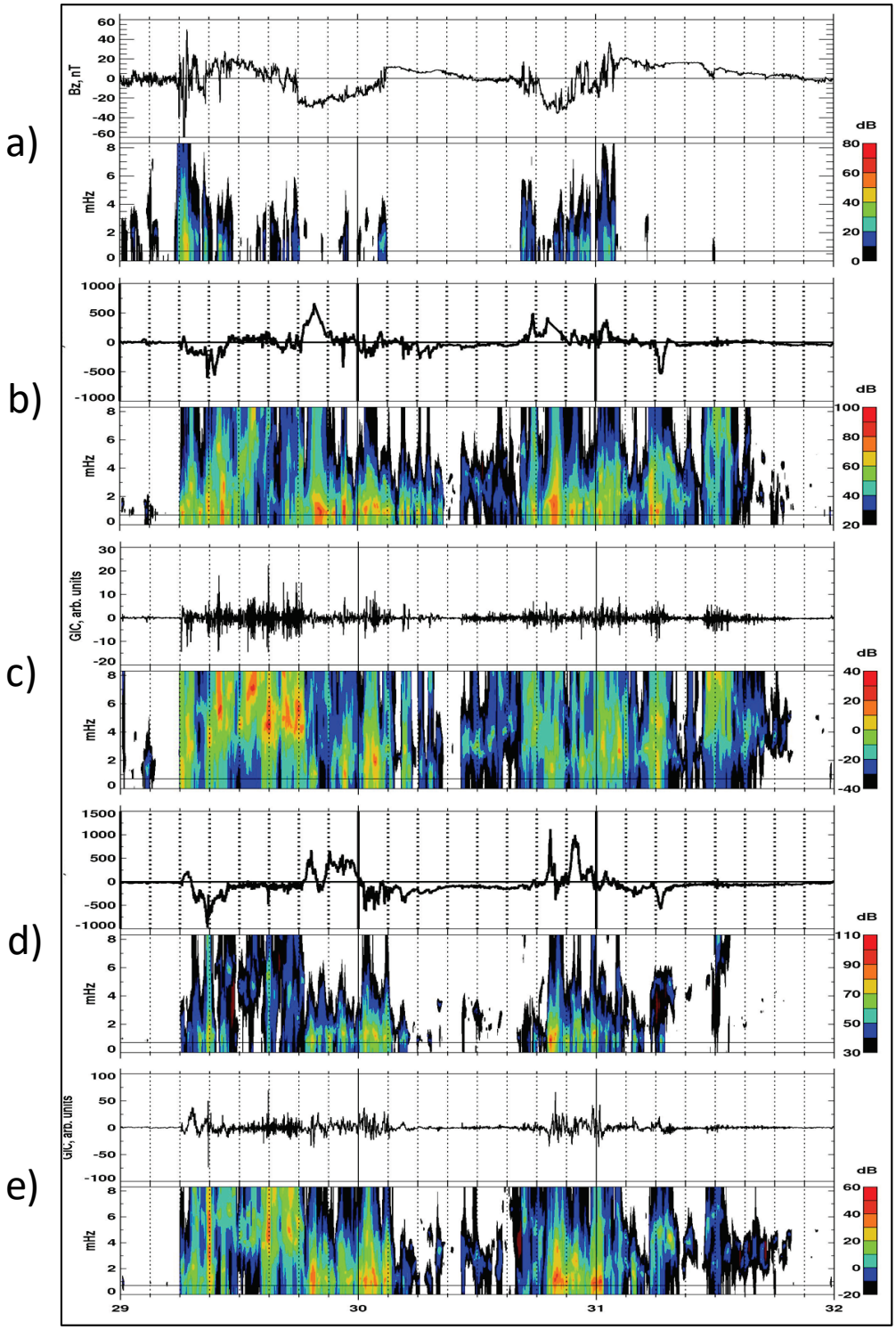

Figure 6.9. Space Weather Events on October 29-31:
a) IMF Bz and corresponding spectra (sonogram); b) magnetic field in OTT and corresponding sonogram; c) GIC in power system close to OTT and corresponding sonogram; d) magnetic field in GLN and corresponding sonogram; e) GIC in power system close to GLN and corresponding sonogram.

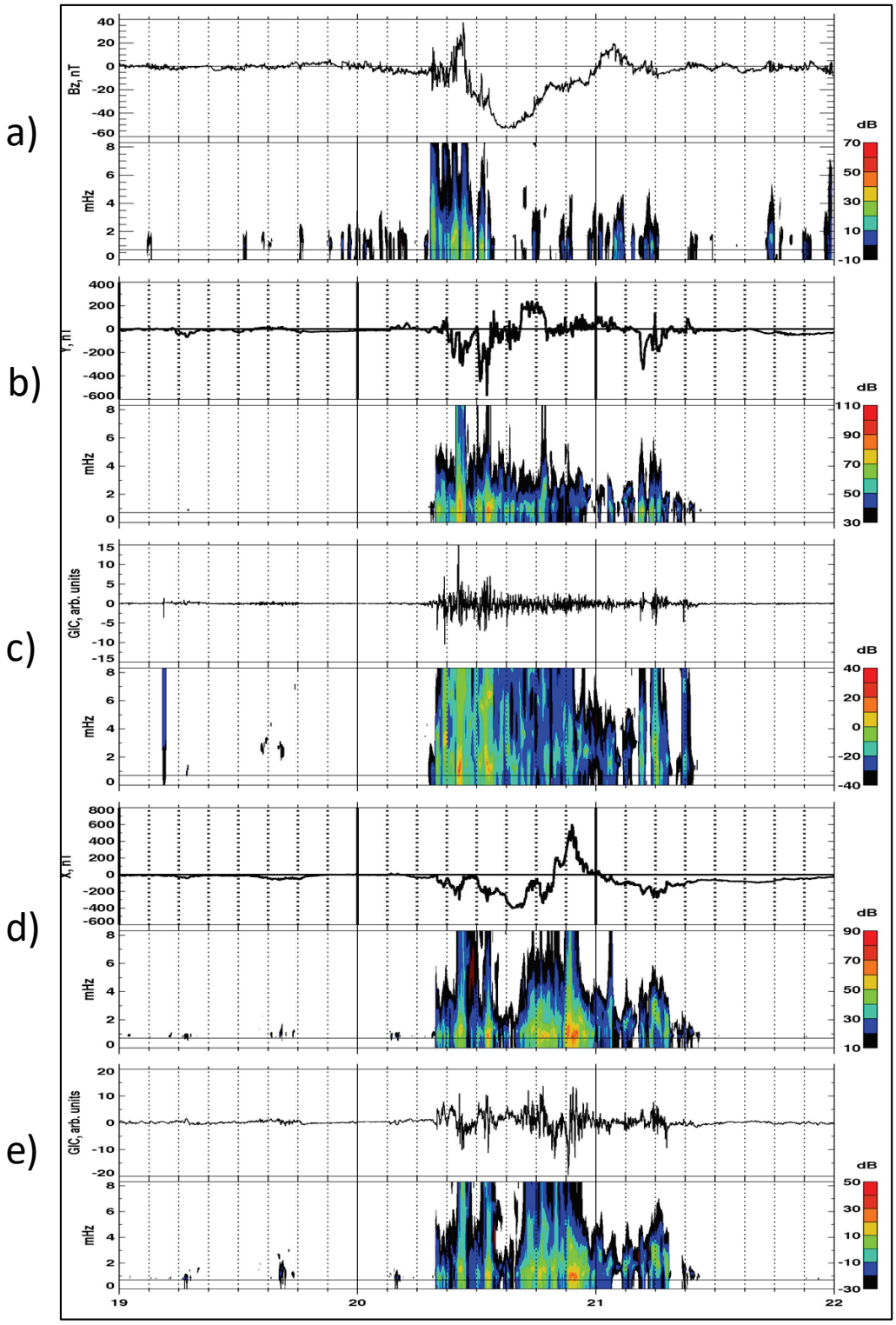

Figure 6.10. Space Weather Events on November 29-22:
a) IMF Bz and corresponding spectra (sonogram); b) magnetic field in OTT and corresponding sonogram; c) GIC in power system close to OTT and corresponding sonogram; d) magnetic field in GLN and corresponding sonogram; e) GIC in power system close to GLN and corresponding sonogram*
*The Burg spectrum method is used to evaluate the power spectral density (nT^2/Hz) for each sonogram.

The colour indicates the intensity of the spectrum at each frequency. A solid line shows the inverse of the window size (~0.8 mHz) which is the lower limit of the technique. The Nyquist frequency for one minute data is 8.3 mHz.

References

L. Trichtchenko, H.-L. Lam and D. Danskin, Space Weather Events and Geomagnetic Activity in 2003, poster presented at the Space Weather Week in Boulder, April 2004.

PART 7

Review of space weather in year 2004

Summary

Part 7 presents a synopsis of solar activity, solar wind conditions, global geomagnetic activity, and geomagnetic activity in Canada for the entire year 2004. High-speed solar wind streams emanating from coronal holes were primarily the source of active and stormy geomagnetic conditions during 2004, which is in the declining phase of the solar cycle 23. However, there were two intense space weather events that were triggered by coronal mass ejections (CMEs). The first event occurred on July 24-27 with maximum geomagnetic indices of Kp=9-, Ap=186 and Dst=-197 on July 27. The second (complex) event occurred on Nov. 7-10 with maximum geomagnetic indices of Kp=9-, Ap=140 and Dst=-373 on Nov. 8 (Nov 10 had a larger Ap of 161). This part 7 presents highlights of the space weather events of July 24-27 and November 7-10 with particular emphasis on November 8, when aurora displays were seen in southern Canada. Power systems in North America experienced severe level of geomagnetically induced currents (GIC) of up to 50A and high harmonics for the July event, and even larger GIC reaching 116A for the November event.

Solar activity

Daily sunspot numbers maximum of 100 and 10.7 flux density variations maximum of 180.8 (in July) indicated the general low level of solar activity during the year (Figure 7.1).

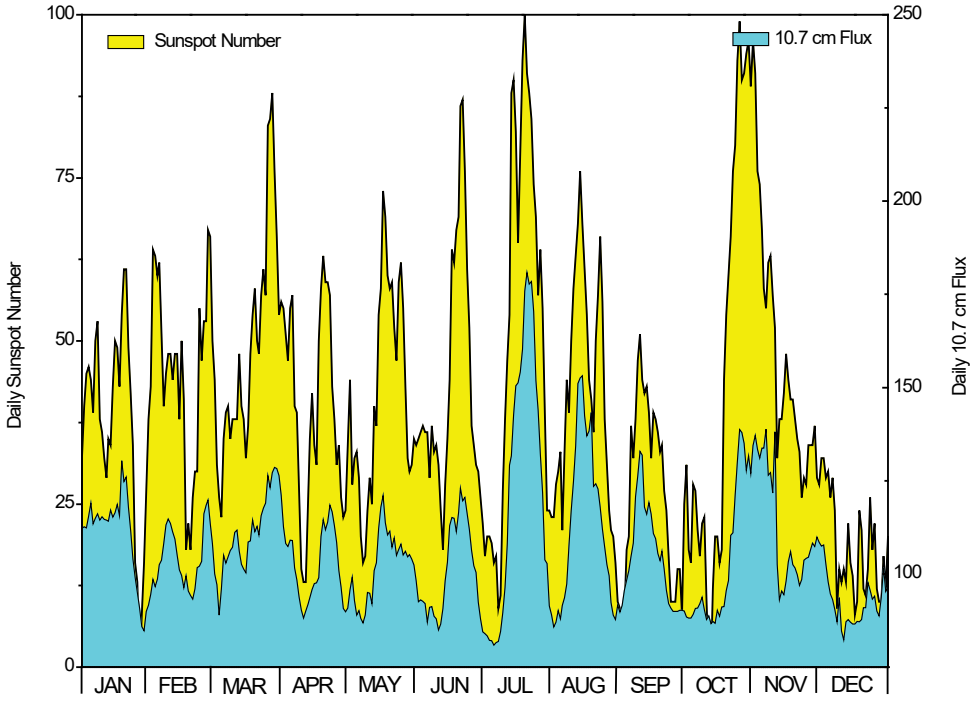

Figure 7.1. Daily sunspot number (yellow) ftp://ftp.ngdc.noaa.gov/STP/space-weather/solar-data/solar-indices/sunspot-numbers/ and 10.7 adjusted solar flux density (blue) https://spaceweather.gc.ca/solarflux/sx-en.php in units 10^{-22} Joules/s/m^2/Hz

The peak sunspot number in November was 99 and 10.7 flux was relatively moderate (138.7), although the associated solar activity resulted in large geomagnetic storms.

Solar Proton Events

The most significant solar proton events are evaluated based on daily fluences of high energy protons (>10 MeV and >100MeV) at GOES satellite, presented in Figure 7.2 together with the daily fluences of energetic electrons.

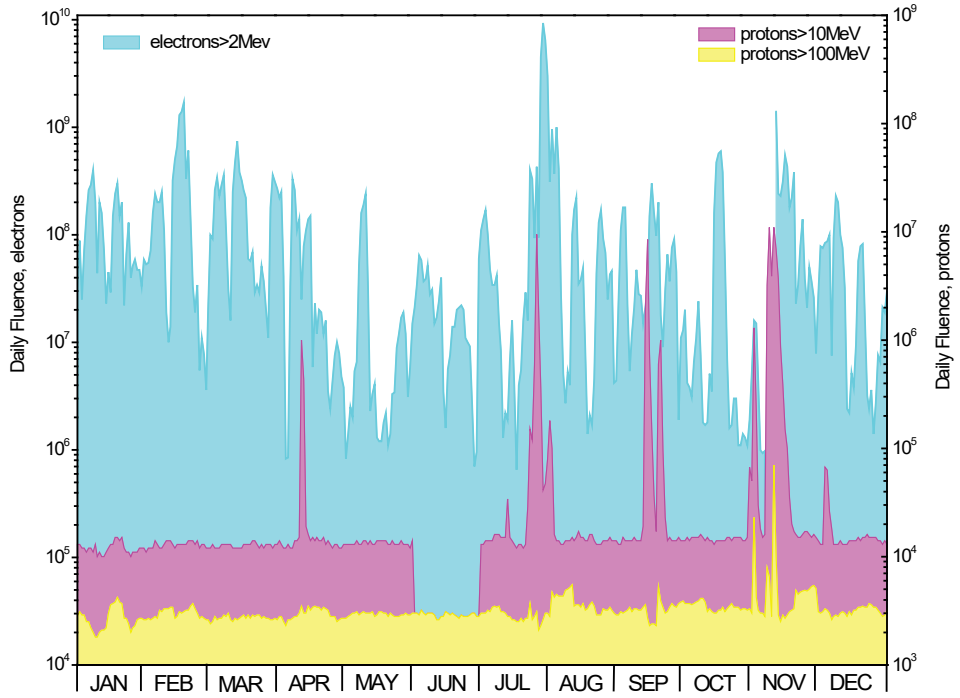

Figure 7.2. Daily fluences of electrons with energies>2MeV (blue), protons > 10 MeV (pink) and >100 MeV (yellow) obtained from GOES satellite data ftp://ftp.ngdc.noaa.gov/STP/SOLAR_DATA/SATELLITE_ENVIRONMENT/.

The most significant solar proton events with proton >10 MeV fluence about 107 pfu are:

- July 20-27, source – AR 652. For the period 20-28 July region produced 18 M-class flares with 3 major flares (>M5), the largest was M9.1 on 22 July started at 00:14 UT and M8/3B flare on 20th. Halo and full halo CMEs, Type II, Type IV, and 10 cm bursts accompanied these solar events.
- September 14: Proton event peaking on 14 September was a result of M4.8 flare of 12th September and associated CME.
- November 3-10, source – AR 696. For the period of 3 – 10 November, the region produced 13 M-class flares (five were M>5) and two X-class flares. The largest was X2.5/sf on 10th November, started at 02:04), X2.0/3b on 7 November (15:42) and M8.8/2n on 9th November (at 17:45). There were numerous CMEs (highest plane-of sky speed about 2000) and type II/ type IV radio bursts. Proton >10 MeV event associated with X2.0 flare began at 07/1910 and ended at 13/16:00. There were also significant enhancements in > 100 MeV proton fluxes on 1st and 7 – 8 November.

Energetic electrons at geostationary orbit

The level of >2 MeV relativistic electrons fluence was high through the year, mostly because of the recurrent coronal hole activities (Figure 7.2). It reached above 10^9 daily pfu on 15-20 February, due to coronal hole-associated activity; on 28 July–4 August and on 11-15 November due to complex effects of flares and coronal holes.

Interplanetary and Solar Wind conditions

As presented in Figure 7.3, the most significant episodes of southward IMF Bz (ftp://ftp.ngdc.noaa.gov/STP/swpc_products/weekly_reports/PRFs_of_SGD/) occurred on:

- January 22, with Bz min.~-20, possibly due to CME associated with long duration C5-flare on January 20th .
- July 25 and 29, Bz= -21 nT due to multiple CMEs from AR 652
- November 7– 10, Bz=-48.5 nT due to multiple CMEs (nine) from AR 696.
- Solar wind speed above 800 km/s produced by high speed streams of coronal holes on 11-12 March (max 801 km/s) and 22-29 March (max 918 km/s) and during two space weather events due to CMEs in July (max 1018 km/c) and November (max.832 km/s)

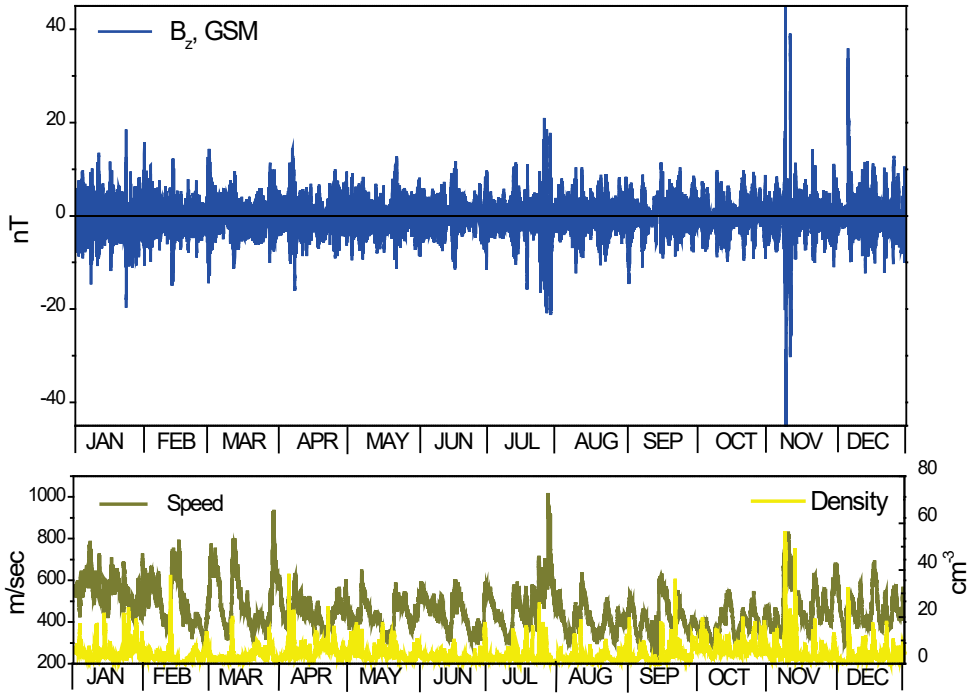

Figure 7.3. Top panel: 4-min. average of IMF Bz and, bottom panel: hourly solar wind speed (dark yellow) and density (yellow) at ACE satellite. http://www.srl.caltech.edu/ACE/ASC/

Global Geomagnetic Activity

Variations of the global indices Kp (ap), Dst and the polar cap index for Thule (PC-North) are presented in Figure 7.4.

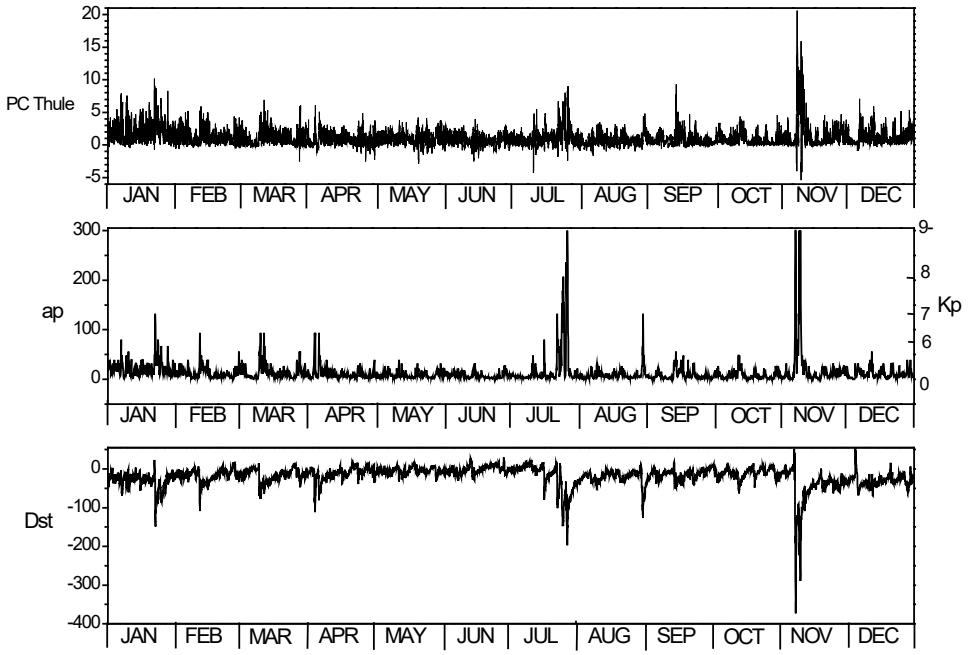

Figure 7.4. Geomagnetic indices for the year 2004 http://isgi.unistra.fr/data_download.php. Top to bottom:Top-15-min PC index at Thule, Middle-3-hour ap (left scale) and Kp (right scale) indices and Bottom-Dst index.

As shown in Figure 7.4, the largest geomagnetic storms of the year were associated with the November 3-10 solar activity.

- PC index was large on November 8 (max 20.6), on November 9 (max. 13) and on November10 (max 13).
- Kp index was 9- during two 3-hour periods on November 8, again 9- on November 9 and 9- on November10. July event was more moderate with Kp =9- only for one 3-hour period on July 27.
- The largest hourly Dst indices were also on November 8 (-373), November 9 (-223) and November 10 (-289). On July 27, Dst minimum was only –197.

Geomagnetic Activity in Canada

Figures 7.5-7.7 present the hourly ranges https://spaceweather.gc.ca/data-donnee/indices/si-en.php of the magnetic field components at three Canadian magnetic observatories, Resolute (RES, GML =83.1°), Yellowknife (YKC, 69.0°) and Ottawa (OTT, 57.0°) which represent the activity in the polar cap, auroral and subauroral regions in Canada.

The largest disturbance in auroral and subauroral zones was on 7-10 November and 27 July, with auroral zone moved to Ottawa. On the contrary, the largest disturbance in polar zone was on January 7 due to the combined effect of the CME-like transient from long duration M6 flare on Jan. 5th and coronal hole.

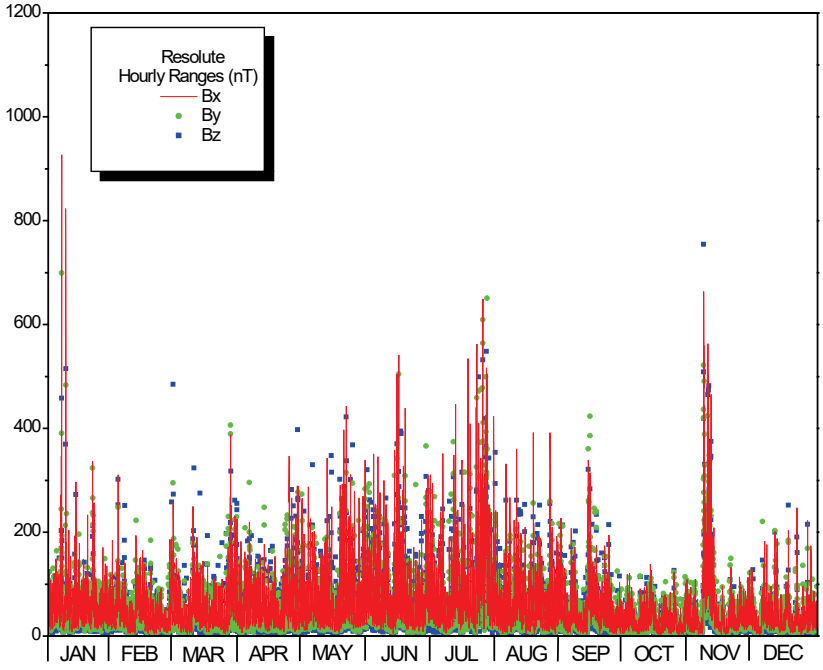

Figure 7.5. Hourly ranges of the magnetic field components at Resolute.

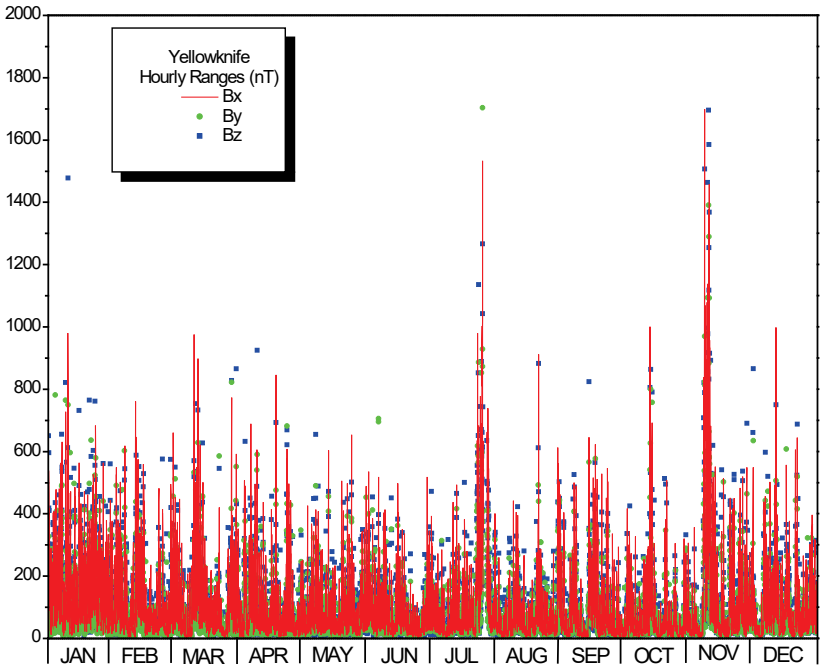

Figure 7.6. Hourly ranges of the magnetic field components at Yellowknife.

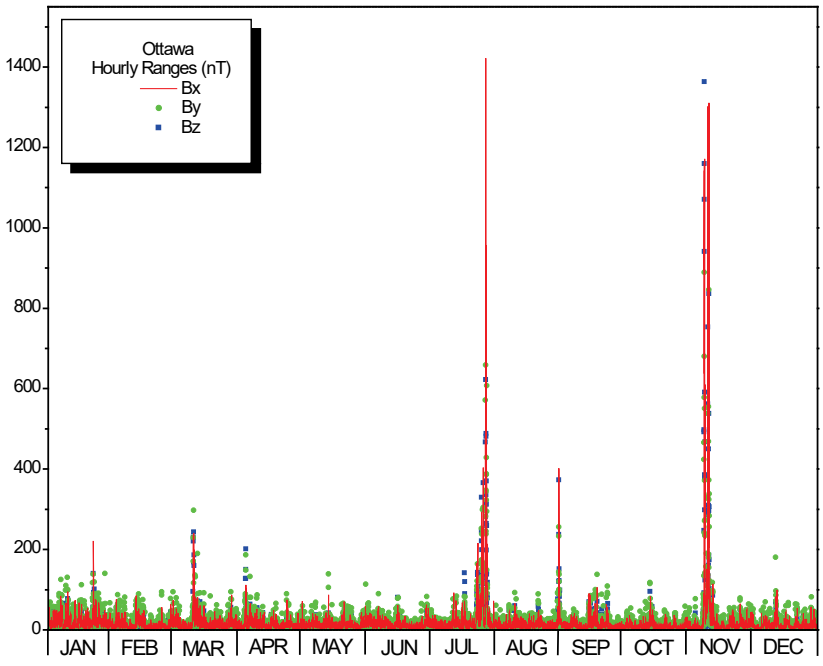

Figure 7.7. Hourly ranges of the magnetic field components at Ottawa.

Details of the largest space weather events and GIC

The space weather event of July 24-27 was preceded by a series of CMEs associated with complex solar activity originating from AR652 which was wider than Jupiter (Figure 7.8).

Figure 7.8. Active Region 652, initiated the series of CMEs on July 24-28.

The most significant in this time period was the full halo CME on July 25th (~1228 km/s) associated with a M2.2 flare.

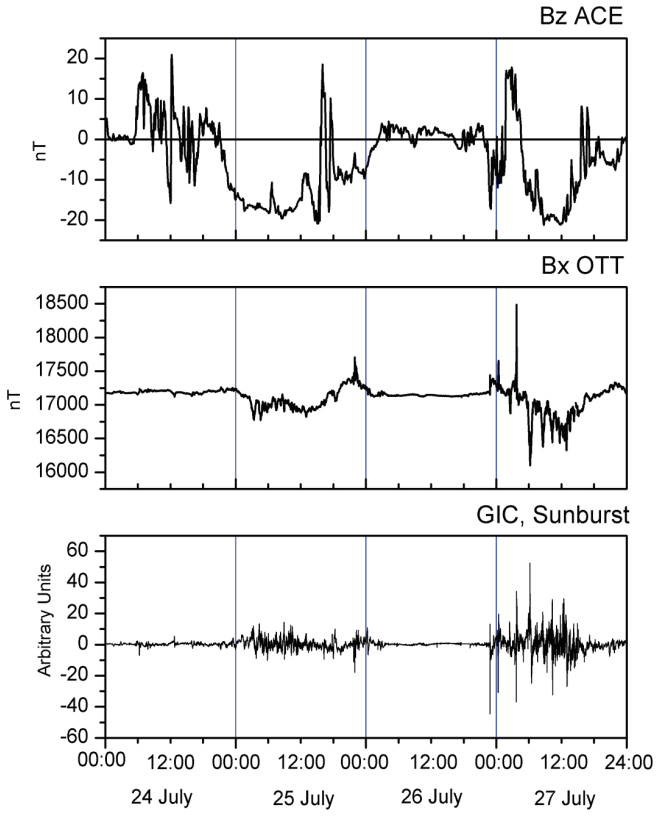

Figure 7.9. Interplanetary and ground results of July 24-27 event: top panel is IMF Bz at ACE, middle panel is Bx at Ottawa and the bottom panel is GIC variations at one of the North American power grid.

During the events of July 24-27, the IMF Bz (top panel, Fig.7.9) shows two major periods of southward turning, with the first one on July 25th slightly affecting the geomagnetic field in Ottawa (middle panel) and the second on July 27th producing major magnetic storm activity and large GIC in North America (bottom panel).

The November 2004 space weather event was produced by a chain of solar events from AR 696,

- started off with a partial halo CME (~750 km/s) associated with M1.6 and an asymmetric full halo CME(~1016 km/s) associated with M5 on Nov 3rd,
- followed by a partial halo CME (~635 km/s) associated with C6.3 and a complex halo CME (~625 km/s) associated with M5.4 on Nov 4th ,
- by a full halo CME (~960 km/s) associated with M9.3 on Nov 6th (shown in Figure 7.10) ,
- by a full halo CME (~1770 km/s) associated with X2 on Nov 7th ,
- a full halo CME (~520 km/s) associated with C7.9 on Nov 8th ,
- by an asymmetric full halo CME (~1853 km/s) associated with M8.9 on Nov 9th.

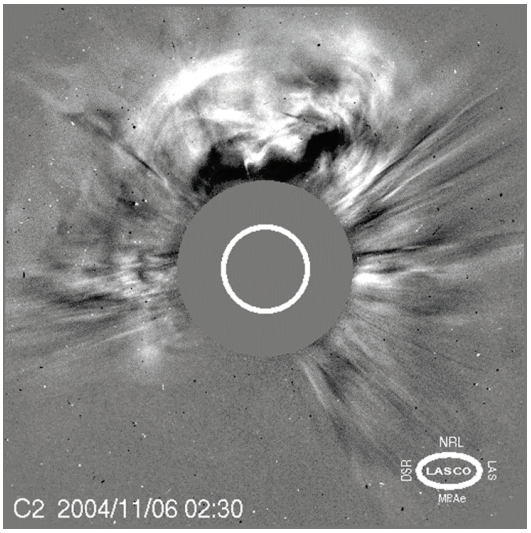

Figure 7.10. CME image taken by C2 EIT on November 6, 2004

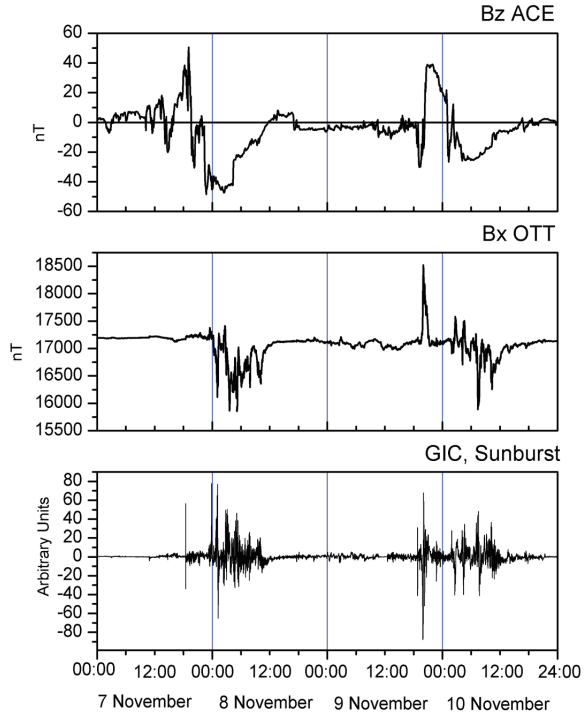

Figure 7.11. Interplanetary and ground results of November 7-10 event: top panel is IMF Bz at ACE, middle panel is Bx at Ottawa and the bottom panel is GIC variations at one of the North American power grid.

As presented in Figure 7.11, both long periods of strong (up to –50 nT) southward IMF Bz produced major storm conditions on the ground on 7-8 November and on 9-10 November.

The storm on 7-8 November triggered intense aurora displays in southern Canada. The ground magnetic records show large fluctuations in the order of 1000 nT and more. Concomitant with the sharp negative bay at ~1 UT in OTT was the spectacular northern light display in Ottawa at ~8 PM local time on November 7, resulting in wide-spread media, in particular in Ottawa (Figure 7.12).

Figure 7.12, Page of "Ottawa morning" presenting the auroral images taken by one of Ottawa resident.

References:

L. Trichtchenko, H.-L. Lam, L. McKee and D. Danskin, Year 2004: Space Weather Events and Geomagnetic Activity, poster presented at the Space Weather Week in Boulder, April 2005.

PART 8

Review of space weather in year 2005

Summary

This part presents a synopsis of solar activity, solar wind conditions, global geomagnetic activity, and geomagnetic activity in Canada for the entire year 2005, highlighting the causes and ground effects of the space weather events in May 13-15 and August 22-24.

Space weather and geomagnetic conditions during 2005 were mostly quiet. However, there were some geoeffective space weather events triggered by coronal mass ejections (CMEs). The first event in the year 2005 has occurred on January 17-22 with two active periods, max Kp=8- and Dst=-121 on Jan 18, max Kp =8.0 and Dst=-105 on Jan. 21-22 respectively. Event of May 15 was characterized by Kp=8+ and Dst=-236, but the largest Kp index of 9- (Dst=-216) occurred during the August 24 geomagnetic storm. Power systems in North America experienced high levels of geomagnetically induced currents (GIC) during these events, with the highest GIC of near 97 A on August 24. A significant proton event on September 7 was not associated with any significant geomagnetic activity.

Solar activity

The values of sunspot numbers and F10.7 flux density (Figure 8.1) were generally low, indicating the low level of solar activity during the year. The maximum daily sunspot numbers of 107 and F10.7 flux of 140.2 occurred in July (associated with AR 786), were not followed by any significant geomagnetic activity.

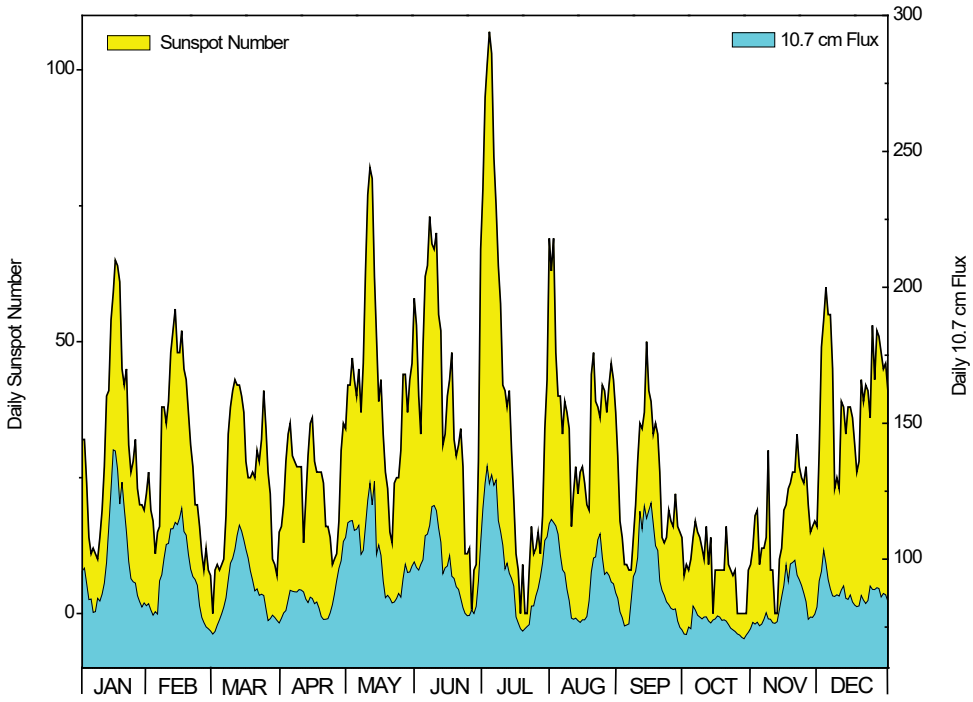

Figure 8.1. Daily sunspot number (yellow) ftp://ftp.ngdc.noaa.gov/STP/space-weather/solar-data/solar-indices/sunspot-numbers/, and F10.7 adjusted solar flux density (blue) https://spaceweather.gc.ca/solarflux/sx-en.php in flux units 10^{-22} Joules/s/m^2/Hz

Solar Proton Events

The most significant solar proton events are evaluated based on daily fluences of high energy protons (>10 MeV and >100MeV) at GOES satellite (Fig. 8.2).

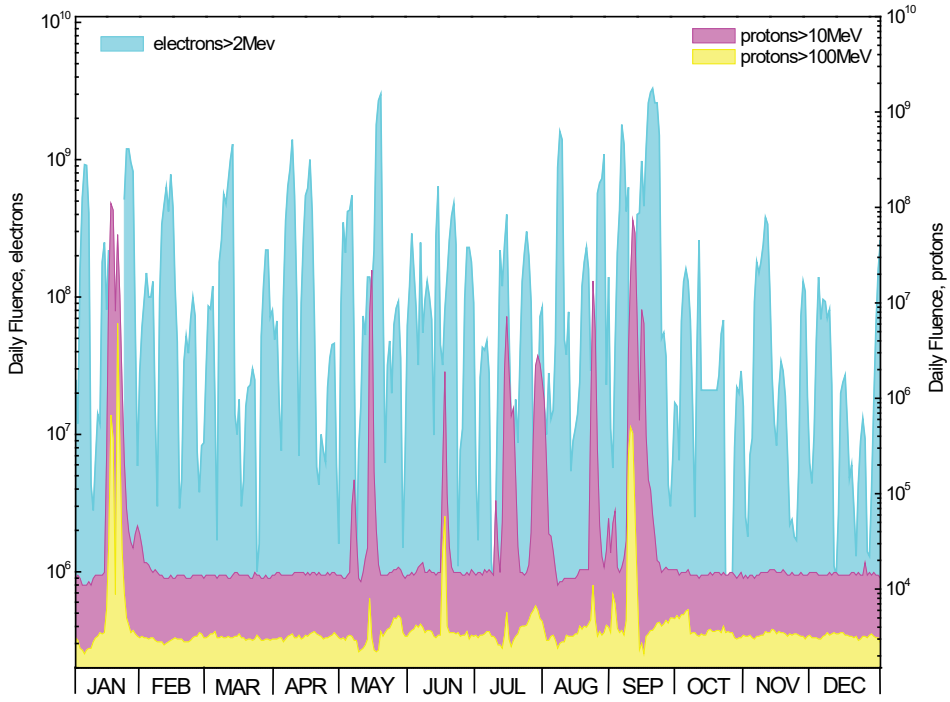

Figure 8.2. Daily fluences of electrons with energies>2MeV (blue), protons > 10 MeV (pink) and >100 MeV (yellow) extracted from GOES satellite data.
ftp://ftp.ngdc.noaa.gov/STP/SOLAR_DATA/SATELLITE_ENVIRONMENT/

The most significant solar proton events (https://umbra.nascom.nasa.gov/SEP) during 2005 are:

- Jan. 17-27, source – AR 720. This region produced 25 C-class flares, 8 M-class flares and 3 X- flares with the largest being X3.8/sf proton flare at 17/0952 and X7.1/2b proton flare flare on Jan. 20, although the peak proton>10 MeV flux was 5040 pfu at 17/01750 due to X2.3/3b flare of Jan.17. Full halo CMEs, Type II and Type IV radio bursts accompanied these solar events.
- May 13-15, source- AR 759. Proton event peaking on May 15 was a result of M8.0/2b LDE at 13/1657 and associated Type II / IV bursts and full halo CME.
- Aug. 22-24, source – AR 798. This region produced 3 long-duration M-flares all associated with CMEs (highest plane-of sky speed of 1700 km/s) and Type II/ Type IV radio bursts.

Proton >10 MeV event began at 22/2040 and ended at 25/0040.

- Sept. 7-11, source – AR 808 (return of AR 798). This period was initiated from far side and southeast limb activity with the largest X17/3b proton flare on 07/1740. Region produced 14 M-class and 7 X-class flares.

Energetic electrons at geostationary orbit

According to Figure 8.2, the >2 MeV relativistic electrons fluence was high throughout the year, mostly due to recurrent coronal hole activities. It exceeded 109 daily pfu during

- Jan. 17-25 space weather event (due to complex effects of coronal holes, CMEs and flares),
- on Mar.13 and Apr. 9 (effects of coronal holes),
- May 17-19 (due to multiple CME and flares effect),
- Aug. 8, 9 (sector boundary crossing) and
- Aug. 28 (effect of the multiple CMEs, flares and coronal hole),
- Sept. 5-6 (effect of multiple CME and flares) and
- Sept. 16-22 (due to multiple CMEs and flares).

Interplanetary and Solar Wind conditions

Analysis has been partially based on information from ftp://ftp.ngdc.noaa.gov/STP/swpc_products/weekly_reports/PRFs_of_SGD/.

As presented in Figure 8.3, the most significant southward IMF Bz occurred on:

- Jan. 21, with Bz min. ~-26, possibly associated with X7.1-flare on Jan. 20. Solar wind and LASCO data were sparse due to proton contamination of the instruments.
- May 15, with Bz min = -44.4 nT due to CME/ M8 flare from AR 759 on May 13.
- July 10, with Bz min = -22.2 nT due to CME /M4.9 flare and filament activity from AR 786 on July 7.
- Aug. 24, Bz min.=-55.4 nT due to two CMEs/M5 flares of August 22.

- Solar wind speed above 800 km/s produced by high speed streams of coronal holes occurred on Jan 2 (max 845 km/s), Mar. 08 (max 811 km/s). On May 8 high speed (max 856 km/s) was due to combination of coronal hole and CME effects, on May 15 (max 985 km/s) was due to CME effect. During space weather events of January and September speed values were high but sparse due to contamination, with highest measured speed of 1007 km/s on September 12.

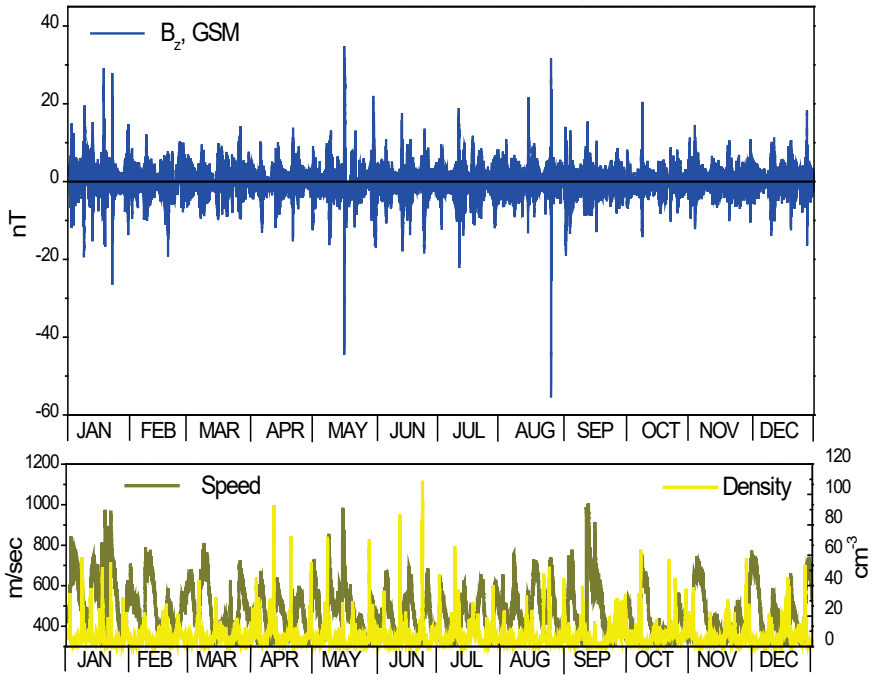

Figure 8.3. Top panel: 4-min. average of IMF Bz; bottom panel: hourly solar wind speed (dark yellow) and density (yellow) at ACE satellite. http://www.srl.caltech.edu/ACE/ASC/

Global Geomagnetic Activity

Variations of the global geomagnetic indices Kp (ap), Dst and the polar cap index for Thule (PC-North) are presented in Figure 8.4.

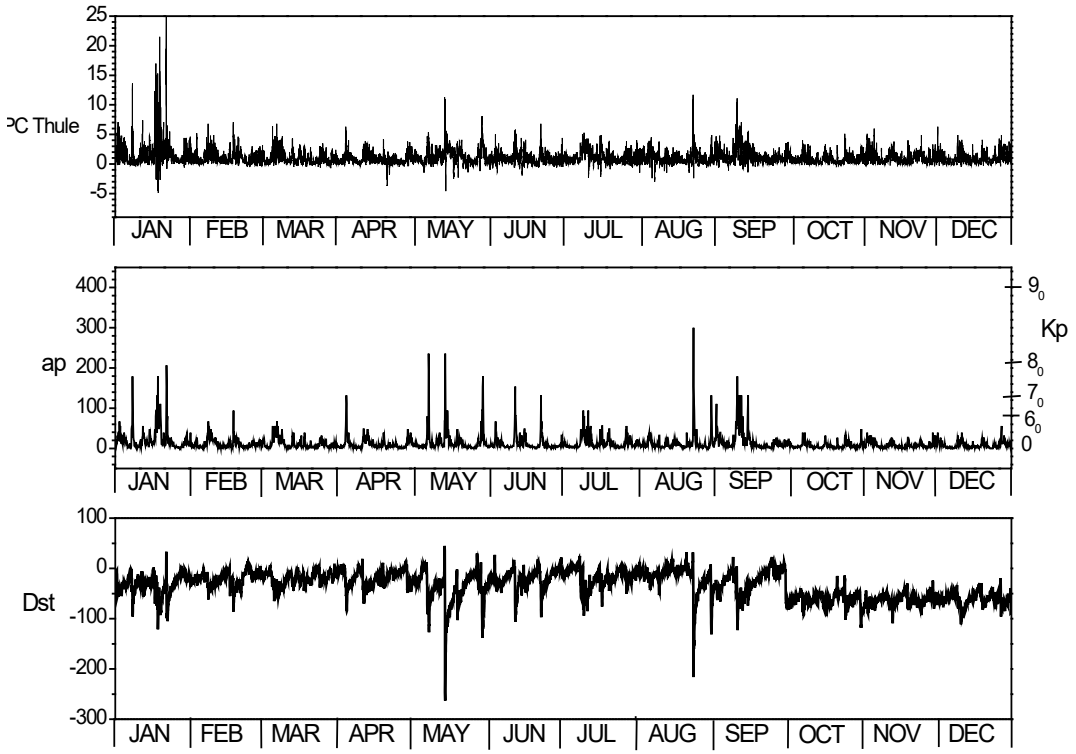

Figure 8.4. Geomagnetic indices for the year 2005 http://isgi.unistra.fr/data_download.php. Top to bottom:Top-15-min PC index at Thule, Middle-3-hour ap (left scale) and Kp (right scale) indices and Bottom-Dst index.

The largest disturbed polar cap (PC) index was during January event (max. 25.6) with enhanced (>10) values during other events (May 15, August 24 and September 11).

The largest geomagnetic storm of the year with Kp=9- on August 24 was associated with the August 22-23 solar activity. The Kp index was 8+ on May15, was 8o on January 21, and 8- on September 11. Additionally, Kp=8- on May 30 was the joint result of the HSS from coronal hole and CME/flare activity of AR 767 on May 26.

The hourly Dst index minimum was -263 May 15, and -216 on August 24. The third largest value of Dst=-138 was on May 30 with Dst = -121 on January 18.

Geomagnetic activity in Canada

Figures 8.5-8.7 show the hourly ranges (https://spaceweather.gc.ca/data-donnee/indices/si-en.php) of the magnetic field components at three Canadian magnetic observatories, Resolute (geomagnetic latitude 82.9°), PBQ (65.46°) and Ottawa (55.6°) which represent the activity in the polar cap, auroral and subauroral regions in Canada. Data gap at PBQ in November is due to technical problems at the observatory.

The largest disturbance in polar cap was during January 17-22 Space Weather events, in auroral zone was during August and in subauroral zone during May 13-15 Space Weather event, with the auroral oval moving to Ottawa.

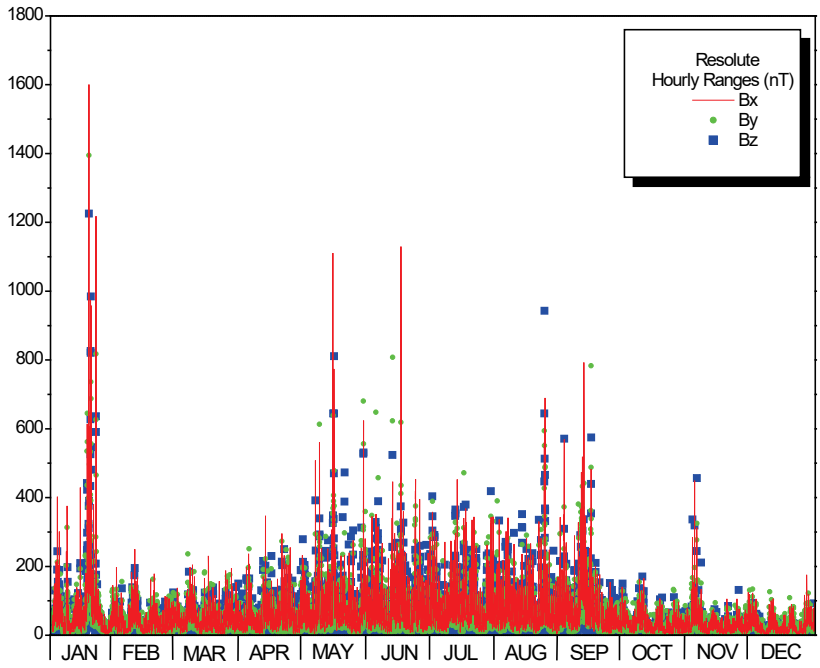

Figure 8.5. Hourly ranges of the magnetic field components at Resolute.

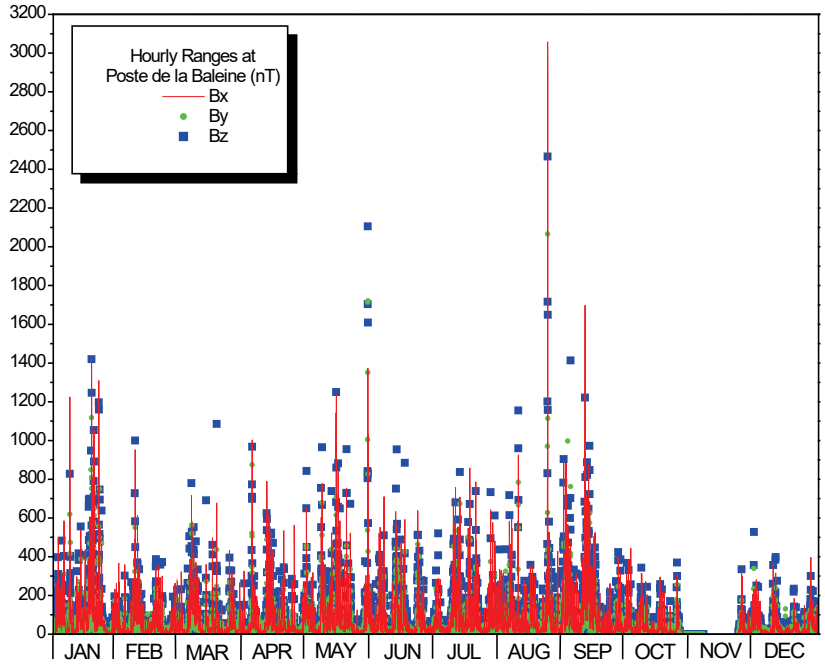

Figure 8.6. Hourly ranges of the magnetic field components at Poste-de-la-Baleine.

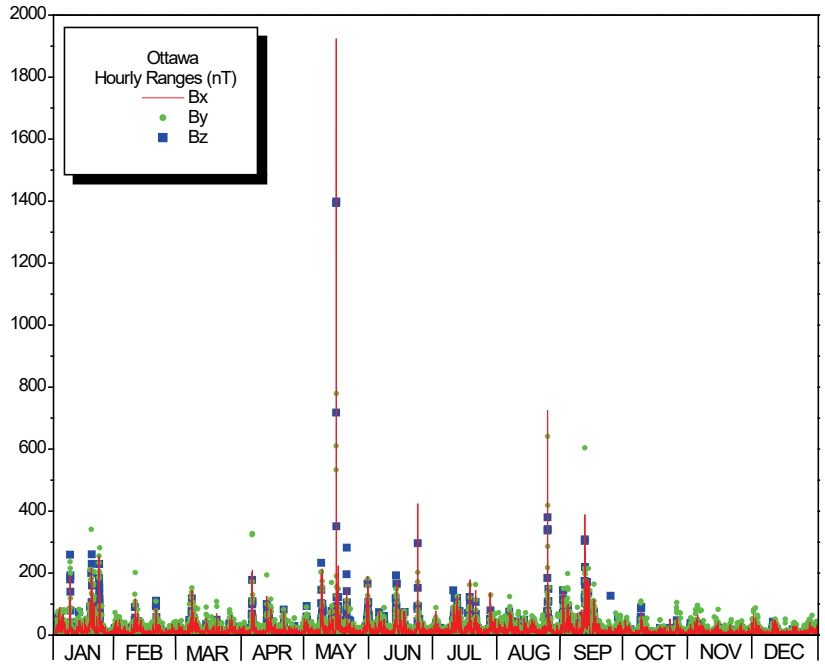

Figure 8.7. Hourly ranges of the magnetic field components at Ottawa.

Details of the largest space weather events and GIC

The space weather event of **May 15** was initiated by the full halo CME associated with an M8.0/2b long duration event (N12E12) and Type II(1349) and Type IV radio bursts, originated from centrally positioned AR 759 (Figure 8.8). The plane of sky speed has been estimated (due to limited imagery) as 794-1020 km/s.

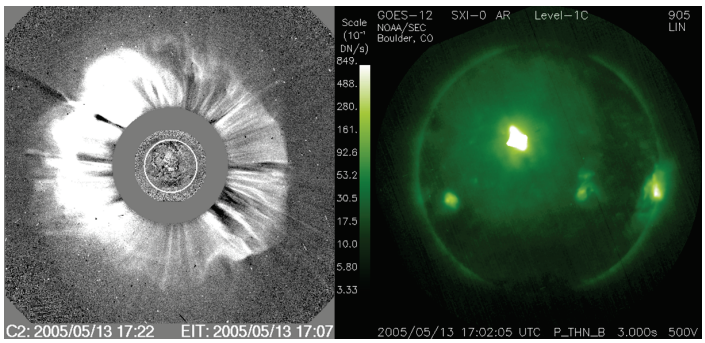

Figure 8.8. CME image taken by C2 EIT (left panel) and location of the source active region (right panel), taken by GOES SXI on May 13, 2005.

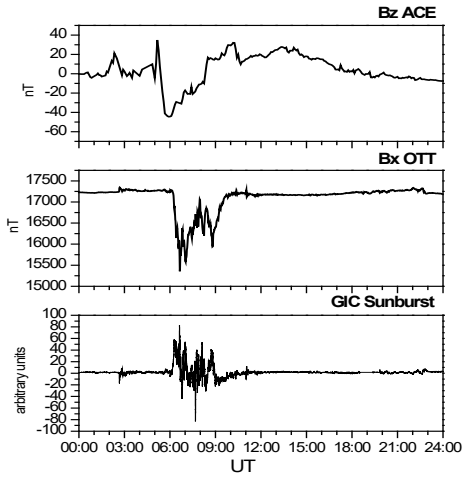

Figure 8.9. Interplanetary and ground results of May 13 event: top panel is IMF Bz at ACE, middle panel is Bx at Ottawa and the bottom panel is GIC variations at one of the North American power grid.

As presented in Figure 8.9, IMF Bz at ACE (top panel) shows sharp southward turning from 05:00 UT and became min=-43 nT at about 0600 UT. This produced a major geomagnetic storm in Ottawa with decrease in magnetic field ~1800 nT (middle panel), rate-of-change ~400nT/min. and significant GIC in power system (bottom panel) with maximum value of 83 A.

The space weather event of **August 24** was the result of the activity in Region 798. The two earth-directed CME (pos speed 720 km/s and 1700km/s, see Figure 8.10) were associated with two long duration flares on 22 August, M2.6 (S08W50) and M5.6 (S12W60).

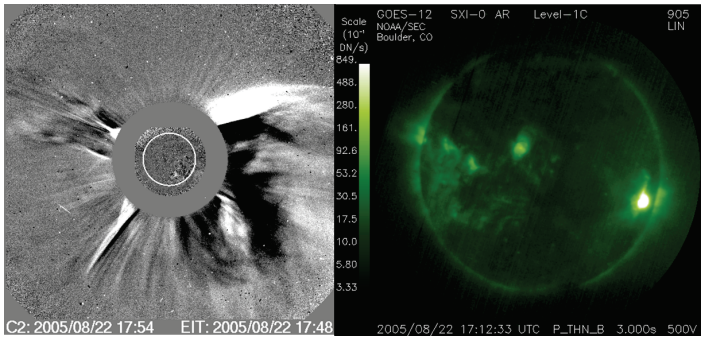

Figure 8.10. CME image taken by C2 EIT (left panel) and location of the source active region (right panel), taken by GOES SXI on August 22, 2005.

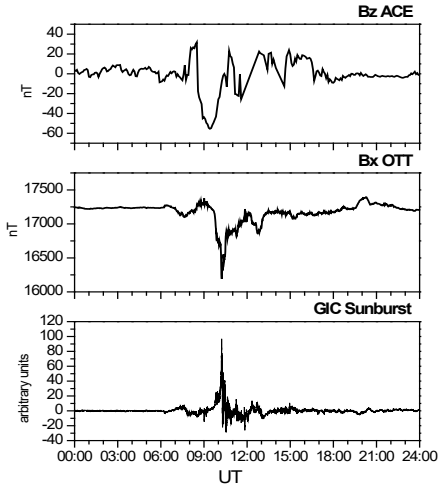

Figure 8.11. Interplanetary and ground results of May 13 event: top panel is IMF Bz at ACE, middle panel is Bx at Ottawa and the bottom panel is GIC variations at one of the North American power grid.

As presented in Figure 8.11, IMF Bz turned negative at about 08:00 UT and became min.=-55 nT at about 09:30 UT. The major magnetic storm in Ottawa produced a decrease in magnetic field ~1000 nT, dBx/dt of 150 nT/min. and GIC in power system with maximum value of 96.9 A.

References

L. Trichtchenko, H.-L. Lam, and D. Danskin, Space Weather Events 2005, poster presented at the Space Weather Week in Boulder, April 2006.